JGP Journal of General Physiology

REVIEW

Structural mechanisms of CFTR function and dysfunction

Tzyh-Chang Hwang[1,2,3], Jiunn-Tyng Yeh[1]*, Jingyao Zhang[1,3]*, Ying-Chun Yu[1,2], Han-I Yeh[1,2], and Samantha Destefano[1,2]

Cystic fibrosis (CF) transmembrane conductance regulator (CFTR) chloride channel plays a critical role in regulating transepithelial movement of water and electrolyte in exocrine tissues. Malfunction of the channel because of mutations of the *cftr* gene results in CF, the most prevalent lethal genetic disease among Caucasians. Recently, the publication of atomic structures of CFTR in two distinct conformations provides, for the first time, a clear overview of the protein. However, given the highly dynamic nature of the interactions among CFTR's various domains, better understanding of the functional significance of these structures requires an integration of these new structural insights with previously established biochemical/biophysical studies, which is the goal of this review.

Introduction

Cystic fibrosis (CF) is an autosomal recessive hereditary disease that afflicts more than 85,000 people worldwide (De Boeck and Amaral, 2016). The culprit of this illness, the *cftr* gene (Riordan et al., 1989), encodes a PKA-activated but ATP-gated anion channel in the epithelial cells lining the airway, the gastrointestinal tract, the biliary duct, the sweat ducts, the pancreas, and part of the reproductive organs. As a member of the ATP-binding cassette (ABC) transporter superfamily, the CFTR protein inherits the canonical motifs of two transmembrane domains (TMDs; transmembrane segments [TMs] 1–6 in TMD1 and TM7–TM12 in TMD2), each followed by a cytosolic nucleotide-binding domain (NBD1 and NBD2). A unique regulatory domain, located between two TMD–NBD complexes (Fig. 1, A and B), contains multiple consensus serine/threonine residues for PKA-dependent phosphorylation, which is a prerequisite for CFTR to function effectively as an ATP-gated ion channel (Sohma and Hwang, 2015).

More than two decades of research have accumulated a plethora of data mostly from biochemical and biophysical studies of CFTR, which no doubt did shed some light on the structure/function relationship of this medically important molecule, but high-resolution structures of CFTR have not been available until very recently (Zhang and Chen, 2016; Liu et al., 2017; Zhang et al., 2017). Although for human CFTR (hCFTR), only an unphosphorylated, closed channel conformation was reported, these pioneering structural studies already offer investigators an unprecedented opportunity to reexamine previously published biochemical/biophysical results as well as to propose possible new directions of research using the structure as a guide. In this article, instead of reviewing the literature across the board, we will focus our discussion on the "functional anatomy" of CFTR by explaining as much as possible published biochemical/biophysical data in the context of the first atomic structure of hCFTR or zebrafish CFTR (zCFTR). Five areas will be covered: roles of the R domain in CFTR function, asymmetrical pore and gate in CFTR, CFTR's gating machinery NBDs and TMD–NBD interfaces, molecular understanding of disease-associated mutations, and structural mechanisms of CFTR pharmacology. In light of the evolutionary relationship between CFTR and ABC exporters, we also take advantage of this opportunity to conjure up a possible schema depicting how the structural changes during evolution in CFTR make it a channel instead of a transporter. To avoid repetition with previous review articles, we refer our readers to other works focused more on specific subjects, e.g., Gadsby and Nairn (1999) for the R domain function, Sohma and Hwang (2015) for the roles of NBDs in CFTR gating, Linsdell (2017) for the CFTR pore, and Jih et al. (2017) for CFTR potentiators.

Roles of the R domain in CFTR function

Phosphorylation of the R domain is essential for the activation of CFTR proteins (Seibert et al., 1999; Ostedgaard et al., 2001). However, the detailed mechanism of how the R domain regulates the channel remains unclear despite extensive studies in the past decades. One technical difficulty in functional studies (perhaps biochemical/structural studies, too) of phosphorylation-dependent regulation is the uncertainty and likely large variability in the initial phosphorylation status of CFTR expressed in cells bearing unpredictable levels of kinase/phosphatase balance

[1]Dalton Cardiovascular Research Center, University of Missouri, Columbia, MO; [2]Department of Medical Pharmacology and Physiology, University of Missouri, Columbia, MO; [3]Department of Biological Engineering, University of Missouri, Columbia, MO.

*J.-T. Yeh and J. Zhang contributed equally to this paper; Correspondence to Tzyh-Chang Hwang: hwangt@health.missouri.edu.

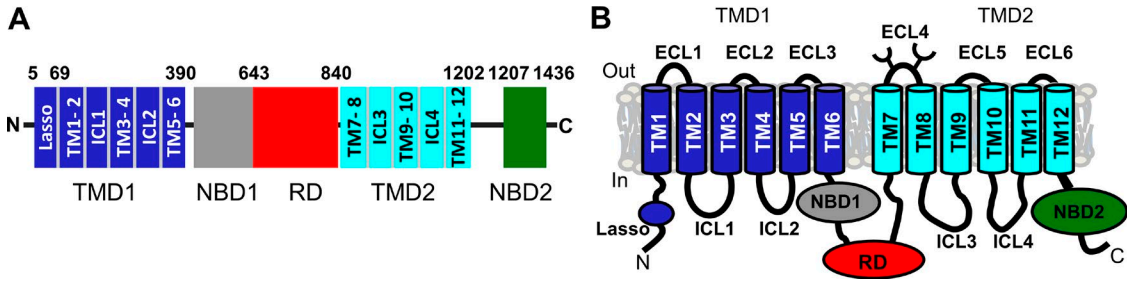

Figure 1. **CFTR topology. (A)** Organization of different domains in CFTR. CFTR is a 1,480–amino acid polytopic glycoprotein in the ABC transporter family (ABCC7). It contains two TMDs (TMD1 and TMD2) that form the channel pore, two cytosolic NBDs (NBD1 and NBD2) that drive channel gating, and an intrinsically unstructured regulatory domain (RD) that controls channel activity via PKA-mediated phosphorylation. Each of the TMDs comprises six TMs. Each ICL or ECL represents the helical extensions of two adjacent TMs. Individual TM and ICL are numbered from the N terminus to the C terminus. **(B)** Topology of CFTR. The TMs are linked by six ECLs and four ICLs. ECL4 contains two consensus N-glycosylation sites (N894 and N900), which are depicted as branches. C, C terminus; N, N terminus.

(Fig. 2 A). Although several phosphatases, such as λ-phosphatase, PP2A, PP2C, and alkaline phosphatase, were used to dephosphorylate the CFTR channel, the exact efficacy of these reagents and the effects on channel gating remained unclear (Chappe et al., 2003). The fact that a counterpart of the R domain is not found in other members of the ABC transporter family or any other proteins further complicates the issue. Indeed, bioinformatics research revealed that the R domain may have evolved from a previously noncoding sequence in the genome to bequeath CFTR a regulatory capacity for its channel function (Sebastian et al., 2013). In the reported hCFTR structure (Liu et al., 2017), the electron microscopy (EM) map of a presumably unphosphorylated R domain of CFTR is shown as an amorphous density that lies between two NBDs (Fig. 3 A). Different from the earlier structure of zCFTR (Zhang and Chen, 2016), an additional helical structure wedged in the internal vestibule of human orthologue is partially resolved (Fig. 3 A). This helix, likely consisting of residues 825–843 in the C terminus of the R domain, is proposed to interact with TM9, 10, and 12 of TMD2.

Although the structure of the overall R domain was not as well resolved as other parts of the CFTR protein, close examinations of the location of the density reveal contacts of the R domain with several functionally critical components of CFTR. These interactions may provide mechanistic insights into multifaceted functions of the R domain. By examining biophysical and biochemical data with respect to the functional role of the R domain, we will discuss the structure/function relationship of the R domain by covering several topics, including the intrinsic structural properties of the R domain, the interactions of the R domain with other domains such as NBDs, N- or C-termini, NBD–TMD interfaces, and the pore. This section will end by discussing the pros and cons of several hypothetic models for R domain function in the literature and pointing to some possible future directions of research.

Intrinsic structural properties of the R domain

The structural properties of an isolated R domain have been studied previously using biophysical and biochemical methods. These studies (Ostedgaard et al., 2000; Baker et al., 2007) led to a consensus conclusion that the R domain is largely disordered irrespective of its phosphorylation status. As expected, the unphosphorylated and phosphorylated R domains in the cryo-EM structure are mostly unresolved (Zhang and Chen, 2016; Liu et al., 2017; Zhang et al., 2017). Proteins like the R domain that lack stable secondary or higher-ordered structure but are biologically active are categorized as intrinsic disordered proteins (IDPs; Wright and Dyson, 1999). IDPs play an essential role in a variety of biological processes, such as protein–protein interaction, signaling, and regulation. The disordered nature of IDPs is thought to endow them the ability to interact with a broad range of binding partners, from small molecules to protein subdomains or other proteins (Dyson and Wright, 2005).

From the structural point of view, a low mean hydrophobicity and a high net charge are important features for not having a more compacted higher-ordered structure (Uversky, 2011). Such properties allow IDP to assume a better interaction with the aqueous environment, to bear a lower driving force for protein compaction, and to exert a stronger electrostatic repulsion to favor an unfolded structure (Oldfield and Dunker, 2014). Indeed, the R domain in hCFTR exhibits all these characteristics. The number of charged residues is 59 amid a total of ∼200 amino acids in the R domain (residues 645–843), and 60% of R domain residues are hydrophilic. Interestingly, the negatively charged residues in the R domain aggregate into two clusters, named NEG1 (725–733) and NEG2 (817–838) by Xie et al. (2002). The sequence of NEG2, which coincides with the aforementioned segment of the R domain that interacts with TMDs, is highly conserved among species, and mutations that alter the charge in this region are identified, e.g., E822K, E826K, D828G, and D836Y, in the Cystic Fibrosis Mutation Database. Among them, E822K and E826K found in patients with CF were reported to have a reduced cAMP-induced chloride current (Vankeerberghen et al., 1998).

In addition to the high charge density the R domain already possesses, phosphorylation of several consensus sites can further increase the negative charges in this domain. Such a mechanism, along with other posttranslational modifications, is common among IDPs as a way to alter the binding affinity for different targets (Iakoucheva et al., 2004). It was also shown that the serines subjected to phosphorylation remain highly conserved, whereas the rest of the R domain tolerates a relatively larger variation in sequence (Ostedgaard et al., 2001). In the same review article, Ostedgaard et al. (2001) also summarize studies using a variety of

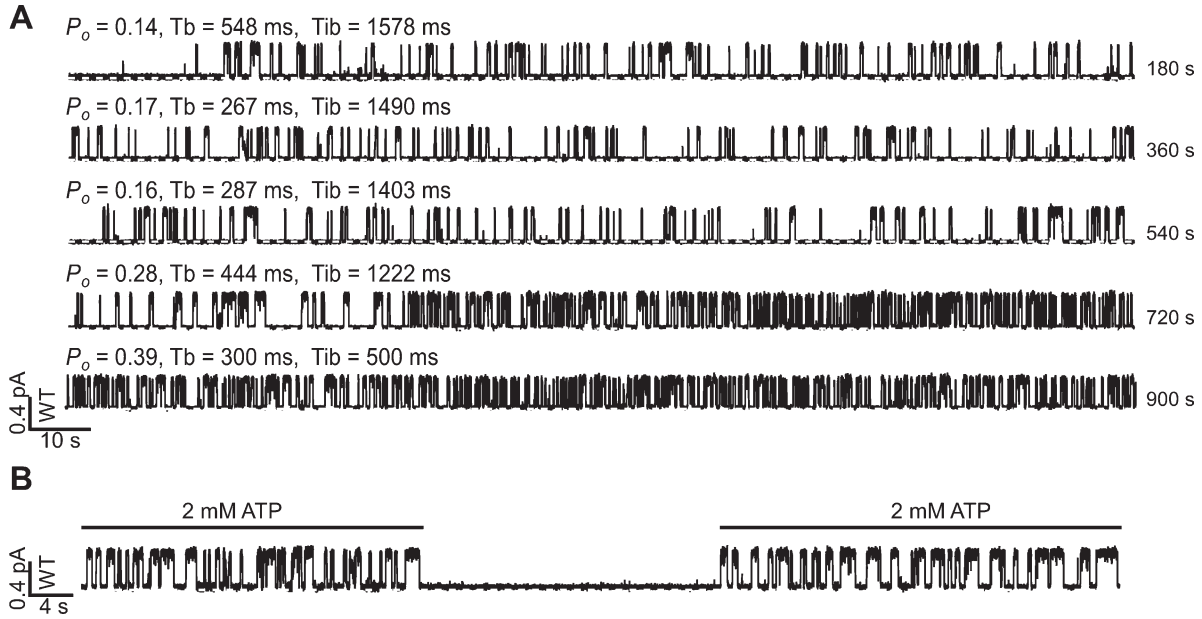

Figure 2. **Single-channel behavior of human WT CFTR. (A)** A representative continuous single-channel trace of human WT CFTR in an excised inside-out patch showing an incremental activation of the channel activity upon addition of PKA (25 IU) and ATP (2 mM). Currents were recorded at room temperature with symmetrical 154 mM [Cl^-]. Membrane potential was held at −50 mV; upward deflections represent channel opening (signals were inverted purely for the purpose of presentation). Dashed lines on the bottom of each trace mark the zero-current level. Microscopic kinetic parameters including open time (Tb), interburst duration (Tib), and open probability (P_o) of each segment of the recording are presented above the trace. Of note, one can barely discern one single opening event in the first ∼20 s of the recording despite the presence of millimolar ATP, suggesting that before phosphorylation, the P_o is exceedingly low even at millimolar ATP. However, the status of R domain phosphorylation is not known; one cannot rule out the possibility that some serine/threonine in the R domain had been phosphorylated by cellular PKA before patch excision. (Thus, assuming that the CFTR channel upon patch excision is completely dephosphorylated could be erroneous.) In the second and third traces for an overall time of 6 min, the channel activity is relatively low with a closed time constant >1 s. A stable, high activity was not observed until ∼10 min after the addition of PKA and ATP. This result is consistent with the idea that phosphorylation-dependent activation of CFTR is more complex than a simple on–off switch. **(B)** ATP-dependent gating of a maximally phosphorylated human WT CFTR. Once the channel is fully activated, a P_o of ∼0.4 with a closed time constant <1 s was consistently observed in our laboratory (Zeltwanger et al., 1999; Zhou et al., 2005; Tsai et al., 2010; Jih and Hwang, 2013; Yeh et al., 2015). Because the degree of phosphorylation can alter the P_o of CFTR, the gating parameters reported in the literature are inevitably subject to the phosphorylation status of CFTR, which depends on the balance between kinase and phosphatase in the system. For example, when CFTR is expressed in *X. laevis* oocytes, the strong membrane-associated phosphatase activity will counter the action of exogenous PKA (Csanády et al., 2005); in some studies, CFTR currents in excised patches depend on the continuous presence of PKA as removal of PKA causes a sharp decrease of >50% of the currents in seconds (Weinreich et al., 1997; Csanády et al., 2000; Szellas and Nagel, 2003).

strategies including partial or complete deletion of the R domain and single amino acid substitution on potential phosphorylation sites to address the issue of how the R domain modulates CFTR gating. Although these studies suggest that it is the spacing between these consensus serines instead of the overall structure of the R domain that is important for phosphorylation-dependent regulation of CFTR, detailed mechanisms for R domain function remain to be elucidated (Ostedgaard et al., 2001). Nonetheless, the disordered nature of the R domain and the relatively fixed spaces between individual phosphorylation sites imply that its regulatory role depends on how the R domain interacts with different segments of CFTR and the dynamics of these interactions after phosphorylation.

Interactions of the R domain with NBDs and N- and C-termini

Phosphorylation-dependent interactions between the R domain and both NBD1 and NBD2 were first revealed by elegant nuclear magnetic resonance (NMR) studies (Baker et al., 2007; Bozoky et al., 2013). By plotting the ratios of the resonance intensity with or without a binding partner as a function of the residues, the authors found that interactions between NBDs and several local regions of the R domain are attenuated after phosphorylation. Close inspection of the residues involved in the binding suggests that the interactions between NBDs and the R domain likely occur at the interface between NBD1 and NBD2. The cryo-EM structures of unphosphorylated CFTR indeed confirm that a significant portion of the R domain lies between the two NBDs (Fig. 3 B); one can hence deduce that the unphosphorylated R domain controls CFTR gating by preventing NBD dimerization, and phosphorylation relieves this inhibition (Bozoky et al., 2013). Supporting this thesis, other functional studies also indicate that phosphorylation of the R domain facilitates NBD dimerization (Mense et al., 2006) as well as ATP hydrolysis (Li et al., 1996; Liu et al., 2017). The idea that the R domain inhibits CFTR function by interfering with NBD dimerization is further supported by the cryo-EM structure of a phosphorylated zCFTR possessing dimerized NBDs (Zhang et al., 2017). This latest structure showed no density representing the R domain after phosphorylation, indicating the dissociation of the R domain from the NBD interface. However, this simple idea is not likely to represent the whole picture of the regulatory function of the R domain. For instance, activation of CFTR mutants whose NBDs are defective

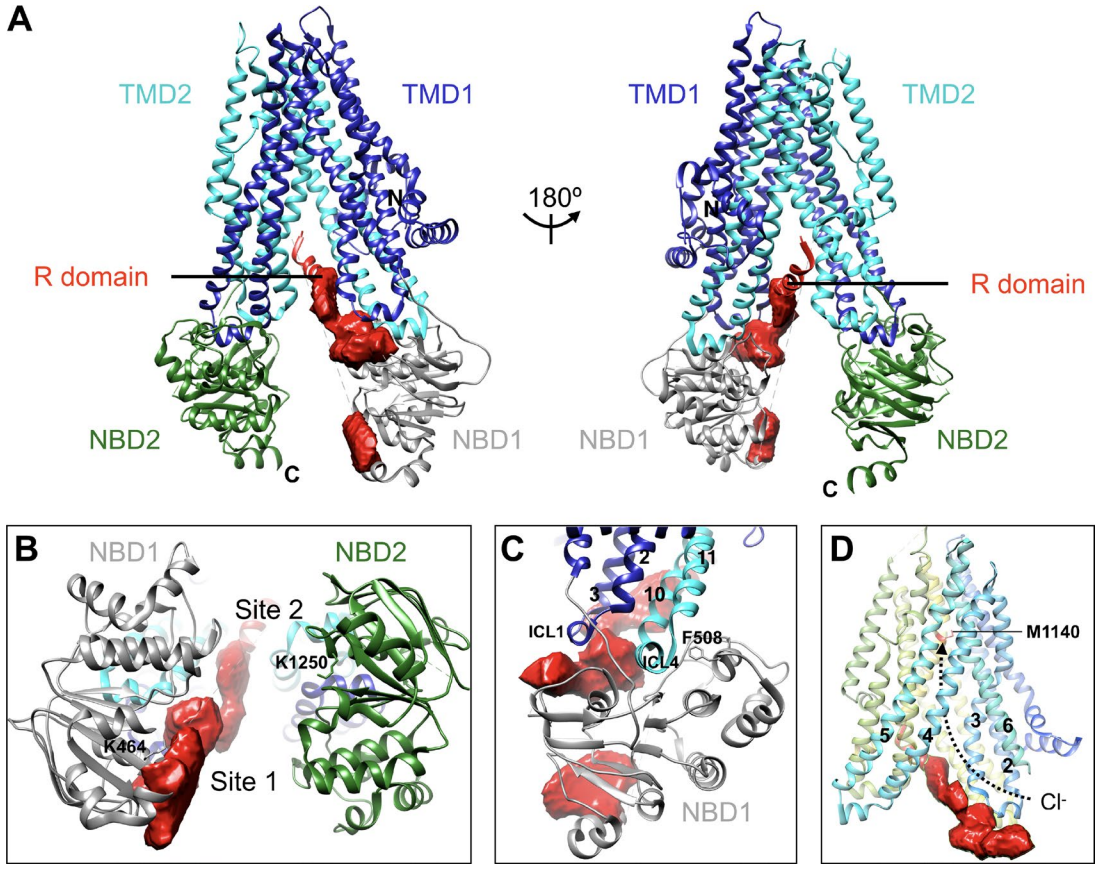

Figure 3. **Interactions between the R domain and other components in CFTR. (A)** The overall ribbon diagram of the front (left) and back (right) view of hCFTR (Liu et al., 2017). The EM density of the R domain is shown in red. **(B)** Bottom view of the structure revealing the interaction between the R domain and the NBDs. The side chains of the Walker A lysine of ATP binding site 1 (K464) and site 2 (K1250) are shown in sticks and labeled. **(C)** Side view of the structure demonstrating the proximity between the R domain and both the NBD1–ICL4 and NBD1–ICL1 interfaces. Individual TMs are labeled in number. **(D)** A graph highlighting the contacts between TMDs and the R domains. The dashed line marks the ion permeation pathway. M1140 in TM12 is labeled (see text).

in dimerization (e.g., G551D) or even partially truncated (e.g., ΔNBD2) remains phosphorylation-dependent (Bompadre et al., 2007; Cui et al., 2007; Wang et al., 2007). Moreover, it has been noted for a long time that different degrees of phosphorylation, as well as different serine residues being phosphorylated, confer different levels of channel activity (Gadsby and Nairn, 1999; Ostedgaard et al., 2001). Such graded regulation of CFTR gating by phosphorylation of the R domain is inconsistent with the simple "on-and-off" idea.

Aside from interacting with NBDs, the R domain has also been shown to interact with the N terminus or C terminus of the CFTR protein. For the N terminus, a cluster of conserved negatively charged amino acids was reported to play a role in controlling CFTR gating by interacting with the R domain (Naren et al., 1999). However, this presumed binding of the R domain to these N-terminal residues is not dependent on phosphorylation. Fu et al. (2001) later showed that neutralizing these negatively charged residues does not alter phosphorylation of the R domain. Interestingly, this cluster of negatively charged residues happens to reside in a region of ∼60 residues (1–60) named lasso motif after its shape (Zhang and Chen, 2016). Although the cryo-EM structures did not show any direct contact between the R domain density and the lasso motif, the strategic position of this motif at the juncture between NBD1 and part of TMD suggests that any structural perturbation induced by mutations may by itself alter CFTR gating.

The interaction between the C terminus and the R domain was first demonstrated by NMR study of isolated peptides (Bozoky et al., 2013). Contrary to the results described above for the N-terminal interaction, the affinity between the C terminus and the R domain increases with phosphorylation. In addition, this interaction between the C terminus and the R domain causes a large chemical shift, indicating significant disorder-to-order conformational changes for a particular subsection of the R domain. Although the structures of CFTR did not show a specific interaction between the R domain and the C terminus (Zhang and Chen, 2016; Liu et al., 2017), this is perhaps not surprising because a significant portion of the C terminus is not resolved in the cryo-EM structures. Nonetheless, an interesting possibility is that part of the unresolved C terminus may serve as a docking site for the phosphorylated R domain.

Interactions of the R domain with NBD–TMD interfaces

Although the cytoplasmic NBDs serve as gating machinery, CFTR's pore and gate reside in its TMDs. Thus, the interfaces between NBDs and TMDs likely play an important role in

coupling NBDs motion and gate opening in TMDs, a subject discussed in the following section. Indeed, the gating trajectory from the ATP binding site to the gate through NBD–TMD interfaces has been extensively mapped (Sorum et al., 2015, 2017). As mentioned above, activation of the mutations like G551D or ΔNBD2 is still phosphorylation dependent, so it's possible that the R domain also regulates the channel activity through interacting with the NBD–TMD interfaces or the pore region. In the cryo-EM structures (Fig. 3 C), we notice a portion of the R domain density located in proximity to the interface between NBD1 and intracellular loop (ICL) 4 (connecting TM10 and TM11). The functional significance of this particular interface is not clear, but it is noted that many disease-associated mutations, including the most common ΔF508, are clustered in this region. There are also studies suggesting that several mutations located at this interface, including ΔF508, are associated with slower phosphorylation-dependent activation (Wang et al., 2000; Chin et al., 2017). Further NMR studies provide evidence that the ΔF508 mutation may affect phosphorylation-modulated domain–domain interactions (Kanelis et al., 2010). Fig. 3 C also shows part of the R domain density near the NBD1–ICL1 interface; however, the functional significance of this interaction is unclear. Nonetheless, because these ICL–NBD interfaces likely undergo conformational changes as the two NBDs approach each other to form a canonical dimer, dissociation of the R domain from these interfaces must also occur after phosphorylation.

Interactions between the R domain and the pore

Perhaps the most intriguing finding in the cryo-EM structure of hCFTR (Liu et al., 2017) is that a helix (residues 825–843) in the R domain protrudes into the internal vestibule of the anion permeation pathway in CFTR (Fig. 3, A and D). This helix happens to overlap with the aforementioned NEG2 (residues 817–838) reported first by Xie et al. (2002). They predicted that the NEG2 is a helix with most of the negatively charged residues lining up on one face of the helix. Deletion of NEG2 (ΔNEG2) results in a phosphorylation-independent channel, albeit with a lower P_o. Also interestingly, cytoplasmic application of synthetic NEG2 to WT CFTR increases the P_o at a low concentration but completely shuts down the channel at a higher concentration, suggesting two binding sites with opposite actions, a conclusion further supported by results that these two actions of NEG2 peptides are differentially sensitive to perturbations of the charges or of the helical tendency. These functional data, together with the strategic position of this helix, suggest that this part of the R domain may serve as a "master switch" for CFTR's TMDs—dislocation of the helix away from the internal vestibule enables the TMDs to undergo gating conformational changes (Liu et al., 2017; also see below).

The observation that a negatively charged helix is wedged in the internal vestibule may also offer a possible explanation for some seemingly conflicting data from substituted cysteine accessibility method (SCAM) studies of the pore-lining residues (see next section for more details). For example, Bai et al. (2011) found that M1140C (methionine to cysteine mutation at position 1140) in TM12 (Fig. 3 D) can be modified by thio-specific reagents from the intracellular side in both closed state and open state after phosphorylation, and thus proposed a gate located external to M1140. In contrast, Qian et al. (2011) reported that M1140C could not be modified before phosphorylation, suggesting a phosphorylation-controlled "gate" internal to this very position. However, if this helix in the R domain does serve as a cytoplasmic gate in the cytoplasmic side of the pore, accessibility to positions between M1140 and this helix should also be phosphorylation dependent; oddly, they are not (Qian et al., 2011). This discrepancy may reflect one of the major difficulties in studying phosphorylation-dependent events again: the uncertainty of the phosphorylation status of the R domain in the initial control condition because of variable balance of cellular kinase/phosphatase activities among cells (Fig. 2 A).

Future direction of research

We have thus far summarized and discussed how previous researchers tackle the protean function and regulation mechanism of the R domain using different biochemical and biophysical approaches and how these functional studies can or cannot account for the newly resolved structures of CFTR. Collectively, three models for the role of the R domain in gating control emerge based on the experimental results. Baker et al. (2007) summarized the dynamic interactions between the R domain and other domains based on NMR studies, which bear a distinct advantage of being able to resolve individual segments responsible for the interaction with different binding partners, as well as providing the structural dynamics upon phosphorylation. This model enables us to understand the regulatory mechanism of the R domain as a series of intricate local interactions instead of a simple on-and-off process. However, the obvious caveat of this approach is that isolated peptides, instead of the whole CFTR protein, are used as experimental materials.

To explain a possible stimulatory role of the phosphorylated R domain, Ostedgaard et al. (2000) proposed a model depicting multiple phosphoserines in the R domain interacting with different locales in CFTR. Such a model nicely explains how a random coil or IDP can regulate a highly structured protein. However, the revelation of multiple interactions between the unphosphorylated R domain and other parts of CFTR by cryo-EM data indicates that the unphosphorylated R domain, by contacting multiple segments of CFTR known to be functionally important, must exert some effects on the channel. Unfortunately, the only structure of a phosphorylated CFTR didn't resolve any density representing the R domain (Zhang et al., 2017).

Based on the idea that the R domain assumes an inhibitory function in CFTR gating, Liu et al. (2017) proposed a model for the regulatory role of the R domain. In this model, the unphosphorylated R domain can dissociate from its original positions slowly, so there's a small fraction of active channel noted before the application of PKA. Phosphorylation of the dissociated R domain will stabilize the structure and prevent the R domain from returning to its inhibition positions. This simple kinetic model precisely explains the sigmoidal time course for phosphorylation-dependent activation of macroscopic CFTR currents. However, a much more complicated scenario is needed to account for the experimental results, suggesting a graded regulation of CFTR gating with different extents of phosphorylation (Hwang et al., 1994),

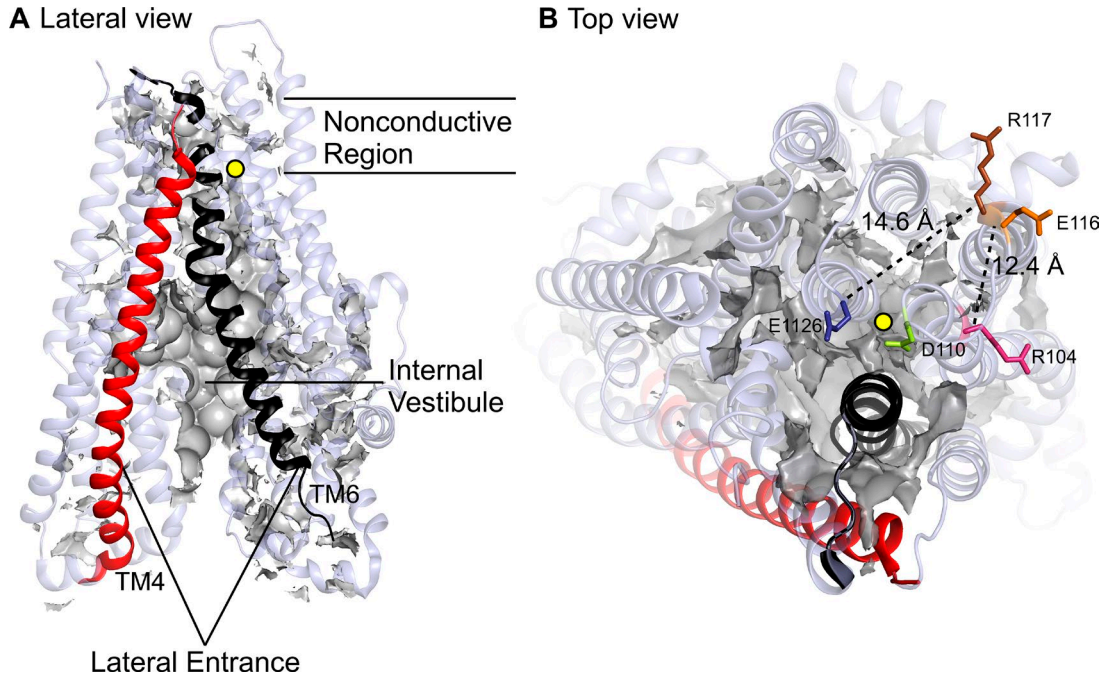

Figure 4. **Lateral view and top view of the TMDs in the cryo-EM structure of hCFTR. (A)** Lateral view of the TMDs featuring a lateral entrance framed by TM4 (red) and TM6 (black), the surface view of the internal vestibule (gray), and a nonconductive region where close contacts among TMs obstruct the pore. Other 10 TMs are shown as ribbons in light purple. A yellow dot marks the end of the water-accessible space in the internal vestibule. Of note, the yellow dot is shifted away from the central axis of the pore. The functional implications of this structural feature are discussed in the text. **(B)** Top view of the TMDs. Color code is the same as used in A. Several residues in the external part of the TMDs (violet, R104; green, D110; gold, E116; brown, R117; salmon, R334; yellow, K335; and blue, E1126) were reported to affect the stability of the channel architecture or permeation properties. The distances between selected residues are shown in dashed lines, and the potential functional significance of these residues is discussed in the text.

or a possible role of inhibitory phosphorylation sites (Wilkinson et al., 1997; Csanády et al., 2005). As discussed above, the uncertainty of the phosphorylation status before the addition of exogenous PKA in patch-clamp experiments also hinders accurate measurements of the activity for a truly unphosphorylated CFTR.

In light of such a complex regulatory process in phosphorylation-dependent gating regulation (Hwang and Kirk, 2013), we believe that attaining a comprehensive model for R domain function may require an integration of many of the mechanistic insights gained from different approaches. For example, one may divide the R domain into several subdomains based on the individual interaction segments revealed by the NMR and cryo-EM data and design biophysical or biochemical assays to probe the functional effects as well as the structural properties of each interaction before and after phosphorylation. As the cAMP-PKA pathway plays a key physiological role in regulating CFTR function in vivo, understanding the molecular mechanism of how the R domain itself is modulated is an imperative task.

Asymmetrical pore and gate in CFTR

An ion channel, CFTR included, is simply a gated pore with the capacity to select for particular ions. Biophysical data collected over the past two decades suggest a continuous chloride permeation pathway in CFTR consisting of, from the cytoplasmic side to the extracellular side, (a) a lateral entrance (El Hiani and Linsdell, 2015; El Hiani et al., 2016) between TM4 and TM6, (b) a large internal vestibule (Bai et al., 2011), (c) a narrow region that may serve as a gate and selectivity filter (Gao and Hwang, 2015; Linsdell, 2016), and (d) a shallow external vestibule (Muanprasat et al., 2004; Norimatsu et al., 2012a). Although the three atomic CFTR structures solved so far all assume nonconductive conformations (Zhang and Chen, 2016; Liu et al., 2017; Zhang et al., 2017), they do reveal a lateral opening between TM4 and TM6, a large internal vestibule, and a nonconductive region located at the external end of the permeation pathway (Fig. 4 A). In the following subsection, we will use the cryo-EM structure of hCFTR as our major reference to summarize previous functional studies that match these structural features. Meanwhile, we will try to resolve some of the discrepancies in the literature regarding the pore-lining amino acids and the location of CFTR's gate. At the end of this section, we will use existing data to project a rough picture of CFTR's anion permeation pathway upon gate opening with additional help from the recently resolved phosphorylated, ATP-bound structure of zCFTR (Zhang et al., 2017).

Structure and function of the internal vestibule

As the open-channel conformation of CFTR possesses a tightly associated cytoplasmic NBD dimer in a head-to-tail configuration (Vergani et al., 2005), it is unlikely for the permeant ions to traverse the pore through a perpendicular, central axis of CFTR that is obstructed by the dimerized NBDs at the cytoplasmic end. Homology models of CFTR's open state based on Sav1866 (Dawson and Locher, 2007) suggest anion entryways on the sides of the protein (Mornon et al., 2008, 2015; Norimatsu et al., 2012a), much like the path for ions entering the pore in K^+ channels (Long et al., 2005). Interestingly, early cryo-EM studies

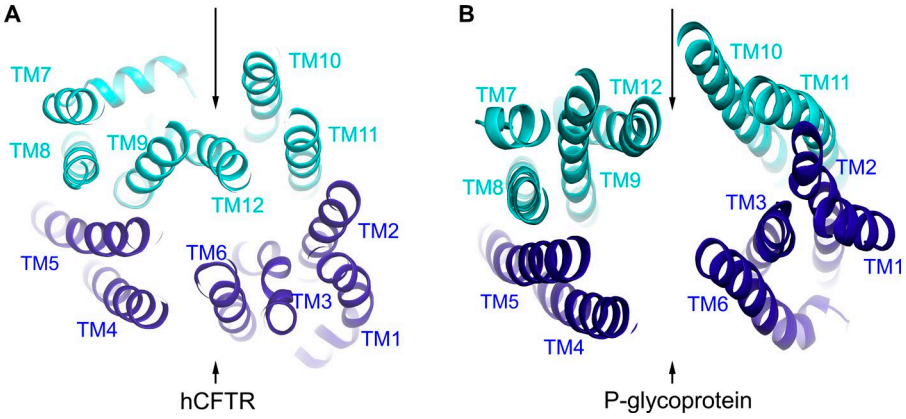

Figure 5. **Comparison of the architecture of TMDs between hCFTR and P-glycoprotein. (A)** Top view of the TMDs in the cryo-EM structure of hCFTR (Protein Data Bank [PDB] accession no. 5UAK). Arrows indicate the cytoplasmic gaps of the internal vestibule between TM4 and TM6 and between TM10 and TM12. Dark blue, TMD1; cyan, TMD2. **(B)** Symmetrical architecture of the TMDs in P-glycoprotein (PDB accession no. 4KSB). The color code is the same as in A. Although CFTR evolves from ABC transporters and serves as an anion channel, the basic architecture of the TMDs in CFTR follows the pseudo-symmetrical mode found in ABC exporters. However, some modifications of this basic architecture are needed for CFTR to work as a channel (an issue discussed throughout this article).

did suggest the presence of "side-windows" in CFTR (Mio et al., 2008). The first piece of functional evidence for a lateral entrance was provided by El Hiani and Linsdell (2015). In their study, all 16 positively charged residues (R, K, and H) along TM5/8, TM2/11, TM10/12, or TM4/6 and their intracellular extensions, which form four potential tunnels proposed by Mornon et al. (2015), were tested. By changing the charge status of these 16 positions, they showed that mutations and/or covalent modification on each of the six cysteine substituted residues, K190C (TM3), R248C (TM4), R303C (TM5), K370C (TM6), K1041C (TM10), and R1048C (TM10), alter the single-channel amplitude in a charge-dependent manner. Interpreting these data in the context of the SAV1866-based homology model (Mornon et al., 2015), El Hiani and Linsdell (2015) proposed that these positively charged residues serve as surface charges at the entry points of the pore. Furthermore, as introducing a negative charge into positions 190 (TM3), 248 (TM4), 303 (TM5), and 370 (TM6) decreases the single-channel current amplitude significantly more than that at positions 1041 (TM10) and 1048 (TM10), it is further suggested that the lateral entrance between TM4 and TM6 serves as a major portal of entry, whereas the entrance between TM10 and TM12 plays a minor role. The cryo-EM structures indeed confirmed that the side chains of all six positively charged residues protrude into the internal vestibule that is constructed by two pseudo-symmetric flanks of the TMDs. The internal vestibule has two opposing lateral clefts opening toward the cytoplasm: a larger opening framed by TM4 and TM6 consistent with what is proposed (El Hiani and Linsdell, 2015), and a smaller one by TM10 and TM12. This latter opening in the unphosphorylated closed state of hCFTR is unlikely to be conductive because of an obstruction by part of the R domain as elaborated above in the R domain section. In the phosphorylated, closed-state structure of zCFTR whose NBDs are in a dimeric form (Figs. 11 and 12), the internal vestibule again opens to the aqueous environment between TM4 and TM6 with an opening smaller than that in the unphosphorylated zCFTR, where the two NBDs are widely separated (Zhang and Chen, 2016; Zhang et al., 2017). However, the widest distance between TM4 and TM6 flanking this cleft is 16.0 Å (measured between two opposing α-C atoms from zL254 in TM4 and zR367 in TM6), large enough for the solvent (or chloride), the MTS reagents,[1] and pore blockers such as glibenclamide to enter the pore. Interestingly, in this phosphorylated, ATP-bound structure of zCFTR where the R domain is no longer wedged between TM10 and TM12 (Zhang et al., 2017), the lateral opening between TM10 and TM12 is still extremely narrow, casting doubt on the conductivity along this very path for an open channel with dimerized NBDs. Indeed, some follow-up experimental data on the cytoplasmic entrance of CFTR from the same group reiterate a major role of the portal between TM4 and TM6 (Li et al., 2018).

If we accept the idea that the latest phosphorylated, ATP-bound zCFTR structure (Figs. 11 and 12) is closely similar to an open-channel conformation at the cytoplasmic end of its TMDs, the observation of a dimerized NBD with clear open access to the internal vestibule supports the "degenerate gate" hypothesis, which states that unlike other ABC exporters with one internal gate and one external gate, the internal gate of CFTR is degraded, resulting in only the external gate regulating the ionic flow. For ABC exporters, dimerization of NBDs provides the "power stroke" to convert an inward-facing conformation of the substrate translocation pathway with a closed external gate to an outward-facing conformation with a closed internal gate (Chen and Hwang, 2008). This alternating access model, together with the degenerate gate hypothesis, has been used to explain CFTR's gating motion (Bai et al., 2011). But why does the external gate remain closed in this structure with dimerized NBDs? This question will be addressed in the next section when we discuss NBD–TMD coupling. Nonetheless, it should be noted that a different picture of degraded transporter hypothesis was proposed by Linsdell's group (Wang and Linsdell, 2012a,b). Their data suggest that the TMDs assume an inward-facing conformation in the open state, but an outward-facing conformation in the closed state. However, part of the evidence used to derive this opposite theory comes from SCAM experiments showing accessibility of engineered cysteines at positions in both TM1 and TM6 to bulky MTS reagents applied from either side of the cell membrane, observations contradicting the idea that CFTR's pore has a narrow segment preventing passage of reagents >5.3 Å (Linsdell and Hanrahan, 1998). Regardless of these controversies, on a closer look at the conformation of these three cryo-EM structures so far published, the basic architecture of CFTR is consistent with that of ABC exporters (Schmitt, 2002; Dawson and Locher, 2007): when one divides the whole protein into halves by these two

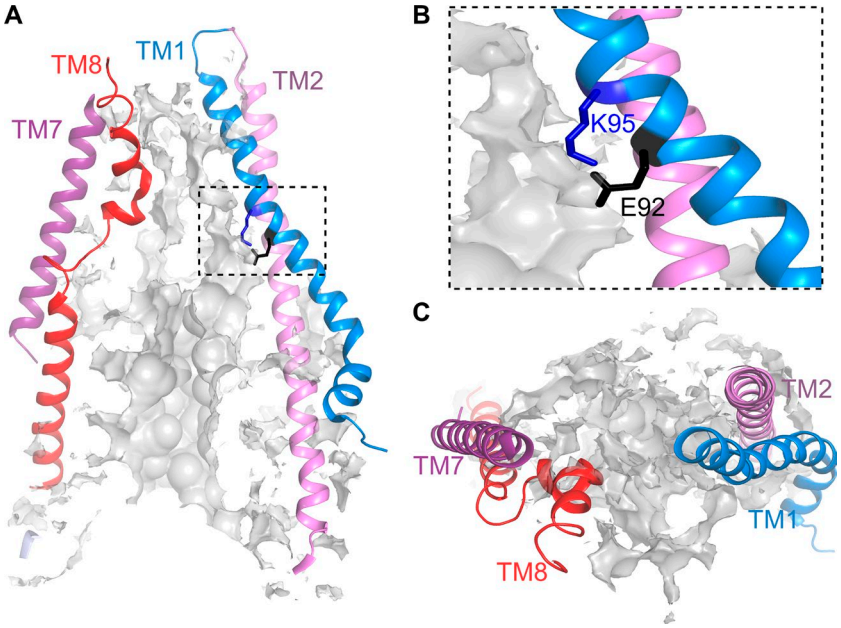

Figure 6. **Distortion of CFTR's TMD2 breaks twofold symmetry of the TMDs. (A)** Lateral view of part of CFTR's TMDs featuring asymmetrical arrangements between TM1 (blue) and TM7 (purple) and between TM2 (violet) and TM8 (red). The internal vestibule is shown in a gray surface view. The loop-like structure in a small segment of TM8 (G921–L935 in hCFTR) is distinct from the typical helical structure of TM2, and the impingement of this loop-like segment of TM8 toward the central vertical axis likely pushes TM7 away from the permeation pathway so that TM7, contrary to TM1, is not pore lining. The dashed box is enlarged in B. **(B)** E92 (black) and K95 (dark blue) in TM1 form an intra-helical salt bridge. **(C)** Top view of the TM pairs in A shows clearly that TM7 is located at the periphery of the protein with little contact with the internal vestibule (in gray surface view).

potential ion entry ports, one half is constructed by TM1, 2, 3, 6, 10, and 11, and the other by TM7, 8, 9, 12, 4, and 5 (Figs. 4 and 5).

The cryo-EM structures also offer an unparalleled opportunity for checking the pore-lining segments proposed based on functional data particularly from SCAM.[1]

To date, functional data collected from SCAM studies have suggested that CFTR's pore is constructed by TM1 (Wang et al., 2011; Gao et al., 2013), TM3 (Norimatsu et al., 2012a; El Hiani et al., 2016), TM4 (El Hiani et al., 2016), TM5 (Zhang and Hwang, 2015; El Hiani et al., 2016), TM6 (Fatehi and Linsdell, 2008; Alexander et al., 2009; Bai et al., 2010; El Hiani and Linsdell, 2010; Norimatsu et al., 2012a; El Hiani et al., 2016), TM9 (Norimatsu et al., 2012a), TM10 (El Hiani and Linsdell, 2015), TM11 (Wang et al., 2014a), and TM12 (Bai et al., 2011; Qian et al., 2011; Norimatsu et al., 2012a; Gao and Hwang, 2015). Table S1 summarizes the published positions of each TM where engineered cysteines can be modified by either internal or external application of thiol modification reagents. Through checking the solvent accessibility (Lee and Richards, 1971) and surface exposure of each residue in the internal vestibule of the cryo-EM hCFTR structure, we found that, with some exceptions (elaborated below), many of the pore-lining residues reported in SCAM studies are indeed water accessible in this closed-state cryo-EM structure (Table S1).

Perhaps the most intriguing and surprising finding in the cryo-EM structures is that the pore is architecturally asymmetrical. Unlike other ABC exporters, which show a twofold symmetry of the TMDs along the central axis of the protein (Fig. 5 B) because their TMD1 and TMD2 are structurally similar if not identical, CFTR's TMD2 is quite different from its TMD1 in that TM8 bears a short segment of loop-like structure interrupting the continuity of the helix (Fig. 6). The distorted segment of TM8 impinges toward the central vertical axis of the pore. The accompanied lateral displacement of TM7 away from the core of the protein renders TM7 being located at a different position than its counterpart TM1 (Fig. 6 A). This breakdown of twofold symmetry nicely explains why TM7 does not contribute to the pore formation (Wang et al., 2014a; Zhang and Hwang, 2015), whereas TM1 is pore-lining (Wang et al., 2011; Gao et al., 2013). This same local impingement of TM8 also enables its contacts with TM9 and TM12, which are not seen between their counterparts TM2, TM3, and TM6 in TMD1. These structural deviations away from twofold symmetry may explain some of the existing data supporting the asymmetry of the pore. For instance, a slight displacement of TM12 medially toward the central axis not only results in an obvious asymmetry in relation to the central axis between TM6 and TM12 but also brings TM12 closer to TM10 to form a smaller lateral entrance between these two segments as discussed above. This different positioning of TM6 and TM12 likely accounts for the functional data that implicate an asymmetrical contribution of these two pivotal TMs in forming the ion permeation pathway (Table S1; Gao and Hwang, 2015). For example, pore-lining residues from the bent TM12 are more consecutive (M1137–T1142 and V1147–S1150), as if more than two faces of an α helix are exposed to the pore, a feature not seen with the straight TM6 (Bai et al., 2010, 2011). As elaborated in more detail below, whereas T338 and S341 in TM6 may contribute to the formation of the narrowest segment in the pore, there is little functional evidence supporting an equivalent role for residues in TM12 (Gao and Hwang, 2015).

[1]SCAM has been considered a gold standard for the identification of pore-lining residues in the ion channel field since its conception (Akabas et al., 1992). The basic idea of this method is to introduce a cysteine to the positions of interest one at a time through mutagenesis. Then whether the engineered cysteine could be accessible and modified by thiol-specific reagents applied from either the extracellular or intracellular side to alter the channel conductance is used as the indicator for its pore-lining role. The availability of a spate of thiol-specific reagents with different charges and sizes including bulky methanethiosulfonate reagents such as $MTSES^-$ (width, ∼5 Å), $MTSET^+$ (width, ∼6 Å), $MTSEA^+$ (width, ∼5 Å; Angelow and Yu, 2009), and smaller, potentially channel-permeant reagents such as $[Au(CN)_2]^-$ and $[Ag(CN)_2]^-$ makes SCAM an unrivaled tool for the studies of CFTR's ion permeation pathways. The high water solubility of these reagents, the requirement for ionized cysteine side chain for effective reaction, and the extremely fast reaction rate infer an aqueous environment for the reacted cysteine, and the reactivity patterns can also suggest a secondary structure of the segment of interest. However, like other function-based assays, a positive hit does not guarantee the location of the targeted cysteine in the pore, especially in cases solely dependent on macroscopic current measurements. It is essential and yet oftentimes difficult to exclude the possibility that the positive effect is due to alterations in gating. Nonetheless, a large drop of the macroscopic current is expected if a negative charge is placed into the chloride permeation pathway.

Of note, these unexpected asymmetrical structural features can also serve as a guide for further experimental explorations. For example, five yet-to-be-studied residues (H146, I142, H139, L138, and R134) in TM2, but none in its counterpart TM8, are solvent accessible in the internal vestibule. Furthermore, as these atomic structures of CFTR show that the wider internal vestibule becomes narrower as the permeation pathway ascends toward the external end, one expects far more TMs making contributions to pore construction in the cytoplasmic end than at the periplasmic end of the anion permeation pathway. However, so far, the strongest functional data only support TM1 and TM6 as major players in making up the narrow portion of the pore. Thus, it takes at least one more TM to make the way for the last mile of chloride permeation. The definitive answer to this issue will have to await the solution of an open state, because neither current SCAM data nor available structures are of significant help.

Ion channel proteins have evolved to solve a fundamental problem in every living being: the rapid translocation of ions across the insurmountable energetic barrier of lipid bilayers. For CFTR to work as an effective anion channel, it has to be equipped with the structural characteristics that bestow energetically favorable conditions facilitating every step in the translocation process for an anion. This will include attraction of bulk anions to the cytoplasmic entrance, entry of ions into the pore, sloughing off some of the hydration water molecules to pass through the narrowest region, and final rehydration and exit out of the channel.[2]

This "design" principle for an ion channel is perhaps best exemplified in the crystal structure of the KcsA K^+ channel (Doyle et al., 1998), where negatively charged amino acids located at the entrance of the pore serve as surface charges to concentrate cations around the channel mouth, negative electrostatic dipoles from the pore helices stabilize K^+ ion in the center of the pore, and partial negative charges of the backbone carbonyl oxygen cage multiple K^+ ions in the selectivity filter. Given that the electrostatic charge–charge or charge–dipole interaction is one of the basic laws of the universe, it is reasonable that equivalent design principles should also apply to anion channels. In the absence of an evolutionary pressure for selecting different anions, most anion channels do not need to equip themselves with a highly selective mechanism; they nonetheless do require a mechanism for differentiating anions from cations. Indeed, as discussed above, some positively charged residues, such as K190 (TM3), R248 (TM4), and R370 (TM6), at the cytoplasmic entrance in CFTR may attract chloride from the bulk solution to the channel mouth to ensure a higher chloride conductance through a long-range surface-charge mechanism (El Hiani and Linsdell, 2015). Some charged residues seen within the internal vestibule such as K95, R352, and R303 (Zhang and Chen, 2016; Liu et al., 2017), neutralization of which dampens the single-channel conductance (Aubin and Linsdell, 2006; Cui et al., 2008; Bai et al., 2010; Zhou et al., 2010; El Hiani and Linsdell, 2012, 2015; Norimatsu et al., 2012b; Gao et al., 2013; Zhang and Hwang, 2015), may serve to tune the energetic profile within the internal vestibule to favor the movement of anions from the cytoplasmic entrance to the interior of the pore. As the chloride ion moves into the spatial internal vestibule that is large enough to accommodate ∼180 water molecules (seen in the phosphorylated ATP-bound zCFTR structure; Norimatsu, Y., personal communication), it is likely still fully hydrated and thus won't be stalled by these positively charged residues. Contrary to the idea that these charged side chains serve as individual "anion binding sites" proposed in Linsdell (2017), we think the role of positively charged residues in the internal vestibule is to create a favorable electropositive potential for anions.

If chloride permeation is indeed facilitated and tuned globally by the charged residues along the permeation pathway following the basic laws of electrostatics, it is not surprising that similar electrostatic forces also work on other negatively charged molecules such as channel blockers. Indeed, the K95Q mutation shows dramatically weakened blocking effects of $[Au(CN)_2]^-$, SCN^-, and $C(CN)_3^-$ (Rubaiy and Linsdell, 2015). Furthermore, mutations of K95 were also reported to weaken the blocking effects of 4,4-dinitrostilbene-2,2-disulfonic acid, lonidamine, 5-nitro-2-(3-phenylpropylamino)benzoate (NPPB), or taurolithocholate-3-sulfate (Linsdell, 2005). Similarly, R303Q or R303C, R248Q, and K370Q weaken the inhibitory effects of suramin and 4,4-dinitrostilbene-2,2-disulfonic acid (St. Aubin et al., 2007; Li et al., 2018). Glibenclamide block is weakened by the neutralization mutations within the internal vestibule such as K95Q, R303Q, R303C, or R352C (Linsdell, 2005; St. Aubin et al., 2007; Bai et al., 2010; Zhang and Hwang, 2015). As the anion translocation—for chloride or large organic anions—is a continuous process and is deemed to be affected by the local electrostatic potential in the internal vestibule, the apparent affinities of anionic blockers are inevitably affected by charge manipulations along their path. Without better evidence, it is inappropriate to assign these charged residues as definitive binding sites for chloride ions or anionic blockers (compare Linsdell, 2005; Rubaiy and Linsdell, 2015). As the internal vestibule of the phosphorylated ATP-bound zCFTR can accommodate a plethora of water, we consider the whole internal vestibule as one "anion binding site" where the relatively electropositive potential stabilizes the presence of a fully hydrated chloride ion in CFTR's internal vestibule—a picture emulating the hydrated potassium ion in the central cavity of the KcsA K^+ channel (Doyle et al., 1998).

Another important role assumed by the positively charged residues in the pore is to neutralize the negatively charged side chains that may pose unfavorable local energetic profile for anion permeation. For instance, Cui et al. (2008) reported that the decreased single-channel amplitude by the R352E mutation was reversed by R352E/D993R, suggesting a local charge network between TM6 and TM9. The cryo-EM structures indeed show that R352 and D993, two conserved amino acids, mutations of

[2]At a physiological concentration of chloride ions (∼150 mM) immersed in an abundance of water molecules, it is strategically important that chloride ions are attracted to the entrance of the pore before entering into the internal vestibule. Then, the pore should be equipped with a favorable energy profile to attract the ion toward the internal vestibule and move it along to the narrow segment where some of the water molecules have to be stripped from the hydration shell to fit the dimension of the "selectivity filter." The energy penalty due to dehydration is paid by the intricate interactions between the dehydrated ions and the side chain or backbone of amino acids in this region. During the whole translocation process, proper chemical mechanisms need to be in place to avoid stalling of ion movement. For instance, a fixed charge (i.e., arginine or lysine) is useful to attract chloride, but the electrostatic force could be too strong if it is placed in a narrow region when chloride is mostly dehydrated. On the other hand, negatively charged side chains in the pore (especially near the narrow segment of the pore) may electrostatically repel chloride ions and hence should be neutralized by positively charged residues (e.g., the E92–K95 salt bridge in hCFTR). To speed up the exit of chloride from the selectivity filter, it may be necessary to have two close-by chloride binding sites in the selectivity filter region, where the resulting electrostatic repulsion could destabilize ion binding.

which are associated with CF, reside on a similar horizontal level in the internal vestibule. Although this charged pair is separated by a distance of 14.7 Å in the hCFTR structure, and 13.7 Å in the newly solved structure of phosphorylated ATP-bound zCFTR (Zhang et al., 2017), biochemical studies show that they can be cross-linked by a lengthy cross-linker when mutated to cysteines (Das et al., 2017). In addition, supporting a role of this charge–charge interaction in gating, neutralization of R352 decreases the P_o (Cui et al., 2008).

Although examining the positions of charged residues in the pore, we also noticed an intra-helical salt bridge between E92 and K95 in TM1 (Fig. 6 B). Because E92 is positioned at a region where the internal vestibule becomes fairly narrow in dimension, it seems critical to neutralize this negative charge to ensure a fast anion movement across the pore. Previous studies indeed showed a drastic decrease of the single-channel amplitude by the K95S or K95Q mutation (Zhou et al., 2010; El Hiani and Linsdell, 2012). The functional importance of this charged pair is further testified to by the fact that E92K is pathogenic (Gené et al., 2008), but a rigorous study on this mutant is missing. Collectively, an energetically favorable profile for anion movement in the pore requires a balanced and well-tuned cross talk involving multiple charged residues along the permeation pathway, although different charged residues may play different functional roles in gating, permeation, or even protein folding/maturation.

Functionally important residues in the extracellular domain

SCAM and site-directed mutagenesis have also been used to identify functionally relevant residues on the extracellular side of CFTR. To date, these studies have identified a few externally accessible residues in TM1 (Gao et al., 2013) and TM3 (Norimatsu et al., 2012a), TM5 (Zhang and Hwang, 2015), TM6 (Smith et al., 2001; Beck et al., 2008; Fatehi and Linsdell, 2008; Alexander et al., 2009; Norimatsu et al., 2012a), TM9 (Norimatsu et al., 2012a), TM11 (Fatehi and Linsdell, 2009; Wang et al., 2014a), and TM12 (Norimatsu et al., 2012a; Table S1). Compared with the results from SCAM experiments with internally applied thiol-specific reagents, many fewer positive hits on the external side of the channel suggest that the extracellular vestibule, if it exists, is much shallower than the internal vestibule. We also noted that in many cases, introducing a bulky negatively charged adduct in these "positive hits" only decreases the macroscopic current <50% (e.g., A107C in TM1, A326C and L323C in TM5, and T1121C, S1118C, and T1115C in TM11; Gao et al., 2013; Wang et al., 2014a; Zhang and Hwang, 2015). In contrast, much larger effects were observed only for a few positions in TM1 (e.g., I106C and Y109C) and TM6 (e.g., R334C, I336C, and T338C; Norimatsu et al., 2012a; Gao et al., 2013). Without further experimental evidence, we should be cautious in assigning the role of TM5, 9, 11, and 12 in the construction of the external portion of the pore.

Sequence alignment and homology modeling have also identified a few conserved positively charged residues on the extracellular part of CFTR. Several studies show that neutralization mutations of R104 (TM1), R117 (TM2), R334 (TM6), or K335 (TM6) reduce the single-channel amplitudes and may cause an inward rectification of the I-V relationship (Smith et al., 2001; Zhou et al., 2008). In addition, abundant evidence supports an electrostatic role of R334 (and perhaps K335) in promoting chloride conductance. For instance, independent SCAM studies not only corroborate the idea that TM6 lines the whole length of the anion permeation pathway (Bai et al., 2011; Norimatsu et al., 2012a) but also suggest R334 as a pore-lining residue (Fatehi and Linsdell, 2008; Alexander et al., 2009; Norimatsu et al., 2012a). As a closed-state conformation, the cryo-EM structures may provide limited molecular insights into the constituents of the external portion of the pore. It is nonetheless worth noting that the positively charged side chains of R104, R117, R334, and K335 are all oriented away from the central axis of the protein in three cryo-EM structures (Fig. 4 B). These observations, plus the fact that the internal vestibule makes up the largest part of the pore with little room for a major contribution from the extracellular residues to the pore construction, lead us to propose that the external pore entrance is sitting on a shallow "vestibule" with some of the aforementioned positively charged residues serving in the role of concentrating chloride ions to the pore.

Some of the external charged residues have also been shown to be important for CFTR gating. For instance, Cui et al. (2014) reported that D110R, E116R, and R117A mutations dramatically reduced the P_o by decreasing the open burst duration. They also provided evidence for electrostatic interactions between D110 and K892, as well as between R117 and E1126 (Cui et al., 2014). Indeed, in the cryo-EM structure, D110, E116, and R117 are located at the external surface of CFTR, but without the open-channel structure that reveals the relative positions of these residues, it is difficult to assign the functional roles of these potential charge–charge pairs. Nonetheless, in the cryo-EM structure of hCFTR (Liu et al., 2017), the distances between R117 and E1126 and between E116 and R104 are 14.6 Å and 12.4 Å, respectively (Fig. 4 B). The equivalent pairs in zCFTR are also widely separated by 10.7 Å and 10.5 Å, respectively, in unphosphorylated zCFTR (Zhang and Chen, 2016), and 9.5 Å and 11.7 Å, respectively, in phosphorylated zCFTR (Zhang et al., 2017).

One obvious limitation with the current cryo-EM structures is that they do not reveal the conformational details of the external portion of an open pore so that some of the positions shown to be functionally relevant do not find a clear mechanistic explanation (Table S1). In addition to the charged residues discussed above, the case in point here includes residues T338 in TM6 and I106 in TM1 identified by SCAM studies (Norimatsu et al., 2012a; Gao et al., 2013) as the accessibility limit for channel impermeant thiol-reagent $MTSES^-$ applied from the extracellular side. They are actually buried deeply in the protein core in the cryo-EM structures. This discrepancy, as well as many that will be elaborated on below, begs for answers that probably will be granted once the structure of CFTR's open state is solved. Nonetheless, as the phosphorylated zCFTR structure suggested an unexpected contribution of the external segment of TM8 to gating and external pore construction (Zhang et al., 2017), it seems urgent to gather functional data on this long-neglected TM.

Location of CFTR's gate

In the absence of a high-resolution open-channel structure, we can only rely on data from functional studies to get a rough picture of an open pore. Both SCAM and classical biophysical

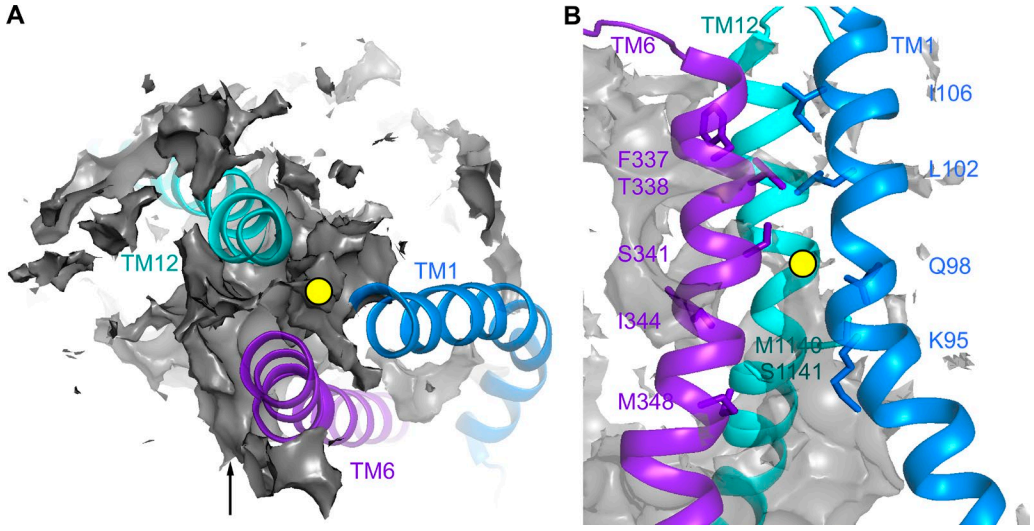

Figure 7. **Narrow region of the internal vestibule largely contributed by TM1, TM6, and TM12. (A)** Top view of the narrow region of the internal vestibule lined by TM1, TM6, and TM12. The external end of the internal vestibule is indicated with a yellow dot as in Fig. 4. Marine, TM1; deep purple, TM6; and cyan, TM12. Arrow indicates the lateral entrance between TM4 and TM6. **(B)** Lateral view of the alignment of TM1, TM6, and TM12 contributing to the narrow region. Residues are shown as sticks and labeled in the same color as the TMs. Of note, the yellow dot is in close proximity to S341 in TM6 and L102 in TM1, both of which define the internal limits of the narrowest region of the pore from SCAM studies.

experiments suggest a narrow region that may serve at least as a size filter between the shallow external vestibule and the large internal vestibule (Hwang and Kirk, 2013; Linsdell, 2014a, 2017; Sohma and Hwang, 2015). On the one hand, by externally applying bulky MTS reagents, external accessibility limit positions (i.e., the external edge of the narrow region) are identified as I106 in TM1 and T338 in TM6. On the other hand, internal applications of the same reagents have identified positions that serve as the internal accessibility limit at L102 in TM1 and S341 in TM6. This alignment of internal and external edges of the narrow region in the pore at TM1 and TM6 is further supported by experiments using the strategy of cross-linking a pair of cysteines. Gao and Hwang (2016) show that cysteine pairs such as L102C/S341C, L106C/F337C, A107C/F337C, and A107C/T338C can be coordinated by Cd^{2+}. On the contrary, S1141C in TM12 coordinates Cd^{2+} with K95C and M348C, positions two helical turns internal to L102 and S341, respectively (Zhou et al., 2010; Gao and Hwang, 2016). This close alignment between residues in TM1 and TM6 is also supported by the results that cysteine pairs Q98C/I344C and K95C/I344C form disulfide bonds in the presence of the oxidizing agent copper(II)-o-phenanthroline (Wang et al., 2011). Indeed, the current cryo-EM structure of CFTR confirms the close distance between L102 and S341 (9.1 Å) with L102 buried in the protein core and S341 positioned at the internal limit of the water accessible area in the internal vestibule (Fig. 7 B). Although, based on SCAM data, the internal accessibility limit residues such as I215 in TM3 (Norimatsu et al., 2012a; El Hiani et al., 2016), G241 in TM4 (El Hiani and Linsdell, 2015), F311 in TM5 (Zhang and Hwang, 2015), V1010 in TM9 (Norimatsu et al., 2012a), S1118 in TM11 (Wang et al., 2014a), and M1140 in TM12 (Alexander et al., 2009; Bai et al., 2011; Qian et al., 2011) also contribute to the pore formation (Table S1), none of these residues are close to L102 or S341 in the three cryo-EM structures. Thus, if we accept the idea that the accessibility limits structurally define the points where the ion permeation pathway becomes physically constricted, the narrowest segment of the pore in CFTR might also be constructed asymmetrically with TM1 (not TM7) and TM6 (not TM12), making major contributions. However, the cryo-EM closed-state hCFTR structure does show a close association of TM12 with TM1 and TM6 at the narrowest point of the internal vestibule (Fig. 7). One possibility to resolve this apparent contradiction is that gate opening involves motions that move TM12 away from the narrowest segment of the pore.

The SCAM studies using positively charged reagents such as $MTSET^+$ and Cd^{2+} also provide some surprising insights: as they can readily reach residues sitting deep in the internal vestibule (e.g., S341 in TM6 and L102 in TM1), or positions at the external edge of the narrow region (e.g., T338 in TM6), the narrow region itself must be able to exclude these cations but allow small anions to pass by. In other words, the narrow region should play a key role in differentiating cations from anions. We can take one step further: to be differentiated from cations, permeating anions should be dehydrated to some degree before entering the narrow region. In this regard, only anions with radii similar to those of chloride ions (3.6 Å) such as NO_3^- and HCO_3^- are permeant within this narrow region that spans one helical turn (T338–S341 in TM6). Hence, we propose that the narrowest region of CFTR's pore serves as both a size filter and a charge filter. This latter idea is supported by some mutational studies. For instance, mutations of F337 lead to a loss of the characteristic lyotropic selectivity sequence for various anions with different hydration energy (Linsdell et al., 2000). Furthermore, mutations of S341 or T338 significantly but L102 weakly alter the permeation properties of CFTR (Linsdell et al., 1998; Linsdell, 2001; McCarty and Zhang, 2001; Negoda et al., 2017).

The functionally defined narrow segment of the pore (i.e., between T338 and S341 in TM6) also may be the exact location (or part) of the gate as proposed by Gao and Hwang (2015). Using the

channel-permeant thiol probe $Au[CN]_2^-$, which has a size similar to chloride (Smith et al., 1999), Gao and Hwang (2015) showed that I334C, F337C, and T338C (residues external to the narrow region) are only reactive to internal $Au[CN]_2^-$ in the presence of ATP but not in the absence of ATP (see Fig. 7 B for relative position), whereas a substituted cysteine engineered at position 344 one helical turn internal to the narrow region can be modified, albeit with a much slower rate, in the presence or absence of ATP. These results suggest an ATP-controlled gate located between I344 and T338 in TM6. Indeed, when we followed the water-accessible space of the internal vestibule in all three closed-state cryo-EM structures, we found that the whole extracellular part of the TM6 above S341 is not exposed to the intracellular space. Therefore, contrary to the idea that a single amino acid, F337, may serve in the role of a gate (Corradi et al., 2015; Zhang and Chen, 2016), it is likely that when the "gate" opens, a short segment of TM6 (and perhaps other TMs too) will be reexposed to the aqueous pore. Consistent with this picture, T338C also reacts faster with externally applied $Au[CN]_2^-$ in the open state. Hence the same segment in the pore plays the critical roles of the selectivity filter and the gate.

Here we have used mostly our own data to pinpoint the location of the gate. But this picture of selectivity filter and gate colocalized at the more external end of TM6 and TM1 (and likely other TMs) contradicts some of the functional studies reported by Linsdell's laboratory. Although some studies including ours showed clear accessibility demarcations at S341 and T338 for internally and externally applied MTS reagents, respectively (Table S1), El Hiani and Linsdell (2010) reported that F337C, T338C, and S341C can be modified by both internal and external MTS reagents. Wang et al. (2014a) also reported that T1115C and S1118C in TM11 are modifiable by the bulky $MTSES^-$ reagent from either side of the membrane. To explain this unusual reactivity pattern, they proposed a more cytoplasmic gate (internal to I344 in TM6) and a more externally located size filter at T338 in TM6 (El Hiani and Linsdell, 2014). In their model, the external vestibule expanded in the closed state with F337, T338, S341, T1115, S1118, and I1132 becoming more accessible from the external side. However, the external part of the closed-state cryo-EM structure does not assume a typical vestibule, and F337, S341, T1115, S1118, and I1132 are not accessible from extracellular side (Table S1). Furthermore, their hypothesis that the gate is internal to I344 also suggests that Q98, S341, N1138, and M1140 should reside in a region that is external to the closed gate. In contrast, all four residues are exposed to the internal vestibule in the cryo-EM closed-state structures (Table S1). Moreover, in a recent cross-linking study of engineered cysteine pairs (L333C/G1127C and I106C/G1127C) located on the external edges of TM1, TM6, and TM12 (Wang and Linsdell, 2012b; Negoda et al., 2018), the authors proposed that the extracellular parts of these TMs are close together in the closed states as seen in the cryo-EM structures, but separate apart from each other in the open states. This latest picture seems more in line with the idea that the gate resides closer to the external end of TMDs discussed in the previous paragraph.

Unresolved functional data await more structures

Although most of the pore-lining residues identified from functional studies are consistent with those lining the internal vestibule of the pore in the cryo-EM structure of hCFTR, careful examination of the cryo-EM structure reveals two major categories of discrepancies between functional results and structural data (Table S1).

First, several residues reported as not lining the pore from the SCAM studies are widely exposed to the aqueous environment according to the solvent accessible surface view of the cryo-EM structure in the unphosphorylated apo form of hCFTR. These include the residues on the cytoplasmic parts of TM3 (S185, S182, V181, Q179, G178, and I177; El Hiani et al., 2016), TM4 (A238, R242, and D249; El Hiani et al., 2016), TM6 (G366, Y362, Q359, V358, F354, and V350; Norimatsu et al., 2012a; El Hiani et al., 2016), TM9 (D985; Norimatsu et al., 2012a), and TM12 (S1159, R1158, S1155, and I1151; Norimatsu et al., 2012a; Table S1). One possible explanation for these discrepancies is that in SCAM studies, modifications of cysteines introduced in these positions do not affect channel function. It is also possible that a large conformational change upon PKA-dependent phosphorylation and channel opening happens in the cytoplasmic portion of the pore. Comparing the accessibilities of the aforementioned residues between unphosphorylated and phosphorylated zCFTR, some of the aforementioned residues in TM3 (S185, S182, V181, Q179, G178, and I177), TM4 (R242 and D249), TM6 (G366, Q359, and V358), TM9 (D985), and TM12 (S1159, S1155, and I1151) are indeed less exposed to the aqueous environment in the phosphorylated zCFTR (Table S1). Thus, this apparent discrepancy actually supports the notion of a narrowing of the internal vestibule upon PKA phosphorylation and NBD dimerization (Bai et al., 2011; Zhang and Hwang, 2017), if we accept the idea that the internal vestibule structure of phosphorylated zCFTR with dimerized NBDs indeed resembles that of an open state.

The cryo-EM structures also offer an opportunity to examine some of the discrepancies in SCAM studies of TM1. For example, E92, K95, and Q98 in TM1 are largely exposed to the aqueous pore in all three structures. However, Wang et al. (2011) reported that Q98C cannot be modified by $MTSES^-$ in the unphosphorylated state, a conformation likely to be similar to the reported cryo-EM structure (Liu et al., 2017). In contrast, Gao et al. (2013) showed that after being fully phosphorylated, K95 and Q98 are only accessible in the open state and not accessible in the closed state. This state-dependence of accessibility is also inconsistent with the cryo-EM data summarized in Table S1 that the side chains of E92, K95, and Q98 are exposed to the aqueous environment in all three structures.

Second, a few residues reported in functional studies as pore-lining are not exposed to the aqueous environment in the cryo-EM structure (Table S1). These include L102 (Wang et al., 2011; Gao et al., 2013), I215, G213, and F191 (Norimatsu et al., 2012a), I344 (Alexander et al., 2009; Bai et al., 2010; El Hiani and Linsdell, 2010; Norimatsu et al., 2012a), F337 (Fatehi and Linsdell, 2008; Alexander et al., 2009; El Hiani and Linsdell, 2010; Norimatsu et al., 2012a), T339 and I340 (Alexander et al., 2009; Norimatsu et al., 2012a), V1010, A1009, V1008, G1003, I1000, L997, and P988 (Norimatsu et al., 2012a), S1118, T1115, and I1112 (Wang et al., 2014a), S1150 (Bai et al., 2011), V1147 (Bai et al., 2011; Qian et al., 2011; Norimatsu et al., 2012a), and D1154 (Norimatsu et al., 2012a). Although some of these discrepancies

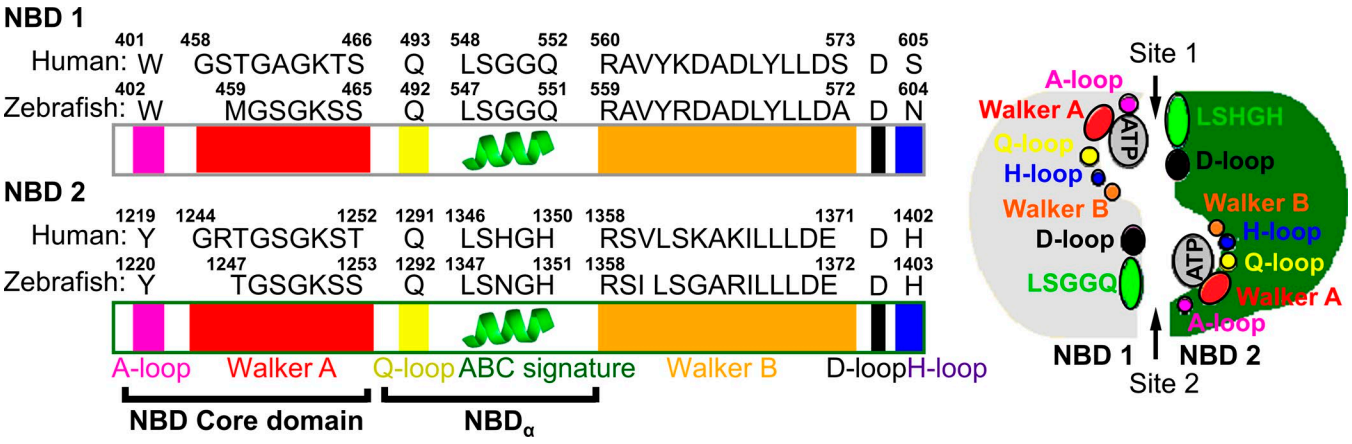

Figure 8. **Conserved sequences and motifs in CFTR's NBDs.** Left: a cartoon depicting the relative positions of the conserved motifs in NBD1 and NBD2 with the characteristic motifs highlighted in different colors. The color code is also used for the cartoon on the right showing the head and tail subdomains of NBDs with two ATP molecules sandwiched in the dimer interface.

can be attributed to the limitation of SCAM,[3] especially when one relies solely on macroscopic mean current measurements, it is also possible that the residues identified in SCAM studies may line the pore only in the open state, but the cryo-EM structures so far solved are all closed states. Supporting this latter notion is the result with L102 in TM1. Gao et al. (2013) shows at a single-channel level that L102C can be modified by internal MTS reagents in a state-dependent manner, but in all three cryo-EM structures, this amino acid is buried in a region inaccessible from either side of the membrane. Hence, opening of a phosphorylated CFTR should be associated with a conformational change that renders this particular residue (and likely others) accessible from the cytoplasmic end of the pore.

CFTR's gating machinery NBDs and TMD–NBD interfaces

Numerous electrophysiological and biochemical studies in the past two decades have established a working mechanism by which the NBD engine uses the energy of ATP binding and hydrolysis to drive the conformational changes in TMDs that open and close CFTR's gate (Sohma and Hwang, 2015). Although the atomic details of the TMDs in the cryo-EM structures offer exquisite molecular insights into CFTR's pore and gate, the resolution of NBDs, unfortunately, is not high enough to reveal molecular details (Zhang and Chen, 2016; Liu et al., 2017; Zhang et al., 2017). However, previously solved crystal structures of the two isolated NBDs in hCFTR (Lewis et al., 2004, 2005; Atwell et al., 2010) can serve as a template for the construction of the structural model. In this section, we set our aims to (a) briefly review the roles of NBDs in controlling CFTR gating, (b) discuss possible functional roles of the interfaces between NBDs and TMDs, (c) debate an important controversy: whether a complete separation of the NBD dimer is required for gate closure, and (d) examine the functional significance of the newly solved zCFTR structure (Zhang et al., 2017). Understanding the coupling mechanism for CFTR gating is expected to bear far-reaching ramifications as all ABC transporters share the same engine.

Conserved structures of NBDs

Although the structurally conserved NBDs are the universal components in all members of the ABC transporter superfamily, there exists a variation on the theme: not all ABC proteins possess two catalysis-competent ATP-binding sites (Davidson and Chen, 2004; Aller et al., 2009; Rees et al., 2009). Regardless of the capability of ATP hydrolysis, all NBDs in ABC proteins, including CFTR's two NBDs, shared canonical architectures (Fig. 8): an ATP-binding core subdomain and an α-helical (NBDα) subdomain (Lewis et al., 2004, 2005). The core subdomain, also known as the "head" subdomain, includes (a) an A loop, in which W401 (W402) in hNBD1 (zNBD1) and Y1219 (Y1220) in hNBD2 (zNBD2) form π-electron interactions with the adenine ring of ATP; (b) the Walker A motif (GXXGXGKS/T, with X being any residue); (c) the Walker B motif (ΦΦΦΦDE, Φ representing a hydrophobic residue); and (d) the switch regions (Q loop and H loop). The α-helical (or "tail") subdomain, named after the predominant α-helices in this part of NBD, contains the conserved signature sequence (LSGGQ in NBD1 but LSHGH in NBD2 of hCFTR) that defines this family of proteins.

Crystallographic studies on swaths of ABC proteins (Hung et al., 1998; Hopfner et al., 2000; Karpowich et al., 2001; Yuan et al., 2001; Smith et al., 2002; Chen et al., 2003) have led to a proposition that ATP serves as a molecular glue that affixes two NBDs into a head-to-tail configuration (Fig. 8). Two ATP molecules are hence sandwiched at the NBD dimer interface. In addition to the base-stacking interaction between the A loop and the

[3]Two strategies were used to isolate the open-state modification from the closed-state modification. In Bai et al. (2010), the state-dependent modification protocol allows measurements of the apparent modification rates in the absence or presence of ATP. This protocol was adopted from experiments done on voltage-gated K^+ channels (Liu et al., 1997). Together with the P_o value, the real modification rates in the open state and the closed state can be calculated (Bai et al., 2011; Gao et al., 2013; Zhang and Hwang, 2015). A different strategy of measuring the modification rate in the open state is to introduce a hydrolysis-deficient mutant such as E1371Q (Linsdell, 2014b) or K1250A together with the mutant of interest or to use nonhydrolytic ATP analogue PP_i (El Hiani and Linsdell, 2015) to lock open the channel so as to increase the P_o close to unity in the presence of ATP, assuming that the hydrolysis-deficient mutation does not alter the accessibility of the mutant of interest. This latter method is somewhat problematic since the difference in P_o between locked open channels and native channels is too small (usually less than twofold) to compensate for the high variability intrinsic to SCAM. Moreover, the assumption that abolishing ATP hydrolysis by altering E1371 in a mutant background guarantees a P_o close to unity is problematic (e.g., Yu et al., 2016). Therefore, once this strategy is used, the P_o of resulting constructs should be rigorously assessed for a more accurate interpretation of the experimental data.

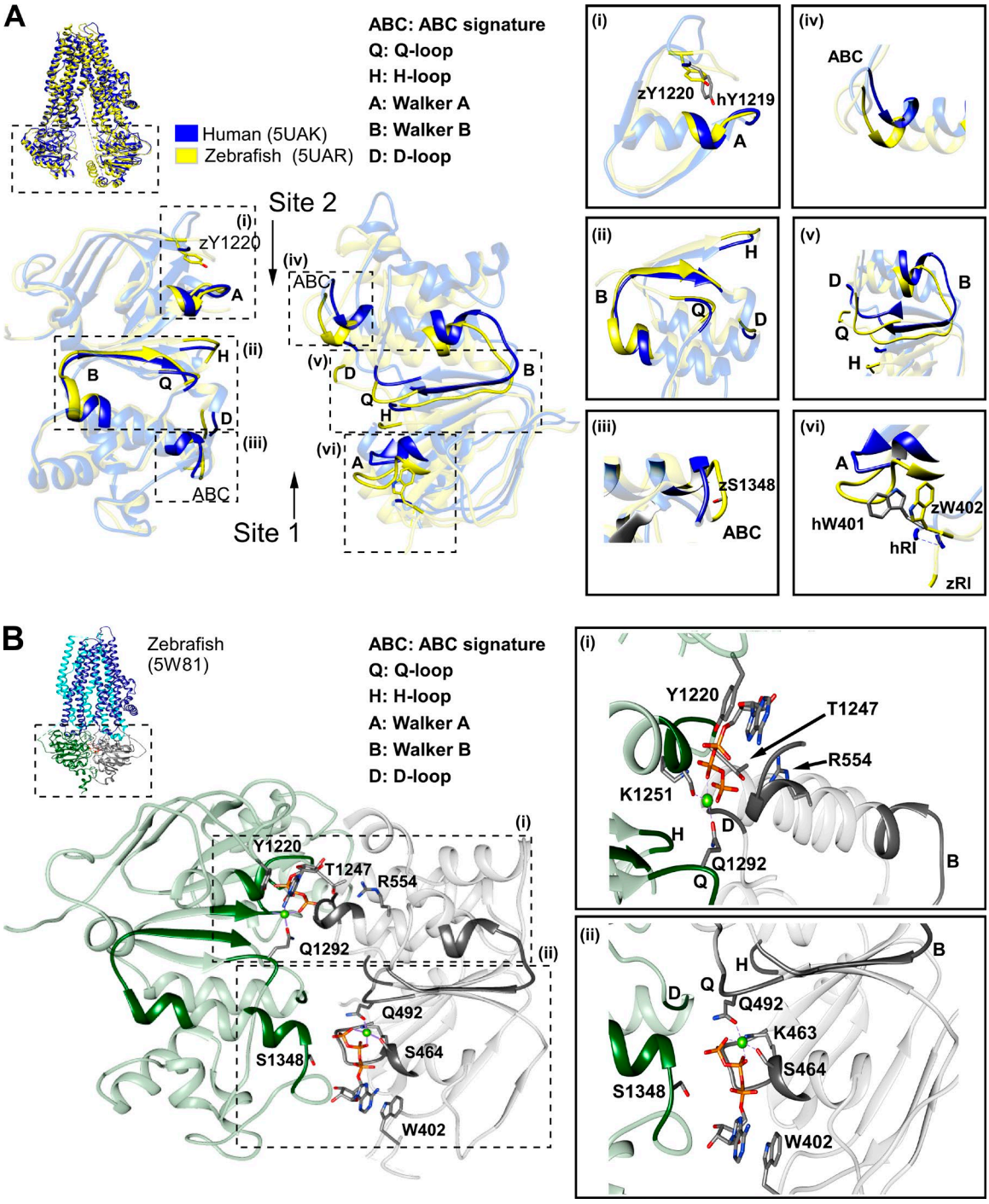

Figure 9. **Conformational changes of NBDs in CFTR. (A)** Widely separated NBDs in unphosphorylated CFTR. Top left: Superimposed cryo-EM structures for hCFTR (blue; Protein Data Bank [PDB] accession no. 5UAK) and zCFTR (yellow; PDB accession no. 5UAR). Bottom: Top view of NBDs. All conserved motifs are labeled as ABC, ABC signature sequence; Q, Q loop; H, H loop; A, Walker A; B, Walker B; and D, D loop. Right: magnified views of those labeled i–vi in the top view. **(B)** Phosphorylated E1372Q-zCFTR (PDB accession no. 5W81). The catalytic glutamate E1372 (E1371 in hCFTR) was mutated to glutamine to abolish ATP hydrolysis in site 2. Top left: cryo-EM structure of zCFTR (PDB accession no. 5W81; TMD1 in blue; TMD2 in cyan; NBD1 in gray; NBD2 in green). Bottom: Top view of NBD. Right: i and ii are magnified images showing the interactions between conserved motifs and ATP in dimeric NBDs.

adenine ring of ATP, the Walker A lysine stabilizes the β and γ phosphates of ATP and the Walker B aspartate coordinates Mg^{2+}, a cofactor for ATP hydrolysis, in the head subdomain of one NBD. On the side of the tail subdomain in the partner NBD, the signature sequence LSGGQ motif provides hydrogen bond donors to further stabilize ATP binding. This canonical structure feature of NBD dimer, demonstrated functionally for CFTR (Kidd et al., 2004; Vergani et al., 2005; Mense et al., 2006), was verified in the new cryo-EM structure of zCFTR in Zhang et al. (2017). However, the two ATP-binding sites in CFTR are inherently asymmetric (Figs. 8 and 9). Only site 2 hydrolyzes ATP; site 1 is catalysis incompetent partly because of a lack of the catalytic glutamate,

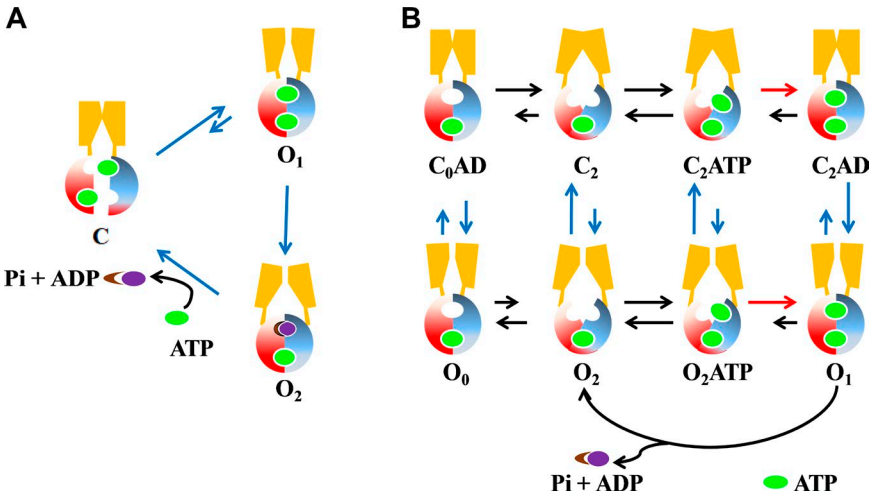

Figure 10. **Two gating models for CFTR. (A)** Strict coupling scheme: The strict coupling model adopted from Liu et al. (2017) dictates that the gating cycle is strictly coupled to the ATP hydrolysis cycle. The opening of the channel is initiated by the formation of NBD dimer, and terminated by dimer disruption triggered by ATP hydrolysis. Of note, although in this model the NBDs are completely separated in the closed channel conformation (state C), a different thesis was proposed in Csanády et al. (2010) where the NBD dimer is not completely separated in the closed state. **(B)** Energetic coupling mechanism proposed in several previous studies (Jih and Hwang, 2012; Lin et al., 2014, 2016). This model follows the classical allosteric modulation principle that the conformational change in one domain facilitates the conformational change in the other domain. Note subtle shape change in TMDs between O_1 and O_2 (see text). Pi, inorganic phosphate.

and the canonical H-loop histidine. Perhaps because of this deficit in ATP hydrolysis, ATP can remain bound for minutes in site 1 as demonstrated biochemically (Aleksandrov et al., 2002b; Basso et al., 2003). In the apo forms of CFTR (Zhang and Chen, 2016; Liu et al., 2017), the two sites are separated to a different degree (Fig. 9 A; see Fig. 2 in Liu et al., 2017). Interestingly, even in the newly solved zCFTR structure with dimeric NBDs (Zhang et al., 2017), site 1 and site 2 exhibit different degrees of "tightness" (Fig. 9 B): whereas the γ phosphate of ATP in site 2 interacts intimately with both the head and the tail subdomains, much weaker interactions were seen for the site 1 ATP (see Fig. 4 in Zhang et al., 2017). This structural asymmetry may also explain different degrees of exposure of the residues in these two sites to the aqueous environment (Fig. 9 B and Fig. 11). For example, the side-chain hydroxyl group of the conserved serine in the signature sequence of site 2 (S548 in zCFTR, or S549 in hCFTR) forms hydrogen bonds with both β and γ phosphate groups of ATP. In contrast, this hydrogen bond network is missing in site 1 (S1348 in zCFTR, or S1347 in hCFTR). Of note, biochemical studies on P-glycoprotein indeed suggest the existence of two different NBD dimeric conformations: one with two ATP molecules bound and the other with only one ATP occluded (Sauna and Ambudkar, 2007).

Roles of NBDs in CFTR gating

Once the R domain is phosphorylated by PKA, robust activity of CFTR requires a continuous presence of MgATP (Anderson et al., 1991; Nagel et al., 1992). Several review articles have thoroughly discussed the gating mechanism of CFTR (Gadsby et al., 2006; Hwang and Sheppard, 2009; Jih and Hwang, 2012; Hwang and Kirk, 2013; Sohma and Hwang, 2015); our readers are encouraged to get a more comprehensive view in those reviews. To avoid too much repetition, here we just briefly summarize some generally accepted theories and focus our discussion on two contested issues: (1) whether the gating cycle and the ATP hydrolysis cycle are tightly coupled, resulting in a one-to-one stoichiometry and (2) whether gate closure requires a complete separation of the NBD dimer.

As a member of the ABC transporter superfamily, CFTR may share with its cousins not only common structural characteristics but also the mode of action. For technical reasons, structural studies of ABC transporter proteins are way ahead of that of CFTR. By comparing ATP-bound and ATP-free forms of ABC proteins, it is proposed that two NBD–TMD complexes undergo a flip-flop motion fueled by ATP binding-induced NBD dimerization and ATP hydrolysis-driven separation of NBDs (Chen et al., 2003; Higgins and Linton, 2004). This flip-flop motion causes the TMDs to switch back and forth between an inward-facing and an outward-facing conformation to expose the substrate binding site alternately to the intracellular and extracellular milieus, necessary steps for a complete transport cycle. Such a highly coordinated movement, when applied to the gating motion of CFTR, projects a strict coupling between the gating cycle and ATP hydrolysis cycle in CFTR. Indeed, elegant single-channel kinetic analysis of the open time distribution provides evidence for such a coupling mechanism (Csanády et al., 2010) that echoes an earlier idea championed by Gunderson and Kopito (1995). In this latter study, it was shown that WT CFTR exhibits two distinct open states that differ in single-channel amplitudes (smaller O_1 and larger O_2). Analysis of gating patterns reveals a predominant $C \rightarrow O_1 \rightarrow O_2 \rightarrow C$ (relative to $C \rightarrow O_2 \rightarrow O_1 \rightarrow C$), a phenomenon violating microscopic reversibility and hence demanding an input of free energy. Because eliminating ATP hydrolysis abolishes the $O_1 \rightarrow O_2$ transition, Gunderson and Kopito (1995) proposed that this transition is associated with ATP hydrolysis. It follows that each opening/closing cycle is coupled to the hydrolysis of one ATP (Fig. 10 A).

But a different theory of the coupling mechanism for CFTR gating was proposed by Jih et al. (2012). By using nonhydrolyzable nucleotide analogues as "baits" to capture a short-lived posthydrolytic state, they provided experimental evidence for the existence of a posthydrolytic open state with site 2 already vacated. Subsequently, they found a CFTR mutant, R352Q, that exhibits similar ATP hydrolysis-dependent transitions between two open states O_1 and O_2 (Jih et al., 2012). Consistent with the observations in Gunderson and Kopito (1995), most of the opening bursts in R352Q show a preferred transition $C \rightarrow O_1 \rightarrow O_2 \rightarrow C$, but repeated cycles ("reentry" events) of the $O_1 \rightarrow O_2$ transition before gate closure were observed. These data lead to a model that depicts nonstrict coupling between ATP hydrolysis and gating

with a probabilistic relationship between NBD dimerization and gate opening (Fig. 10 B).

Interestingly, discernable O_1 and O_2 states can be seen in a variety of mutations around a local charged network involving R303, R352, and D993 in the internal vestibule (Zhang and Hwang, 2017). This latest study, together with the cryo-EM structures pinpointing the location of these residues, suggests that altering local potential in the internal vestibule confers this O_1O_2 phenotype. However, exactly how perturbations of this local charge network result in a hydrolysis-dependent change in chloride permeation awaits further studies. Nonetheless, these data do suggest that some conformational changes occur in TMDs after ATP hydrolysis but before gate closure. If we assume that the O_1 state represents an open-channel configuration in the TMDs with dimerized NBDs, the O_2 state should represent a different open-channel configuration in the TMDs that is associated with posthydrolytic NBDs. Taking one step further, supposing ATP hydrolysis is indeed the driving force that separates two tightly associated NBDs as proposed in ABC proteins (Smith et al., 2002; Vergani et al., 2005; Ward et al., 2007; Oldham et al., 2008; Hwang and Sheppard, 2009; Rees et al., 2009), it seems reasonable to deduce that the posthydrolytic O_2 state possesses at least transiently separated NBDs at site 2 (the O_2 state in Fig. 10 B). This then raises the question of whether the lateral entrance between TM10 and TM12 described in the pore section may be conductive to chloride in the posthydrolytic open state, as the separation of NBDs at site 2 likely will exert some structural perturbation at this very location. The cryo-EM structures solved so far, although this question cannot be answered directly, could serve as a guide for further exploration into the physiological role of this presumed nonfunctional lateral entrance.

Although these studies may suggest an open state with (partially) separated NBDs, a recent study on R117H (Yu et al., 2016), a pathogenic mutation that is associated with the mild form of CF (Sheppard et al., 1993; Hämmerle et al., 2001), provides solid evidence for the existence of a closed state with dimerized NBDs. Gating of R117H is ATP dependent, but in contrast to WT CFTR with a long opening burst that is interrupted occasionally by very brief closures (Fig. 2 B), R117H shows opening bursts within which fairly long closed events are seen. This gating anomaly together with a much prolonged interburst results in a reduced P_o (Yu et al., 2016). The most intriguing observation is that abolition of ATP hydrolysis by the E1371Q mutation, like that in the WT background, drastically prolongs the opening burst duration, but contrary to a P_o of ∼0.9 under the WT background, the P_o of R117H/E1371Q double mutant is ∼0.1, a result of abundant closures in a "lock-open" event. If we accept the generally held idea that the lock-open state represents a CFTR structure with a stable NBD dimer, this observation in R117H suggests the existence of both open and closed conformations in TMDs, whereas the two NBDs stay bound (O_1 and C_2AD states, respectively, in Fig. 10 B), which means the gate can close when NBDs are in a dimeric form. To our knowledge, this closed state with an NBD dimer has not been formally incorporated into the strict coupling model (compare Zhang et al., 2017; also see below). In contrast, in the recent study by Sorum et al. (2017), the R117H mutation only shortens the open burst duration with little effect on the interburst closed time, leading to a different conclusion that the sole effect of this mutation is to destabilize the open state. The reason for this discrepancy is unknown and should be addressed in the future, but one possible reason is that the experiments in Sorum et al. (2017) were performed in a hydrolysis-deficient background (D1370N) with the R domain removed.

The two models mentioned above connote different interpretations on the structure of phosphorylated, ATP-bound zCFTR (Fig. 9 B) reported lately by Zhang et al. (2017). Based on the strict coupling model, Zhang et al. (2017) proposed that this state represents a "post-open" closed state, i.e., the normally short-lived flicker closed state buried in an opening burst. It was also speculated that the single-channel amplitude of hCFTR is underestimated because of incessant visits to this state once the channel opens and the limited bandwidth of the recording system. In contrast, this closed state with dimerized NBDs is inherent in the energetic coupling model as a "pre-open" closed state (C_2AD in Fig. 10 B). Of note, in the absence of electrophysiological data on zCFTR, here we liberally interexchange structure/function data and interpretations between hCFTR and zCFTR. This practice could be problematic because it is known that different CFTR orthologues, even with highly conserved amino acid sequences, exhibit very functional properties, such as an altered anion selectivity sequence in *Xenopus laevis* CFTR (Price et al., 1996), a different pattern of channel gating in mouse CFTR (Scott-Ward et al., 2007), and a different ATP-dependent effect in sheep CFTR (Cai et al., 2015). Although much-needed functional studies of zCFTR will definitely shed more light on this important and yet unresolved issue on CFTR gating, the sheer existence of a closed state with a canonical NBD dimer raises an intriguing question one needs to entertain: Can this very state hydrolyze ATP? The molecular details revealed in the cryo-EM structure suggest an affirmative answer, but it has been assumed for years, regardless of the specific gating model, that ATP hydrolysis only occurs in the open state.

Does gate closure require a complete separation of NBDs?

In the cryo-EM structure of unphosphorylated human and zCFTR (Zhang and Chen, 2016; Liu et al., 2017), the two NBDs are widely separated (Fig. 9 A), and the TMDs are in a closed conformation. The study by Liu et al. (2017) also presented functional evidence for a multistep activation process during phosphorylation-dependent activation of CFTR: spontaneous slow dislodging of the R domain followed by PKA-dependent phosphorylation and subsequent ATP-dependent opening of the channel through NBD dimerization. The issue apropos phosphorylation-dependent activation has been well covered in the R domain section; here we will focus on the question of whether a complete separation of CFTR's two NBDs is required for gate closure.

Several electrophysiological studies have suggested that NBDs do not dissociate completely upon gate closing (Tsai et al., 2009, 2010; Szollosi et al., 2011). Instead, it is the separation of NBDs at site 2 that is coupled to gate closure, whereas site 1 remains connected. In contrast, the necessity of a complete separation of NBDs for channel closure is proposed by Chaves and Gadsby (2015). By showing that cysteine placed at the signature

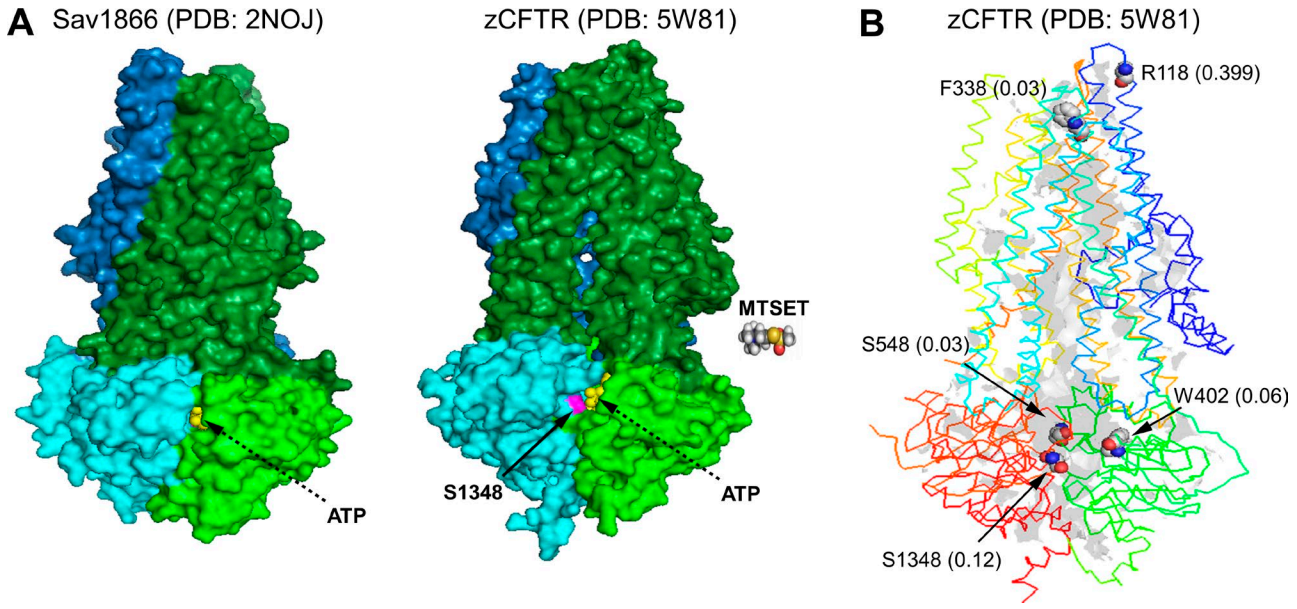

Figure 11. **Accessibility of the NBD dimer interface. (A)** Structural comparison between Sav1866 (left) and CFTR (right). The structures are presented in space-filling model. As a prototypical ABC exporter in an outward-facing conformation, Sav1866 (Protein Data Bank [PDB] accession no. 2ONJ) shows a complete coalesce of the transmembrane helices at the junction between its TMDs (green and blue) and NBDs (lime and cyan). In contrast, a clear gap representing the lateral entrance to the pore is seen in the structure of zCFTR with dimerized NBDs (PDB accession no. 5W81). Yellow marks the bound ATP, and target residues S1348 (equivalent to S1347 in hCFTR) and S548 (S549 in hCFTR) as space-filling spheres in purple. The equivalent residues in Sav1866 are completely buried in the NBD dimer. In contrast, although S548 in site 2 is buried in zCFTR, S1348 is exposed. This analysis suggests that MTSET (labeled as space-filling sphere), even much larger reagents such as MTS-rhodamine, may be able to access the S1348C through the lateral entrance, which is unique to CFTR, an ion channel, not a transporter. **(B)** Solvent-accessible surface in the cryo-EM structure of zCFTR (PDB accession no. 5W81). The solvent-accessible regions were assessed by molecular visualization software PyMOL. The residues were labeled with numbers that indicate relative accessibilities. (The range of 0–1 is used to rank the accessibility: 0, hardly accessible; 1, highly accessible.)

sequence of site 1 (S1347 in hCFTR or S1348 in zCFTR) or site 2 (S549 in hCFTR or S548 in zCFTR) can be modified by bulky MTS reagents after gate closure, Chaves and Gadsby (2015) proposed that the separation between NBDs must exceed 8 Å, indicating a complete separation of NBDs. The idea that NBD dimerization can protect these cysteines from modification was based on a structural model of ABC transporters in an outward-facing conformation (Fig. 11 A), which inevitably shows obliteration of the pore by the coalesced transmembrane helices at the junction between NBDs and TMDs. The structure of zCFTR with dimerized NBDs (Zhang et al., 2017) offers an ideal opportunity to examine this issue more closely. Fig. 11 shows that although S548 (S549 in hCFTR) in site 2 is well protected by the NBD dimer, S1348 (S1347 in hCFTR) is at least partially exposed to the aqueous environment instead of burying within the NBD dimer interface (Fig. 11 B). If we assume that this zCFTR structure with dimerized NBD is any close to the conformation of the open state, it is then not surprising that a cysteine engineered at the dimer interface in site 1 could be accessible to modification even in the open state. Indeed, Cotten and Welsh (1998) showed that modification of the cysteine placed at the signature sequences by *N*-ethylmaleimide does not seem to be state dependent. Some more rigorous tests are needed to resolve this issue.

But what about the closed-state structures of unphosphorylated zCFTR and hCFTR showing two widely separated NBDs (Zhang and Chen, 2016; Liu et al., 2017)? Doesn't this structure support the notion that closure of the channel is associated with a complete separation of CFTR's two NBDs? It should be noted that the two solved CFTR structures are closed states with an unphosphorylated R domain sitting between two NBDs and TMDs. Once the phosphorylated R domain is out of the way so that conformational changes in TMDs and NBDs can occur to open the gate, the closing from this yet-to-be-solved phosphorylated open state is unlikely to sojourn directly to an unphosphorylated closed state. Thus, solving the cryo-EM structures has not helped resolve this controversial issue regarding the fundamental mechanism of CFTR gating. It can be further argued that if the gate can close even when NBDs remain dimerized as in the phosphorylated ATP-bound zCFTR structure (Zhang et al., 2017), a conformational change involving a drastic movement of the two TMD–NBD complexes as depicted in Fig. 10 A may not be necessary for gate closure.

NBD–TMD interfaces

As the gate of CFTR's pore is located closer to the external end of the TMDs, the signal of molecular motions in NBDs after ATP binding must be transmitted through a long distance along the vertical axis of the channel. The simplest scenario borrowed directly from the ABC transporters is to treat each TMD–NBD complex as a rigid body. Before ATP binds, two TMD–NBD complexes are separated at the cytoplasmic end as in the apo form of CFTR (Fig. 9 A). ATP binding to two NBDs triggers lateral motion of the two TMD–NBD complexes converting an inward-facing to an outward-facing conformation

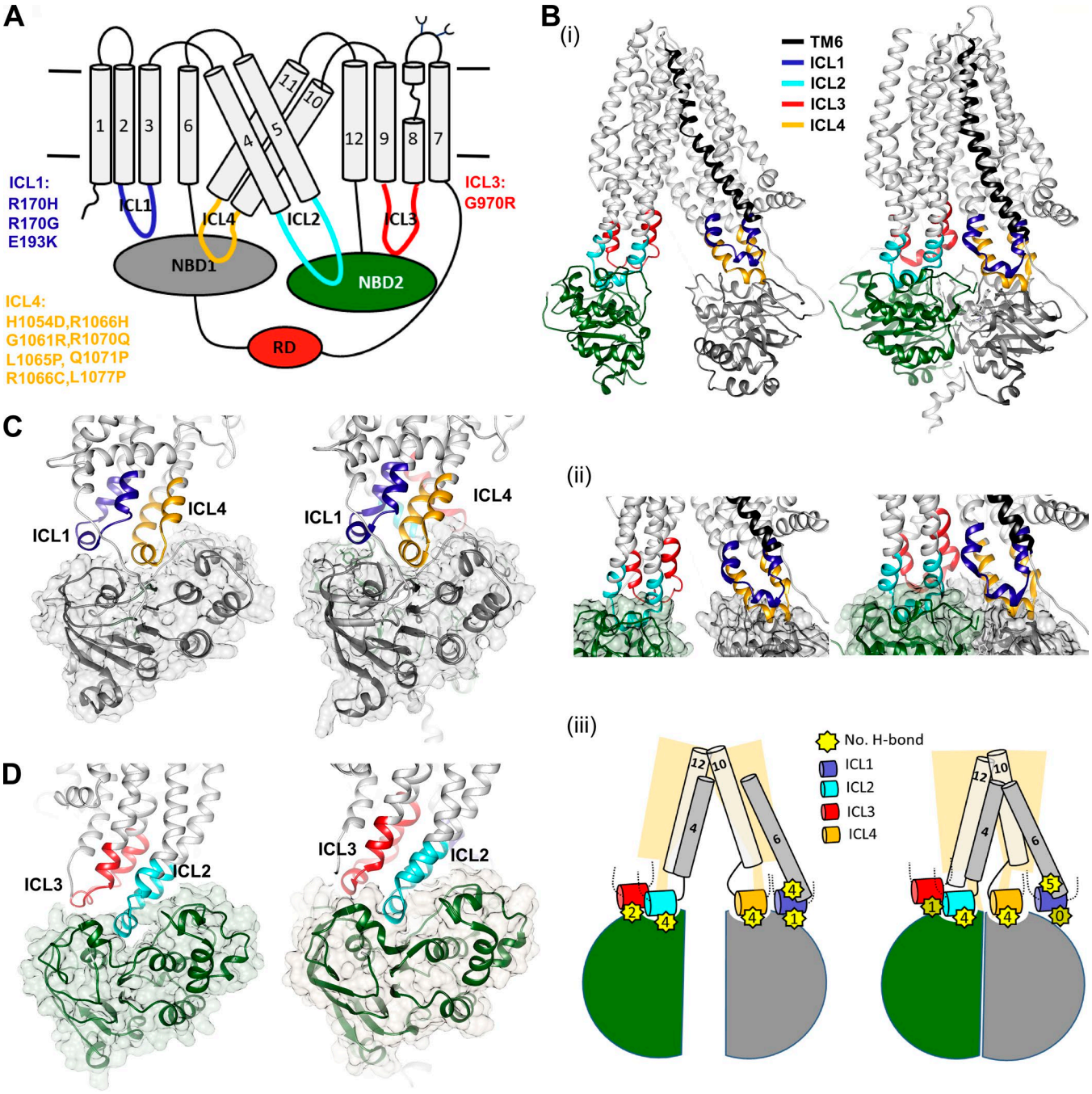

Figure 12. **Molecular interactions at TMD–NBD interfaces. (A)** CFTR topology showing its 12 TMs (1–12), two NBDs (gray, NBD1; green, NBD2), the R domain, and interfaces between ICL1 and ICL4). Note the two ball-and-socket joints are between ICL2–NBD2 and ICL4–NBD1. Labeled residues next to each ICL are mutations that cause a severe form of CF. **(B)** (i) Locations of the four ICLs in the cryo-EM structures of CFTR (Protein Data Bank [PDB] accession nos. 5UAR and 5W81). Left: unphosphorylated zCFTR (PDB accession no. 5UAR). Right: phosphorylated ATP-bound zCFTR (PDB accession no. 5W81). The color codes of ICLs are the same as those in A (blue, ICL1; cyan, ICL2; red, ICL3; and orange, ICL4). (ii) Close-up front view of the ICL–NBD interfaces. The surface views of NBD are shown. (iii) Cartoon depicting the dynamic change of hydrogen bond network upon dimerization. The relative position of each segment is based on the structures of interfaces shown in ii; only TM4, 6, 10, and 12 are shown. Dashed lines mark the regions connecting TMs and their corresponding ICLs. The relatively constant number (shown in the yellow symbols at each interface) of hydrogen bonds before and after NBD dimerization suggests that the ball-in-the-socket interfaces (ICL2–NBD2 and ICL4–NBD1) move in sync with NBD. In contrast, the loose interfaces (ICL1–NBD1 and ICL3–NBD2) lag behind because of many weakened interactions (see text). **(C)** Close-up view of the interfaces between ICL1, ICL4, and NBD1. Left: Unphosphorylated zCFTR (PDB accession no. 5UAR). Right: Phosphorylated ATP-bound zCFTR (PDB accession no. 5W81). **(D)** Similar presentation as C except ICL2, ICL4, and NBD2 interfaces are shown.

that is similar to the one shown in Fig. 9 B. For this scenario to be valid, each TMD and its corresponding NBD have to be connected tightly so they move synchronously. The physiological importance of the junctions between TMDs and NBDs (i.e., ICL1–4 in Fig. 12 A) is testified to by the fact that many CF-causing mutations were found there.

However, the molecular motion during CFTR gating must be somewhat different from that of ABC transporters because the transmembrane helix bundle at the cytoplasmic end of the pore cannot be completely sealed off upon NBD dimerization (Fig. 9, A and B). Specifically, upon NBD dimerization in CFTR, the lateral opening between TM4 and TM6 remains relatively wide (Fig. 9 B). We attempt to see whether examining the TMD–NBD interfaces in CFTR and P-glycoprotein may provide some clues to address the differences in molecular motions between CFTR and ABC transporters.

Similar to those found in ABC transporters, a short helix (so-called coupling helix) in ICL2 (between TM4 and TM5 of TMD1) and one in ICL4 (between TM10 and TM11 in TMD2) are buried in a socket in NBD2 and NBD1, respectively (Fig. 12 B). These conserved ball-in-a-socket assemblies (Oldham et al., 2008), seen in both P-glycoprotein and CFTR, suggest a relatively tight partnership so that as one moves, the other may move synchronously. Some functional data indeed support the notion that the interfaces between both ICL4–NBD1 and ICL2–NBD2 remain relatively tight during the gating cycle (He et al., 2008). Thus, here P-glycoprotein and CFTR may undergo similar conformational transition, in which the coupling helix moves like a ball inside the cleft of the NBD (the socket) to affect the pivot point in the TMD-conformational change (Khare et al., 2009; Jin et al., 2012). However, it is interesting to note that cross-linking cysteines engineered in ICL2 and NBD2 (e.g., C276C and Y1307C or N268C and F1294C) decreases the P_o dramatically (He et al., 2008; Sorum et al., 2015), suggesting some flexibility at this interface is required for normal gating.

Contrary to ICL2–NBD2 and ICL4–NBD1 interfaces, the coupling helices in ICL1 and ICL3 have less contact with NBDs in all three structures of CFTR (Fig. 12, B–D, for zCFTR; see Fig. 2 in Liu et al., 2017 for hCFTR). In fact, these two ICLs do not form ball-in-a-socket assemblies with their corresponding NBDs, but these two loops still interact with ATP-binding sites 1 and 2, respectively (Mornon et al., 2008). A relatively long distance between these ICLs and their partner NBDs casts doubt on the existence of a tight connection at these ICL–NBD interfaces. (This potential disconnect is even more obvious for the ICL1–NBD1 interface; Fig. 12, B–D). Indeed, the contact surfaces of ICL1–NBD1 and ICL3–NBD2 interfaces, calculated with the PDBePISA (Proteins, Interfaces, Structures and Assemblies) service at the European Bioinformatics Institute, are much smaller than those of ICL2–NBD2 and ICL4–NBD1 interfaces. More interestingly, although the total contact areas for ICL2–NBD2 and ICL4–NBD1 interfaces remain relatively unchanged between apo- and ATP-bound zCFTR structures, the contact areas for ICL1–NBD1 and ICL3–NBD2 interfaces decrease in the zCFTR structure with dimerized NBDs. These surface area changes are accompanied by changes in the hydrogen bond network between ICLs and NBDs. For example, the only hydrogen bond between S170 and E473 in ICL1–NBD1 found in apo zCFTR is lost in the ATP-bound structure. It seems difficult to explain these structural changes if TMDs and NBDs are moving as a rigid body. One possibility we envision is that when two ATP-bound NBDs move medially to form a dimer, ICL4–NBD1 and ICL2–NBD2 move more synchronously because of tighter interactions in these two interfaces. But as a result of a weaker interaction in ICL1–NBD1 and ICL3–NBD2 interfaces, ICL1 and ICL3 may not follow NBD motion strictly and thus lag behind when NBDs undergo dimerization (Fig. 12). As ICL1 and ICL3 are intimately associated with TM6 and TM12, respectively, this slippage in NBD motion may constitute the structural basis for the existence of the clefts between TM4–TM6 and TM10–TM12 (cartoon in Fig. 12 B)—the molecular mechanism underpinning the "degraded gate" hypothesis. The structural asymmetry between ICL1–NBD1 and ICL3–NBD2 may also account for the differences in the size of resulting lateral entrances for chloride permeation described in the pore and gate section.

Molecular understanding for disease-associated mutations

Although six different classes of pathogenic mutations have been described based on their molecular mechanisms (Wang et al., 2014b), this section will focus on type III (gating defect) and type IV (conductance defect) as the cryo-EM may shed light on the structural mechanisms explaining these defective functions. In the sections described above, four critical steps are involved in CFTR gating: (1) ATP binding, (2) NBD dimerization, (3) signal transmission from NBDs to TMDs, and (4) movement of TMDs to open the gate. Once the gate opens, chloride ions traverse through CFTR's pore at a rate of >1 million per second. In theory, mutations disrupting any of these events could compromise the channel's ability to function normally and hence cause CF. In this section, we review some of the functional data for 13 representative disease-causing mutations, most of which have been extensively investigated, in important regions of the CFTR molecule.

Mutations in the NBD active sites

Opening of CFTR's gate in TMDs is coupled to ATP binding-induced dimerization of NBDs in a head-to-tail configuration (Vergani et al., 2005). Therefore, it is not surprising that mutations affecting ATP binding or NBD dimerization could impair CFTR gating. Indeed, several pathogenic mutations have been identified in or close to the ATP-binding sites. For example, S1255P, G1244E, S1251N, G551D, and G1349D are all located at the interface between two NBDs (Fig. 13). Specifically, S1251 is a conserved residue in the Walker A motif that directly participates in ATP binding, whereas G1244 and S1255 are just several amino acids apart from this critical motif. Although not all of these mutations have been studied extensively to reveal the detailed mechanism of gating abnormalities, Yu et al. (2012) showed that these mutants respond to VX-770, and Anderson and Welsh (1992) reported a lower apparent affinity of ATP for the S1255P mutant. Otherwise, how exactly G1244E and S1255P mutations cause gating defects awaits further investigation.

Perhaps the most thoroughly studied class III mutation is G551D, located in the signature sequence (or the tail subdomain) of NBD1 and G1349D in the equivalent position of NBD2 (Fig. 8). Cai et al. (2006) showed that both mutants exhibit lower P_o, corroborating the functional importance of the signature sequences in mediating NBD dimerization. Also consistent with the idea that site 2 plays a more significant role than site 1 in controlling CFTR gating, the gating defect associated with G551D located in site 2 is ~10-fold more severe than G1349D, a corresponding mutation in site 1 (Bompadre et al., 2007). More interestingly, sudden

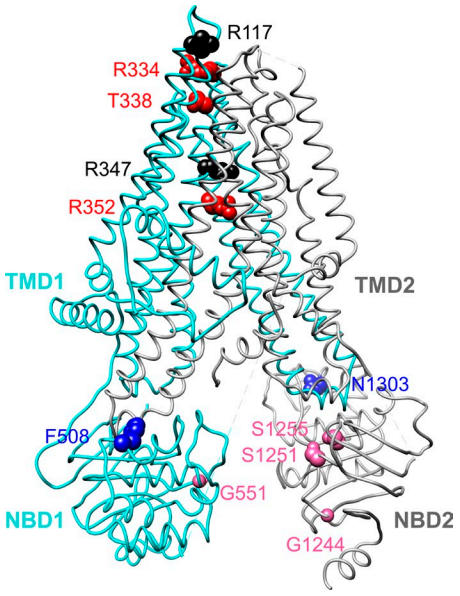

Figure 13. **Locations of pathogenic mutations covered in the current article.** A lateral view of hCFTR structure showing the positions of all disease-associated mutations discussed. Pink, residues in NBDs; blue, residues at NBD–TMD interfaces; red, residues that line the pore; and black, non–pore-lining positions.

removal of ATP after G551D-CFTR channels are activated results in a biphasic response (a fast current rise followed by a slow current decay). Furthermore, a decrease of [ATP] from millimolar to micromolar concentrations causes a paradoxical increase of G551D-CFTR currents. These unique behaviors and other experimental evidence led Lin et al. (2014) to conclude that the mutation converts site 2 to an inhibitory site. As the same phenomenon was seen with G551E, but not in G551S or G551K, it was further proposed that the negative charge of D551 repels electrostatically the negatively charged ATP so that NBD dimerization is prohibited. However, removal of ATP (or lowering the ATP concentration) by eliminating this inhibitory effect allows the two NBDs to undergo spontaneous, albeit slow, dimerization reactions (Lin et al., 2014). The newly resolved structure of phosphorylated zCFTR in the ATP-bound conformation corroborates this proposition, as the residue G551 is physically close to the γ phosphate of bound ATP with its backbone intimately involved in the interactions with the phosphate group (Zhang et al., 2017).

Mutations in the NBDs affecting the NBD–TMD interfaces

For the molecular events happening in the cytosolic NBDs to control gating motion in CFTR's TMDs, the signal of ATP binding-induced dimerization of the NBDs needs to be transmitted to the TMDs via NBD–TMD interfaces. Indeed, using rate-equilibrium free-energy relationship analysis, Sorum and colleagues provided evidence for a signal transmission from NBDs through the NBD–TMD interfaces to the pore (Sorum et al., 2015, 2017). This functional importance of NBD–TMD interfaces is testified to by the fact that many disease-associated mutations were found at these interfaces (Fig. 12 A). Among them, ΔF508 and N1303K, two common mutations that also cause trafficking defects, are well studied. The gating defects caused by the ΔF508 mutation include a P_o of ∼15 times less than WT mostly because of a prolonged closed time (Miki et al., 2010), consistent with the idea that the ΔF508 mutation (Fig. 13) disrupts the interface between NBD1 and TMD2 (He et al., 2008; Mornon et al., 2008; Serohijos et al., 2008). In addition, the ΔF508 mutation also shortens the locked-open time and has a faster ligand-exchange time at site 1 (Jih et al., 2011; Kopeikin et al., 2014), suggesting a destabilization of the NBD dimer by the mutation. Interestingly, the gating defect of ΔF508-CFTR can be completely rectified by high-affinity ATP analogues (Miki et al., 2010) or VX-770 (Van Goor et al., 2009; Kopeikin et al., 2014). In contrast, N1303K, a mutation at the equivalent position of F508 in NBD2, is located at the interface between NBD2 and TMD1 (Fig. 13). In a canonical NBD, this asparagine residue is directly involved in forming a hydrogen bond network with the conserved interfacial Q loop that interacts with bound ATP (Eudes et al., 2005). Residues in the Q loop form part of the NBD–TMD interface (He et al., 2008). Functional studies indeed demonstrated gating abnormalities including increased burst duration and decreased opening rate for N1303K (Berger et al., 2002; Randak and Welsh, 2003, 2005). However, these studies, all performed before the discovery of effective CFTR potentiators, may have underestimated the severity of the gating abnormalities associated with N1303K. More thorough investigations are needed to extract mechanistic insights out of this mutation that resides at a critical position in the NBD–TMD interface.

Mutations in the TMDs

The fundamental role of CFTR's TMDs is to craft a gated pore. Therefore, mutations found in TMDs could affect chloride conductance and/or channel gating. Using cryo-EM structures and functional data as our guide, we categorize disease-associated mutations into pore-lining and non–pore-lining positions.

The first category is the pore-lining mutations such as R334W, T338I, and R352Q. TM6 in the TMDs has been under investigation most comprehensively. The structure/function roles of TM6 have been discussed in the pore section. Not only is TM6 a major component for pore construction, part of TM6 likely also plays a role in gating conformational changes (Bai et al., 2010). For the disease-associated mutations located in TM6, SCAM studies clearly demonstrate that R334, T338, and R352 line the pore. Thus, it is not surprising that R334W and T338I mutations exhibit severe conductance defects so that their single-channel currents are too small to be measured accurately (Sheppard et al., 1993; Linsdell et al., 1998). The tiny single-channel amplitude of these two mutants also precludes assessments of any gating abnormalities. However, considering T338 may be part of the gate in TMDs (Gao and Hwang, 2015), we speculate that the T338I mutation also causes gating defects. In contrast, the R352Q mutation causes a mild conductance defect. Single-channel conductance was reduced from 6.2 pS for WT CFTR to 4.2 pS for R352Q-CFTR (Guinamard and Akabas, 1999). Thus, this moderate reduction of single-channel conductance is by itself insufficient to cause CF; gating defects were reported for this mutation (Cui et al., 2008). In addition, transepithelial chloride transport through R352Q-CFTR is increased dramatically by the CFTR potentiator VX-770 (Van Goor et al., 2014), indicative of a gating defect caused by the mutation.

The second category is the non–pore-lining mutations like R117H and R347P/H. The R117H mutation is usually associated with mild-form CF (Sheppard et al., 1993). The single-channel conductance of R117H-CFTR is ∼25% less than WT CFTR (Sheppard et al., 1993; Yu et al., 2016). Because R117 is located in the first extracellular loop (ECL1) between TM1 and TM2, it was proposed that one reason R117H has diminished conductance may be that the positively charged arginine serves in the role of attracting anions to the entryway of the external vestibule (Zhou et al., 2008; Cui et al., 2014). Regardless of how the R117H mutation causes conductance defects, a 25% reduction of the conductance cannot explain its pathogenesis. Indeed, in excised membrane patches, the P_o for R117H is ∼10-fold lower than WT (Yu et al., 2016). Interestingly, however, no gating defect was found for R117H in reconstituted lipid bilayers (Hämmerle et al., 2001). This discrepancy could be reconciled if R117 actually interacts with the head group of membrane phospholipids. The position as well as the side-chain protrusion of R117 does support this conjecture.

R347 was proposed to be an anion binding site in CFTR's pore (Tabcharani et al., 1993), but SCAM studies fail to verify a pore-lining role for this amino acid (Alexander et al., 2009; Bai et al., 2010; El Hiani et al., 2016). The cryo-EM structures show that R347 (or R348 in zCFTR) is not exposed to the internal vestibule; instead, it is buried in the protein core interacting with D924 (or E932 in zCFTR) in TM8. This salt bridge, first suggested by Cotten and Welsh (1999), may play a role in stabilizing the pore architecture. Thus, the R347H and R347P mutations affect single-channel conductance by disrupting the pore. Because the single-channel conductance of R347P-CFTR was reported to be 30% of WT (Sheppard et al., 1993), this mutant likely exhibits multiple dysfunction including mild trafficking defects (Van Goor et al., 2014).

Although the resolved cryo-EM structures represent a static snapshot of the channel in the closed state, they allow us to conceptualize how structural deviations introduced by disease-causing mutations in functionally important regions of CFTR might lead to dysfunction in gating or permeation. Integration of more functional data with new insight from the emerging CFTR structures should grant us an in-depth understanding of the molecular pathophysiology of CF and may provide the means for structure-based drug design.

Structural mechanisms of CFTR pharmacology

Cloning of the CFTR gene (Riordan et al., 1989) has made it possible to develop expression systems for studying the function of CFTR at a molecular level, unveiling the fundamental defects associated with pathogenic mutations, and using high-throughput drug screening techniques to discover small molecules that can modulate CFTR function. The last endeavor is especially important because although loss-of-function mutations cause CF, secretory diarrhea resulting from hyperactivity of CFTR as a result of bacterial toxins inflicts more mortality and mobility in the developing world (Bhattacharya, 1995; Barrett and Keely, 2000; Al-Awqati, 2002). Great strides have been made in the past decades in developing CFTR modulators (Amaral and Kunzelmann, 2007; Cai et al., 2011; Hanrahan et al., 2013; Rowe and Verkman, 2013). Some of the CFTR modulators have been successfully implemented in clinics (e.g., ivacaftor and lumacaftor), but the availability of high-resolution structures of CFTR now ushers in a new era for structure-based drug design. In this section, we will elaborate on the actions of different CFTR modulators (Fig. 14), including correctors that improve CFTR trafficking, potentiators that increase the P_o of CFTR, and pore blockers and inhibitors that may affect gating or permeation.

CFTR correctors

Many disease-associated mutations of CFTR, including the most prevalent ΔF508 mutation, cause folding defects that lead to a reduction of functional CFTR proteins expressed on the cell surface (Denning et al., 1992; Lukacs et al., 1993; Du et al., 2005; Thibodeau et al., 2010). Compounds that increase the delivery of mature CFTR to the cell membrane are known as CFTR correctors. The readers are referred to recent reviews for detailed discussions (Amaral and Kunzelmann, 2007; Lukacs and Verkman, 2012; Rowe and Verkman, 2013). VX-809 (lumacaftor; Fig. 14 A), one of the ingredients in Orkambi that was approved by the U.S. Food and Drug Administration for the treatment of CF patients carrying the ΔF508 mutation, has been extensively studied (Van Goor et al., 2011; He et al., 2013; Loo et al., 2013; Ren et al., 2013), but exactly where it binds remains unclear. According to docking simulations performed with a homology model of ΔF508-CFTR (He et al., 2013), a hydrophobic pocket formed in the NBD1–ICL4 interface because of the deletion of residue F508 was identified as a potential binding site for VX-809. However, it seems difficult to use this idea to explain why VX-809 also increases the surface expression of WT CFTR or mutants other than ΔF508 (Van Goor et al., 2011). Furthermore, evidence also showed that TMD1 is the shortest-length fragment of CFTR required for the action of VX-809 (Ren et al., 2013), arguing against a role of NBD1–ICL4 interface in forming the binding site for VX-809. A different binding site for VX-809 was lately proposed (Rusnati et al., 2018). Using molecular dynamic simulation and surface Plasmon resonance, they showed that three residues in the NBD1, Y577, V580, and E655, anchored VX-809 through hydrogen bonds. Future functional studies may be required to validate these binding modes predicted by computer simulation.

In addition to VX-809, many experimental CFTR correctors have been developed and it has been shown that combinations of different correctors could have additive or synergistic effects (Bridges et al., 2010; Lin et al., 2010). This is perhaps not surprising as the ΔF508 mutation causes multiple biochemical defects, including not only misfolding of NBD1, where the F508 is located, but also the disruption of the interaction between NBD1 and ICL4, which subsequently impairs domain assembly of CFTR (Du et al., 2005; Thibodeau et al., 2005; Cui et al., 2007; Rosser et al., 2008; Du and Lukacs, 2009; Hoelen et al., 2010). A combination of correctors with different mechanisms of action is thus required to restore ΔF508-CFTR biogenesis, whereas correction on folding of NBD1 alone is insufficient (Mendoza et al., 2012; Rabeh et al., 2012). The idea of combination therapy was validated by Okiyoneda et al. (2013), who showed that surface expression of ΔF508-CFTR partially corrected by VX-809 can be further improved by other correctors to rectify its stability defects in NBD1 and NBD2, highlighting the importance of combination

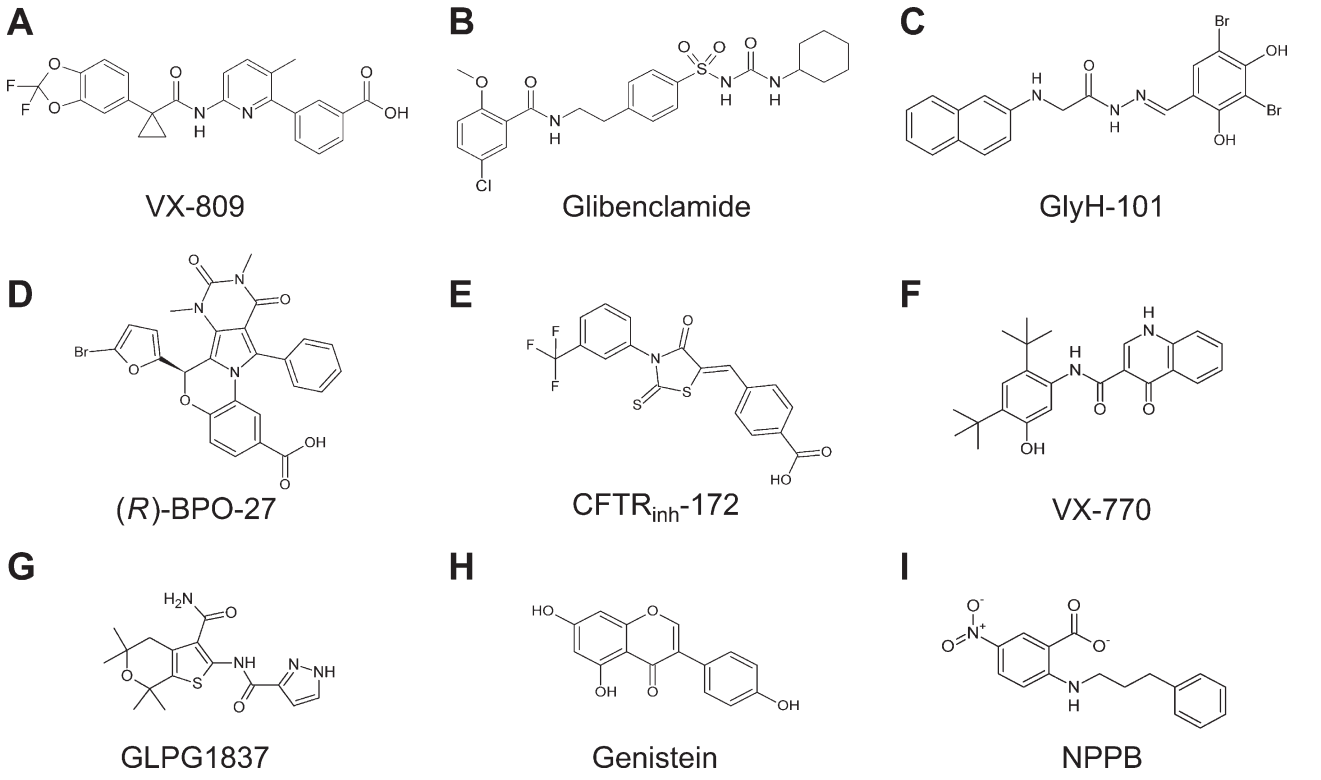

Figure 14. **Chemical structures of representative CFTR modulators. (A)** CFTR corrector. **(B and C)** Pore blocker. **(D and E)** Gating inhibitor. **(F–I)** CFTR potentiators.

therapy in repairing the mutant protein. Although more mechanistic studies on the mechanism of CFTR correctors are warranted, if their actions entail interactions with incompletely folded CFTR or other proteins involved in CFTR maturation, solving the atomic structure of CFTR in its mature form may not be immediately useful for the development of CFTR correctors.

Blockers and inhibitors

As described above, both functional and structural data indicate that the internal vestibule of CFTR is wide enough for a variety of large organic anions (e.g., glibenclamide; Fig. 14 B) serving as channel blockers (Schultz et al., 1996; Sheppard and Robinson, 1997; Gong et al., 2002; Zhou et al., 2002; Linsdell, 2014a). The large size of the internal vestibule seen in the cryo-EM structure may account for the fact that the chemical structures of internal blockers vary a lot, except for the negative charge they possess. A lack of specificity also explains why so far we have not found internal blockers with nanomolar affinity. However, there is a general principle that hydrophobic blockers are more potent than hydrophilic ones (e.g., Zhou et al., 2002). The structure–activity relationship for internal blockers also provides insights into their interactions with the CFTR protein. For example, extensive studies of the sulphonylurea hypoglycemic agent glibenclamide, and the nonsulphonylurea hypoglycemic agents including mitiglinide and meglitinide, suggest that the sulphonylurea moiety and benzamide groups of glibenclamide interact respectively with two different sites in CFTR (Cai et al., 1999; Cui et al., 2012). Cui et al. (2012) further proposed that multiple residues along TM6 and TM12 are involved in binding of the sulphonylurea end of glibenclamide. However, mutagenesis studies done by other groups have identified K95 (Linsdell, 2005) and R303 (St. Aubin et al., 2007) as possible binding sites for channel blockers working from the intracellular side of CFTR. Docking simulation also supports the idea that K95 is a critical and common binding site for several internal blockers including glibenclamide (Dalton et al., 2012). However, as alluded to in the pore section above, these positively charged amino acids (i.e., K95 and R303) sitting in a wide vestibule are likely well shielded by water molecules or negatively charged amino acids (e.g., K95 and E92) to avoid trapping of chloride in its permeation path. Neutralization of positive charges in the internal vestibule is expected to affect the local electropositive energy profile and subsequently impede the movement of anionic blockers into the pore. These positively charged amino acids do not necessarily have to be the binding sites. By the same token, mutations on TM6 and TM12 are also expected to influence the electrostatic profile of charged amino acids along the permeation pathway and thus affect the movement of internal blockers. As the blockade of CFTR by large organic anions exhibits a high voltage dependence, it is likely that these blockers will travel transiently through the internal vestibule and subsequently lodge at a deeper location of the pore (Zhang and Hwang, 2017). As discussed below, we speculate that the wide lateral entrance and spatial internal vestibule revealed in the cryo-EM structure of CFTR's phosphorylated closed state may not undergo a drastic change in the open-channel conformation. However, solving the open-state structure will no doubt lay the foundation for developing more potent CFTR blockers.

Contrary to the internal blockers described above, the external entrance of CFTR's pore seems fairly resistant to blockade by large anions (Zhou et al., 2002). GlyH-101 (Fig. 14 C) is the only blocker that seems to occlude the pore from the extracellular side (Muanprasat et al., 2004; Norimatsu et al., 2012b). A possible binding site for GlyH-101 was proposed at the external end of the pore where the charged head of GlyH-101 lies close to F337 and T338 residues with its hydrophobic tail inserted into the pore (Norimatsu et al., 2012b). As described in the pore section, SCAM studies indeed showed that both F337 and T338 are pore-lining residues in the open-state conformation of CFTR (Linsdell, 2006; Bai et al., 2010). In contrast, in all three cryo-EM structures of CFTR's closed state, the proposed binding site for GlyH-101 is obstructed by the side chains of the surrounding amino acids. Thus, a rearrangement of the TMDs must occur upon gate opening so that the binding site for GlyH-101 is exposed to the anion permeation pathway. Interestingly, this scenario also suggests a state-dependent binding of GlyH-101 to CFTR, which has yet to be demonstrated.

Unlike pore blockers, there are other small molecules that reduce CFTR currents by interfering with CFTR gating. For example, (*R*)-benzopyrimido-pyrrolo-oxazine-dione (Fig. 14 D) inhibits CFTR gating by competing with ATP in the NBDs (Snyder et al., 2013; Kim et al., 2015). On the other hand, $CFTR_{inh}$-172 (Ma et al., 2002), a thiazolidinone derivative (Fig. 14 E), exerts its inhibitory effect on CFTR gating through an unknown binding site (Taddei et al., 2004; Kopeikin et al., 2010). Although site-directed mutagenesis studies have identified the conserved R347 in TM6 as an important residue for the action of $CFTR_{inh}$-172 (Caci et al., 2008), comparing the effect of $CFTR_{inh}$-172 on CFTR orthologues that respond to $CFTR_{inh}$-172 differently, Stahl et al. (2012) argue that the binding site is more likely located elsewhere in the CFTR. Our own kinetic studies provide evidence that $CFTR_{inh}$-172 can bind to both the open and closed states (Kopeikin et al., 2010). More interestingly, binding of $CFTR_{inh}$-172 does not inhibit CFTR, an observation that excludes a direct pore blocking mechanism; instead, an additional step (conformational changes) after binding leads to inhibition. Perhaps the most unique feature of $CFTR_{inh}$-172 is that dissociation of $CFTR_{inh}$-172 is drastically slowed down when CFTR's two NBDs are locked into a stable dimeric configuration, suggesting that $CFTR_{inh}$-172 actually binds more tightly in a closed state with an NBD dimer (Kopeikin et al., 2010). With more and more atomic structures of CFTR becoming available down the road, we are optimistic that the molecular mechanism of $CFTR_{inh}$-172 will be unveiled in the near future.

CFTR potentiators

For obvious reasons, tremendous efforts have been devoted to finding small molecules that can enhance the function of CFTR ever since the CFTR gene was identified (Hwang and Sheppard, 1999; Rowe and Verkman, 2013; Jih et al., 2017). This search paid off almost a decade ago when a highly potent and efficacious reagent, VX-770 (ivacaftor; Fig. 14 F), was discovered through high-throughput screening and a series of structural optimizations (Van Goor et al., 2009). Successful clinical trials soon led to U.S. Food and Drug Administration approval for human use (Accurso et al., 2010; Ramsey et al., 2011). Although the original use of VX-770 was for patients carrying the third most common disease-associated mutation, G551D, VX-770 was eventually approved to treat a wide spectrum of mutations causing gating defects of CFTR (Yu et al., 2012; Carter et al., 2015).

Although the mechanism of action for VX-770 on CFTR gating has been well characterized (Eckford et al., 2012; Jih and Hwang, 2013), the exact binding site for VX-770 remains unknown. Our recent studies at least exclude the R domain and NBD2 as the target for VX-770 (Yeh et al., 2015) and suggest that the binding site for VX-770 resides at the interface between membrane lipids and the TMDs of CFTR (Jih and Hwang, 2013) based on its hydrophobic property and the similar potentiating effects from intracellular and extracellular application. Supporting evidence from small-angle x-ray scattering shows that VX-770 can penetrate the lipid bilayer and predominantly accumulates in the internal leaflet (Baroni et al., 2014). Although there is still limited information about the binding sites for a CFTR potentiator, it is interesting to note that many CFTR potentiators share limited structural similarities (Yang et al., 2003; Pedemonte et al., 2005; Rowe and Verkman, 2013). However, a newly developed CFTR potentiator, GLPG1837 (Fig. 14 G), and VX-770, despite their structural differences, share the same mechanism of action, probably through binding to the same site in CFTR (Yeh et al., 2017), but GLPG1837, compared with VX-770, has a higher efficacy but a lower potency. This latest study also reveals a state-dependent binding of GLPG1837: tighter binding to the open state than the closed state. Thermodynamic analysis of the state-dependent binding of GLPG1837 using a classical allosteric modulation scheme supports the notion that the potency of a CFTR potentiator is determined by the absolute binding affinity of the drug to the CFTR protein, whereas the efficacy is decided by the difference in binding affinities between the closed state and the open state (Yeh et al., 2017). The state-dependent idea also bears a practical implication for drug development: using two potentiators binding to different sites not only enhances the overall efficacy (pharmacological synergism) but also mutually improves their individual potency. As the high-affinity VX-770 is much more hydrophobic than GLPG1837, it is also suggested that the binding site for these CFTR potentiators likely possesses hydrophobic amino acids. With the high-resolution structures of CFTR's TMDs resolved by cryo-EM, the next exciting step is to use this powerful technique to identify the binding sites for these clinically useful drugs. The resulting structural and functional insights may help design better medicines for the treatment of CF.

Not all potentiators share the same mechanism of action; there are potentiators whose chemical structures are very different from VX-770 and GLPG1837. For instance, ATP analogues that bind to the normal ATP binding sites in NBDs with higher affinity have been shown to gate CFTR better than the natural ligand ATP (Aleksandrov et al., 2002a; Zhou et al., 2005; Cai et al., 2006; Bompadre et al., 2008; Miki et al., 2010). The well-known CFTR potentiator genistein is another example (Fig. 14 H). Genistein is the first potentiator shown to target the CFTR protein directly (French et al., 1997; Hwang et al., 1997; Weinreich et al., 1997). Genistein is distinct from VX-770 and GLPG1837 in that it has a bell-shaped dose–response relationship, suggesting at least two binding sites with opposite effects on CFTR: a

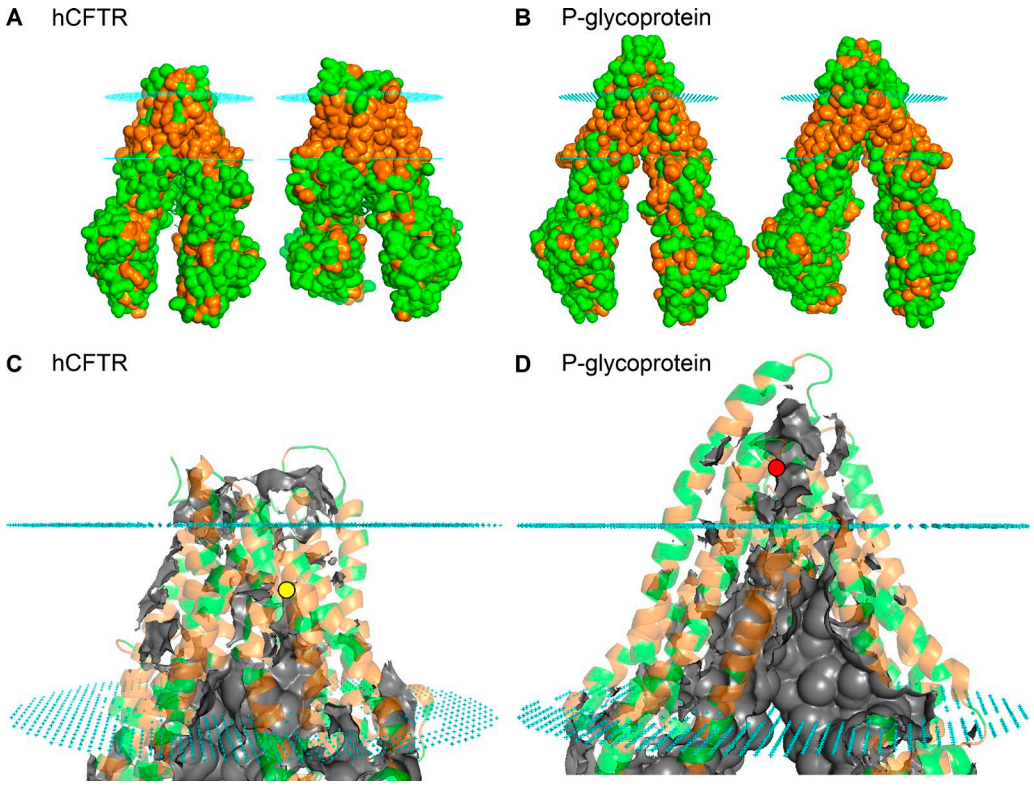

Figure 15. **Comparison of hCFTR and P-glycoprotein oriented within the lipid bilayer. (A)** Lateral view of hCFTR (Protein Data Bank [PDB] accession no. 5UAK) after being oriented within the membrane (left: front view as shown in Fig. 4 A; right: back view). **(B)** Lateral view of P-glycoprotein (PDB accession no. 4KSB) after being oriented within the membrane (left: front view; right: back view). Orientation of proteins in membrane was processed with the Orientations of Proteins in Membranes (OPM) database provided by the University of Michigan. Whole proteins are green with the hydrophobic residues in gold. Lipid bilayers are shown in cyan dots. The two dotted surfaces in each panel depict the boundaries of a whole membrane with a hydrophobic thickness of 31.4 ± 0.6 Å in A and 29.8 ± 1.3 Å in B. The cleft of the lateral entrance of CFTR is sealed so that the deeper part of the internal vestibule is well protected by surrounding TMs from being exposed to the lipid bilayer (31.4 ± 0.6 Å) even thicker than that in B (29.8 ± 1.3 Å). On the contrary, the largely opened inward-facing conformation of P-glycoprotein in B shows that the lateral cleft between halves of the TMDs protrudes deeply into the lipid bilayer, and therefore the internal vestibule of P-glycoprotein is connected to the lipid bilayer. **(C)** Lateral view of hCFTR (PDB accession no. 5UAK) within the boundaries of the membrane with the internal vestibule shown in surface view and all the TMs shown as ribbons. The yellow dot marks the external end of the internal vestibule. **(D)** Lateral view of P-glycoprotein (PDB accession no. 4KSB) within the boundaries of the membrane with the internal vestibule shown in surface view. The red dot indicates the external end of the internal vestibule. More ABC transporters orientated in the membrane showing deep cleft in the lipid bilayer similar to one with the P-glycoprotein can be seen in the Orientations of Proteins in Membranes (OPM) database provided by the University of Michigan.

high-affinity site accounting for potentiation and a low-affinity inhibitory site (Wang et al., 1998; Zhou et al., 1998; Obayashi et al., 1999; Lansdell et al., 2000). Although the exact mechanism of action for genistein remains unclear, different approaches used to localize its binding sites suggest a binding site at the interface of the NBD dimer (Moran et al., 2005; Huang et al., 2009). In contrast, Lansdell et al. (2000) proposed that genistein may also bind within the CFTR pore. Taking advantage of the high-resolution of TMDs in cryo-EM structures, one may now evaluate other potential binding sites for genistein in the TMDs of CFTR.

NPPB (Fig. 14 I), which also blocks the CFTR pore (Wang et al., 2005), is another potentiator that has a dual effect (i.e., pore blocking and modulation of gating) on CFTR. Several studies have demonstrated the effects of NPPB on CFTR gating (Wang et al., 2005; Csanády and Töröcsik, 2014a,b; Lin et al., 2016), but its mechanisms of action remain debated. Although Csanády and Töröcsik (2014a,b) suggested NPPB modulates the transition state of CFTR, Lin et al. (2016) argue that NPPB facilitates NBD dimerization by stabilizing the NBD dimer. This discrepancy from functional data may be resolved by identifying the action site using cryo-EM. Nonetheless, a synergistic interaction between NPPB and VX-770 in rectifying the gating defects associated with the G551D mutation conveys an optimistic outlook in future drug development for combination therapy (Lin et al., 2016). As more cryo-EM structures of CFTR will emerge in the future, we anticipate forthcoming identification of the binding sites for different CFTR potentiators. Successes in this area of research will lay the foundation for structure-based drug design of CFTR potentiators exhibiting pharmacological synergism for gating enhancement.

Epilogue

Solving the atomic structures of CFTR is no doubt a celebratory breakthrough in the CF field. In the current article, we strive to take advantage of the molecular details provided by the structures to get a glimpse of the functional anatomy of CFTR. Decades of biochemical/biophysical studies have generated tremendous amounts of data that help interpretations of the solved structures.

In the meantime, the structures also serve as a guide to scrutinize previous functional data and to plan future studies. We hope that our discussion has successfully integrated these two rich sources of information and hence provided a more comprehensive view of the structure and function of CFTR. We will end our discussion by covering, albeit speculatively, a topic that should interest those readers who may ponder the evolutionary relationship between CFTR, a bona fide ion channel, and ABC transporters that use ATP hydrolysis as the source of free energy to actively pump the substrate across the membrane.

The overall architectural similarities between CFTR and a typical ABC exporter (e.g., P-glycoprotein; Fig. 15) underscore the long-suspected evolutionary track in which a primordial transporter evolves into a channel. But channels and transporters are fundamentally different machines with different operational mechanisms (Gadsby et al., 2006; Chen and Hwang, 2008). As many of the substrates for ABC exporters are hydrophobic in nature, their substrate translocation pathways can be partly exposed to the lipid bilayer. In fact, membrane lipids could partition into the substrate translocation pathway of the P-glycoprotein (Barreto-Ojeda et al., 2018), and some ABC exporters actually transport phospholipids (Linton, 2015; Zhao et al., 2015). This free communication between the substrate translocation pathway and lipid bilayers, however, is an anathema for an ion channel. Fig. 15 shows a comparison between CFTR and P-glycoprotein when incorporated into the lipid bilayer. Although the lateral cleft of P-glycoprotein penetrates into the membrane (Lomize et al., 2012; see http://opm.phar.umich.edu for many more examples), the part of CFTR's internal vestibule that is enclosed in the lipid bilayer is sequestered. We believe that this structural adaptation constitutes one of the essential steps for making a channel from ABC exporters.

It is also worth noting that in the inward-facing conformations of CFTR, the internal vestibule stops within the outer leaflet of the membrane (Fig. 7, A and B, yellow dot; and Fig. 15 C). On the contrary, the more spacious internal vestibule in the P-glycoprotein protrudes from the inner leaflet of the cell membrane all the way over the outer leaflet and only stops outside the external boundary of the membrane bilayer (Fig. 15 D). Thus, the "external gate" of the P-glycoprotein (Fig. 15 D, region above the red dot) is located in the extracellular domain of the protein. As discussed in the pore section, the narrowest region of CFTR's pore may also serve as the gate. Then, contrary to that of P-glycoprotein, the position of CFTR's gate is buried in the membrane-spanning segments. This internal shift of the narrow segment (or gate) may be part of the evolutionary changes that allow CFTR's anion permeation pathway to comprise not only an internal vestibule but also a shallow external vestibule that can effectively attract anions to the external pore entrance.

What about open-channel conformations? We argue that when CFTR undergoes conformational changes to the open state, a state similar to the phosphorylated ATP-bound zCFTR structure (Fig. 9 B), its pore still needs to be isolated from membrane lipids. The flip-flop gating motion proposed for ABC exporters such as Sav1866 suggests that each NBD–TMD complex moves as a rigid body to convert the overall assembly from an inward-facing conformation with external gate closed to an outward-facing conformation with internal gate closed (Ward et al., 2007; Khare et al., 2009). Two problems emerge if one literally borrows this picture of gating motion for CFTR. First, the outward-facing structure of an ABC exporter has an even wider cleft freely communicable with the membrane lipid. Second, a closure of an "internal gate" for CFTR is not allowed for an open-channel conformation. Definitive answers to these issues will have to await the solution of CFTR's open-state structure. But the cryo-EM structure of zCFTR with dimeric NBDs published lately (Zhang et al., 2017) as well as some SCAM data using bulky MTS reagents did provide some hints for possible gating motions after NBD dimerization. As described in the pore section, internally applied bulky MTS reagents can reach the positions deep in the internal vestibule in both the open and the closed states, suggesting that there is no internal gate (i.e., degenerate gate hypothesis). The observation that bulky MTS reagents can enter the lateral entrance and subsequently the internal vestibule in the open state also means that once two NBDs dimerize, those TMs linking the pore domain and NBDs cannot undergo the same kind of motion proposed for ABC exporters lest a collapse of the lateral entrance occurs. In other words, a sizable gap connecting the internal vestibule and the bulk solution has to be present in the open state. Indeed, the most recently published phosphorylated zCFTR confirms the existence of a lateral entrance between TM4 and TM6 (Fig. 9 B), although this opening is smaller than that in the unphosphorylated structure of zCFTR (Fig. 9 A). As described above in the TMD–NBD interface section, the existence of a lateral entrance between TM4 and TM6 may ultimately result from the weakened interaction, particularly at the ICL1–NBD1 interface.

If the newly solved closed state with dimerized NBDs (Zhang et al., 2017) indeed represents a closed conformation right before gate opening (as proposed in the energetic coupling gating model in Fig. 10 B), this means that TMDs movements upon NBD dimerization do not open the gate synchronously. Based on our own SCAM data, we speculate that opening of the gate from this closed state may only need conformational changes that eventually expose the segments between S341 and T338 in TM6 and between L102 and I106 in TM1 (and at least one unidentified TM) to create an anion permeation pathway tilted to one side of the CFTR protein, instead of being right along the central axis. Unique to CFTR as an ion channel, ATP hydrolysis at site 2 then causes a (partial) separation of the NBD dimer, which facilitates conformational changes in TMDs for gate closure and hence to complete a gating cycle. Thus a protein, although it looks like a transporter, can be a real ion channel.

The advancement of cryo-EM technologies culminated in 2017 as the three pioneers in this field were awarded the Nobel Prize in Chemistry. Unlike x-ray crystallographic methods, cryo-EM does not require crystallization of interested proteins, which is often the rate-limiting step in solving the atomic structure of a membrane protein. The successful employment of cryo-EM techniques in solving the high-resolution structures of CFTR is no doubt a remarkable accomplishment. Unquestionably, we all anticipate more CFTR structures in different conformations will emerge in the near future. The next few years should be exciting, as both functional and structural

studies will feed into each other with unique and yet respective insights. Perhaps we are not so far away from fulfilling the revered goal of "intelligent design" of drugs to overcome CF and CFTR-related illnesses.

Online supplemental information

Table S1 shows the pore-lining residue comparison between functional data and cryo-EM CFTR structures.

Acknowledgments

We thank Shenghui Hu and Cindy Chu for their technical assistance. We also thank Dr. Zhe Zhang at the Rockefeller University for providing the EM-density map and technical assistance for mapping the R domain in Fig. 3 and the permeation pathway. We also thank Dr. Liming Qiu at the University of Missouri-Columbia for measuring the relative solvent accessibility in Table S1.

This work is supported by grants from the National Institutes of Health (NIHR01DK55835) and the Cystic Fibrosis Foundation (Hwang11P0) to T.-C. Hwang. J.-T. Yeh is a recipient of a scholarship from The Taipei Veterans General Hospital–National Yang-Ming University Excellent Physician Scientists Cultivation Program in Taiwan (no. 102-Y-A-001).

During the preparation of this manuscript, T.-C. Hwang's lab had service contracts with AbbVie and Proteostatis in addition to a sponsored research grant from AbbVie. S. Destefano's stipend was supported by a gift fund from Nanova, Inc.

Author contributions: T.-C. Hwang formulated the overall content of the article, wrote the summary, abstract, Introduction, and Epilogue, and edited the whole article. J.-T. Yeh wrote the Roles of the R domain in CFTR function section. J. Zhang wrote the Asymmetrical pore and gate in CFTR section. Y.-C. Yu wrote the CFTR's gating machinery NBDs and TMD–NBD interfaces section. H.-I. Yeh wrote the Structural mechanisms of CFTR pharmacology section. S. Destefano wrote the Molecular understanding for disease-associated mutations section.

Lesley C. Anson served as editor.

Submitted: 16 November 2017
Accepted: 5 March 2018

References

Accurso, F.J., S.M. Rowe, J.P. Clancy, M.P. Boyle, J.M. Dunitz, P.R. Durie, S.D. Sagel, D.B. Hornick, M.W. Konstan, S.H. Donaldson, et al. 2010. Effect of VX-770 in persons with cystic fibrosis and the G551D-CFTR mutation. *N. Engl. J. Med.* 363:1991–2003. https://doi.org/10.1056/NEJMoa0909825

Akabas, M.H., D.A. Stauffer, M. Xu, and A. Karlin. 1992. Acetylcholine receptor channel structure probed in cysteine-substitution mutants. *Science.* 258:307–310. https://doi.org/10.1126/science.1384130

Al-Awqati, Q. 2002. Alternative treatment for secretory diarrhea revealed in a new class of CFTR inhibitors. *J. Clin. Invest.* 110:1599–1601. https://doi.org/10.1172/JCI0217301

Aleksandrov, A.A., L. Aleksandrov, and J.R. Riordan. 2002a. Nucleoside triphosphate pentose ring impact on CFTR gating and hydrolysis. *FEBS Lett.* 518:183–188. https://doi.org/10.1016/S0014-5793(02)02698-4

Aleksandrov, L., A.A. Aleksandrov, X.B. Chang, and J.R. Riordan. 2002b. The First Nucleotide Binding Domain of Cystic Fibrosis Transmembrane Conductance Regulator Is a Site of Stable Nucleotide Interaction, whereas the Second Is a Site of Rapid Turnover. *J. Biol. Chem.* 277:15419–15425. https://doi.org/10.1074/jbc.M111713200

Alexander, C., A. Ivetac, X. Liu, Y. Norimatsu, J.R. Serrano, A. Landstrom, M. Sansom, and D.C. Dawson. 2009. Cystic fibrosis transmembrane conductance regulator: using differential reactivity toward channel-permeant and channel-impermeant thiol-reactive probes to test a molecular model for the pore. *Biochemistry.* 48:10078–10088. https://doi.org/10.1021/bi901314c

Aller, S.G., J. Yu, A. Ward, Y. Weng, S. Chittaboina, R. Zhuo, P.M. Harrell, Y.T. Trinh, Q. Zhang, I.L. Urbatsch, and G. Chang. 2009. Structure of P-glycoprotein reveals a molecular basis for poly-specific drug binding. *Science.* 323:1718–1722. https://doi.org/10.1126/science.1168750

Amaral, M.D., and K. Kunzelmann. 2007. Molecular targeting of CFTR as a therapeutic approach to cystic fibrosis. *Trends Pharmacol. Sci.* 28:334–341. https://doi.org/10.1016/j.tips.2007.05.004

Anderson, M.P., and M.J. Welsh. 1992. Regulation by ATP and ADP of CFTR chloride channels that contain mutant nucleotide-binding domains. *Science.* 257:1701–1704. https://doi.org/10.1126/science.1382316

Anderson, M.P., H.A. Berger, D.P. Rich, R.J. Gregory, A.E. Smith, and M.J. Welsh. 1991. Nucleoside triphosphates are required to open the CFTR chloride channel. *Cell.* 67:775–784. https://doi.org/10.1016/0092-8674(91)90072-7

Angelow, S., and A.S. Yu. 2009. Structure-function studies of claudin extracellular domains by cysteine-scanning mutagenesis. *J. Biol. Chem.* 284:29205–29217. https://doi.org/10.1074/jbc.M109.043752

Atwell, S., C.G. Brouillette, K. Conners, S. Emtage, T. Gheyi, W.B. Guggino, J. Hendle, J.F. Hunt, H.A. Lewis, F. Lu, et al. 2010. Structures of a minimal human CFTR first nucleotide-binding domain as a monomer, head-to-tail homodimer, and pathogenic mutant. *Protein Eng. Des. Sel.* 23:375–384. https://doi.org/10.1093/protein/gzq004

Aubin, C.N., and P. Linsdell. 2006. Positive charges at the intracellular mouth of the pore regulate anion conduction in the CFTR chloride channel. *J. Gen. Physiol.* 128:535–545. https://doi.org/10.1085/jgp.200609516

Bai, Y., M. Li, and T.C. Hwang. 2010. Dual roles of the sixth transmembrane segment of the CFTR chloride channel in gating and permeation. *J. Gen. Physiol.* 136:293–309. https://doi.org/10.1085/jgp.201010480

Bai, Y., M. Li, and T.C. Hwang. 2011. Structural basis for the channel function of a degraded ABC transporter, CFTR (ABCC7). *J. Gen. Physiol.* 138:495–507. https://doi.org/10.1085/jgp.201110705

Baker, J.M., R.P. Hudson, V. Kanelis, W.Y. Choy, P.H. Thibodeau, P.J. Thomas, and J.D. Forman-Kay. 2007. CFTR regulatory region interacts with NBD1 predominantly via multiple transient helices. *Nat. Struct. Mol. Biol.* 14:738–745. https://doi.org/10.1038/nsmb1278

Baroni, D., O. Zegarra-Moran, A. Svensson, and O. Moran. 2014. Direct interaction of a CFTR potentiator and a CFTR corrector with phospholipid bilayers. *Eur. Biophys. J.* 43:341–346. https://doi.org/10.1007/s00249-014-0956-y

Barreto-Ojeda, E., V. Corradi, R.-X. Gu, and D.P. Tieleman. 2018. Coarse-grained molecular dynamics simulations reveal lipid access pathways in P-glycoprotein. *J. Gen. Physiol.*. https://doi.org/10.1085/jgp.201711907

Barrett, K.E., and S.J. Keely. 2000. Chloride secretion by the intestinal epithelium: molecular basis and regulatory aspects. *Annu. Rev. Physiol.* 62:535–572. https://doi.org/10.1146/annurev.physiol.62.1.535

Basso, C., P. Vergani, A.C. Nairn, and D.C. Gadsby. 2003. Prolonged nonhydrolytic interaction of nucleotide with CFTR's NH2-terminal nucleotide binding domain and its role in channel gating. *J. Gen. Physiol.* 122:333–348. https://doi.org/10.1085/jgp.200308798

Beck, E.J., Y. Yang, S. Yaemsiri, and V. Raghuram. 2008. Conformational changes in a pore-lining helix coupled to cystic fibrosis transmembrane conductance regulator channel gating. *J. Biol. Chem.* 283:4957–4966. https://doi.org/10.1074/jbc.M702235200

Berger, A.L., M. Ikuma, J.F. Hunt, P.J. Thomas, and M.J. Welsh. 2002. Mutations that change the position of the putative gamma-phosphate linker in the nucleotide binding domains of CFTR alter channel gating. *J. Biol. Chem.* 277:2125–2131. https://doi.org/10.1074/jbc.M109539200

Bhattacharya, S.K. 1995. Cholera outbreaks: role of oral rehydration therapy. *J. Indian Med. Assoc.* 93:237–238.

Bompadre, S.G., Y. Sohma, M. Li, and T.C. Hwang. 2007. G551D and G1349D, two CF-associated mutations in the signature sequences of CFTR, exhibit distinct gating defects. *J. Gen. Physiol.* 129:285–298. https://doi.org/10.1085/jgp.200609667

Bompadre, S.G., M. Li, and T.C. Hwang. 2008. Mechanism of G551D-CFTR (cystic fibrosis transmembrane conductance regulator) potentiation by a high affinity ATP analog. *J. Biol. Chem.* 283:5364–5369. https://doi.org/10.1074/jbc.M709417200

Bozoky, Z., M. Krzeminski, R. Muhandiram, J.R. Birtley, A. Al-Zahrani, P.J. Thomas, R.A. Frizzell, R.C. Ford, and J.D. Forman-Kay. 2013. Regulatory R region of the CFTR chloride channel is a dynamic integrator of phospho-dependent intra- and intermolecular interactions. *Proc. Natl. Acad. Sci. USA.* 110:E4427–E4436. https://doi.org/10.1073/pnas.1315104110

Bridges, R.J., A. Thakerar, Y. Cheng, M. Mense, D. Wetmore, N. Bradbury, Y. Jia, and W. Driessche. 2010. Capitalizing on corrector mechanistic differences to achieve synergy in F508del–CFTR expression. *Pediatr. Pulmonol.* 45(Suppl.):119–120.

Caci, E., A. Caputo, A. Hinzpeter, N. Arous, P. Fanen, N. Sonawane, A.S. Verkman, R. Ravazzolo, O. Zegarra-Moran, and L.J. Galietta. 2008. Evidence for direct CFTR inhibition by CFTR(inh)-172 based on Arg347 mutagenesis. *Biochem. J.* 413:135–142. https://doi.org/10.1042/BJ20080029

Cai, Z., K.A. Lansdell, and D.N. Sheppard. 1999. Inhibition of heterologously expressed cystic fibrosis transmembrane conductance regulator Cl- channels by non-sulphonylurea hypoglycaemic agents. *Br. J. Pharmacol.* 128:108–118. https://doi.org/10.1038/sj.bjp.0702748

Cai, Z., A. Taddei, and D.N. Sheppard. 2006. Differential sensitivity of the cystic fibrosis (CF)-associated mutants G551D and G1349D to potentiators of the cystic fibrosis transmembrane conductance regulator (CFTR) Cl- channel. *J. Biol. Chem.* 281:1970–1977. https://doi.org/10.1074/jbc.M510576200

Cai, Z.W., J. Liu, H.Y. Li, and D.N. Sheppard. 2011. Targeting F508del-CFTR to develop rational new therapies for cystic fibrosis. *Acta Pharmacol. Sin.* 32:693–701. https://doi.org/10.1038/aps.2011.71

Cai, Z., T. Palmai-Pallag, P. Khuituan, M.J. Mutolo, C. Boinot, B. Liu, T.S. Scott-Ward, I. Callebaut, A. Harris, and D.N. Sheppard. 2015. Impact of the F508del mutation on ovine CFTR, a Cl- channel with enhanced conductance and ATP-dependent gating. *J. Physiol.* 593:2427–2446. https://doi.org/10.1113/JP270227

Carter, S., S. Kelly, E. Caples, B. Grogan, J. Doyle, C.G. Gallagher, and E.F. McKone. 2015. Ivacaftor as salvage therapy in a patient with cystic fibrosis genotype F508del/R117H/IVS8-5T. *J. Cyst. Fibros.* 14:e4–e5.

Chappe, V., D.A. Hinkson, T. Zhu, X.B. Chang, J.R. Riordan, and J.W. Hanrahan. 2003. Phosphorylation of protein kinase C sites in NBD1 and the R domain control CFTR channel activation by PKA. *J. Physiol.* 548:39–52. https://doi.org/10.1113/jphysiol.2002.035790

Chaves, L.A., and D.C. Gadsby. 2015. Cysteine accessibility probes timing and extent of NBD separation along the dimer interface in gating CFTR channels. *J. Gen. Physiol.* 145:261–283. https://doi.org/10.1085/jgp.201411347

Chen, T.Y., and T.C. Hwang. 2008. CLC-0 and CFTR: chloride channels evolved from transporters. *Physiol. Rev.* 88:351–387. https://doi.org/10.1152/physrev.00058.2006

Chen, J., G. Lu, J. Lin, A.L. Davidson, and F.A. Quiocho. 2003. A tweezers-like motion of the ATP-binding cassette dimer in an ABC transport cycle. *Mol. Cell.* 12:651–661. https://doi.org/10.1016/j.molcel.2003.08.004

Chin, S., D. Yang, A.J. Miles, P.D. Eckford, S. Molinski, B.A. Wallace, and C.E. Bear. 2017. Attenuation of Phosphorylation-dependent Activation of Cystic Fibrosis Transmembrane Conductance Regulator (CFTR) by Disease-causing Mutations at the Transmission Interface. *J. Biol. Chem.* 292:1988–1999. https://doi.org/10.1074/jbc.M116.762633

Corradi, V., P. Vergani, and D.P. Tieleman. 2015. Cystic Fibrosis Transmembrane Conductance Regulator (CFTR): CLOSED AND OPEN STATE CHA NNEL MODELS. *J. Biol. Chem.* 290:22891–22906. https://doi.org/10.1074/jbc.M115.665125

Cotten, J.F., and M.J. Welsh. 1998. Covalent modification of the nucleotide binding domains of cystic fibrosis transmembrane conductance regulator. *J. Biol. Chem.* 273:31873–31879. https://doi.org/10.1074/jbc.273.48.31873

Cotten, J.F., and M.J. Welsh. 1999. Cystic fibrosis-associated mutations at arginine 347 alter the pore architecture of CFTR. Evidence for disruption of a salt bridge. *J. Biol. Chem.* 274:5429–5435. https://doi.org/10.1074/jbc.274.9.5429

Csanády, L., and B. Töröcsik. 2014a. Catalyst-like modulation of transition states for CFTR channel opening and closing: New stimulation strategy exploits nonequilibrium gating. *J. Gen. Physiol.* 143:269–287. https://doi.org/10.1085/jgp.201311089

Csanády, L., and B. Töröcsik. 2014b. Structure-activity analysis of a CFTR channel potentiator: Distinct molecular parts underlie dual gating effects. *J. Gen. Physiol.* 144:321–336. https://doi.org/10.1085/jgp.201411246

Csanády, L., K.W. Chan, D. Seto-Young, D.C. Kopsco, A.C. Nairn, and D.C. Gadsby. 2000. Severed channels probe regulation of gating of cystic fibrosis transmembrane conductance regulator by its cytoplasmic domains. *J. Gen. Physiol.* 116:477–500. https://doi.org/10.1085/jgp.116.3.477

Csanády, L., D. Seto-Young, K.W. Chan, C. Cenciarelli, B.B. Angel, J. Qin, D.T. McLachlin, A.N. Krutchinsky, B.T. Chait, A.C. Nairn, and D.C. Gadsby. 2005. Preferential phosphorylation of R-domain serine 768 dampens activation of CFTR channels by PKA. *J. Gen. Physiol.* 125:171–186. https://doi.org/10.1085/jgp.200409076

Csanády, L., P. Vergani, and D.C. Gadsby. 2010. Strict coupling between CFTR's catalytic cycle and gating of its Cl- ion pore revealed by distributions of open channel burst durations. *Proc. Natl. Acad. Sci. USA.* 107:1241–1246. https://doi.org/10.1073/pnas.0911061107

Cui, G., Z.R. Zhang, A.R. O'Brien, B. Song, and N.A. McCarty. 2008. Mutations at arginine 352 alter the pore architecture of CFTR. *J. Membr. Biol.* 222:91–106. https://doi.org/10.1007/s00232-008-9105-9

Cui, G., B. Song, H.W. Turki, and N.A. McCarty. 2012. Differential contribution of TM6 and TM12 to the pore of CFTR identified by three sulfonylurea-based blockers. *Pflugers Arch.* 463:405–418. https://doi.org/10.1007/s00424-011-1035-1

Cui, G., K.S. Rahman, D.T. Infield, C. Kuang, C.Z. Prince, and N.A. McCarty. 2014. Three charged amino acids in extracellular loop 1 are involved in maintaining the outer pore architecture of CFTR. *J. Gen. Physiol.* 144:159–179. https://doi.org/10.1085/jgp.201311122

Cui, L., L. Aleksandrov, X.B. Chang, Y.X. Hou, L. He, T. Hegedus, M. Gentzsch, A. Aleksandrov, W.E. Balch, and J.R. Riordan. 2007. Domain interdependence in the biosynthetic assembly of CFTR. *J. Mol. Biol.* 365:981–994. https://doi.org/10.1016/j.jmb.2006.10.086

Dalton, J., O. Kalid, M. Schushan, N. Ben-Tal, and J. Villà-Freixa. 2012. New model of cystic fibrosis transmembrane conductance regulator proposes active channel-like conformation. *J. Chem. Inf. Model.* 52:1842–1853. https://doi.org/10.1021/ci2005884

Das, J., A.A. Aleksandrov, L. Cui, L. He, J.R. Riordan, and N.V. Dokholyan. 2017. Transmembrane helical interactions in the CFTR channel pore. *PLOS Comput. Biol.* 13:e1005594. https://doi.org/10.1371/journal.pcbi.1005594

Davidson, A.L., and J. Chen. 2004. ATP-binding cassette transporters in bacteria. *Annu. Rev. Biochem.* 73:241–268. https://doi.org/10.1146/annurev.biochem.73.011303.073626

Dawson, R.J., and K.P. Locher. 2007. Structure of the multidrug ABC transporter Sav1866 from Staphylococcus aureus in complex with AMP-PNP. *FEBS Lett.* 581:935–938. https://doi.org/10.1016/j.febslet.2007.01.073

De Boeck, K., and M.D. Amaral. 2016. Progress in therapies for cystic fibrosis. *Lancet Respir. Med.* 4:662–674. https://doi.org/10.1016/S2213-2600(16)00023-0

Denning, G.M., M.P. Anderson, J.F. Amara, J. Marshall, A.E. Smith, and M.J. Welsh. 1992. Processing of mutant cystic fibrosis transmembrane conductance regulator is temperature-sensitive. *Nature.* 358:761–764. https://doi.org/10.1038/358761a0

Doyle, D.A., J. Morais Cabral, R.A. Pfuetzner, A. Kuo, J.M. Gulbis, S.L. Cohen, B.T. Chait, and R. MacKinnon. 1998. The structure of the potassium channel: molecular basis of K+ conduction and selectivity. *Science.* 280:69–77. https://doi.org/10.1126/science.280.5360.69

Du, K., and G.L. Lukacs. 2009. Cooperative assembly and misfolding of CFTR domains in vivo. *Mol. Biol. Cell.* 20:1903–1915. https://doi.org/10.1091/mbc.E08-09-0950

Du, K., M. Sharma, and G.L. Lukacs. 2005. The DeltaF508 cystic fibrosis mutation impairs domain-domain interactions and arrests post-translational folding of CFTR. *Nat. Struct. Mol. Biol.* 12:17–25. https://doi.org/10.1038/nsmb882

Dyson, H.J., and P.E. Wright. 2005. Intrinsically unstructured proteins and their functions. *Nat. Rev. Mol. Cell Biol.* 6:197–208. https://doi.org/10.1038/nrm1589

Eckford, P.D., C. Li, M. Ramjeesingh, and C.E. Bear. 2012. Cystic fibrosis transmembrane conductance regulator (CFTR) potentiator VX-770 (ivacaftor) opens the defective channel gate of mutant CFTR in a phosphorylation-dependent but ATP-independent manner. *J. Biol. Chem.* 287:36639–36649. https://doi.org/10.1074/jbc.M112.393637

El Hiani, Y., and P. Linsdell. 2010. Changes in accessibility of cytoplasmic substances to the pore associated with activation of the cystic fibrosis transmembrane conductance regulator chloride channel. *J. Biol. Chem.* 285:32126–32140. https://doi.org/10.1074/jbc.M110.113332

El Hiani, Y., and P. Linsdell. 2012. Tuning of CFTR chloride channel function by location of positive charges within the pore. *Biophys. J.* 103:1719–1726. https://doi.org/10.1016/j.bpj.2012.09.020

El Hiani, Y., and P. Linsdell. 2014. Metal bridges illuminate transmembrane domain movements during gating of the cystic fibrosis transmembrane

conductance regulator chloride channel. *J. Biol. Chem.* 289:28149–28159. https://doi.org/10.1074/jbc.M114.593103
El Hiani, Y., and P. Linsdell. 2015. Functional Architecture of the Cytoplasmic Entrance to the Cystic Fibrosis Transmembrane Conductance Regulator Chloride Channel Pore. *J. Biol. Chem.* 290:15855–15865. https://doi.org/10.1074/jbc.M115.656181
El Hiani, Y., A. Negoda, and P. Linsdell. 2016. Cytoplasmic pathway followed by chloride ions to enter the CFTR channel pore. *Cell. Mol. Life Sci.* 73:1917–1925. https://doi.org/10.1007/s00018-015-2113-x
Eudes, R., P. Lehn, C. Férec, J.P. Mornon, and I. Callebaut. 2005. Nucleotide binding domains of human CFTR: a structural classification of critical residues and disease-causing mutations. *Cell. Mol. Life Sci.* 62:2112–2123. https://doi.org/10.1007/s00018-005-5224-y
Fatehi, M., and P. Linsdell. 2008. State-dependent access of anions to the cystic fibrosis transmembrane conductance regulator chloride channel pore. *J. Biol. Chem.* 283:6102–6109. https://doi.org/10.1074/jbc.M707736200
Fatehi, M., and P. Linsdell. 2009. Novel residues lining the CFTR chloride channel pore identified by functional modification of introduced cysteines. *J. Membr. Biol.* 228:151–164. https://doi.org/10.1007/s00232-009-9167-3
French, P.J., J. Bijman, A.G. Bot, W.E. Boomaars, B.J. Scholte, and H.R. de Jonge. 1997. Genistein activates CFTR Cl- channels via a tyrosine kinase- and protein phosphatase-independent mechanism. *Am. J. Physiol.* 273:C747–C753. https://doi.org/10.1152/ajpcell.1997.273.2.C747
Fu, J., H.L. Ji, A.P. Naren, and K.L. Kirk. 2001. A cluster of negative charges at the amino terminal tail of CFTR regulates ATP-dependent channel gating. *J. Physiol.* 536:459–470. https://doi.org/10.1111/j.1469-7793.2001.0459c.xd
Gadsby, D.C., and A.C. Nairn. 1999. Control of CFTR channel gating by phosphorylation and nucleotide hydrolysis. *Physiol. Rev.* 79(Suppl 1):S77–S107. https://doi.org/10.1152/physrev.1999.79.1.S77
Gadsby, D.C., P. Vergani, and L. Csanády. 2006. The ABC protein turned chloride channel whose failure causes cystic fibrosis. *Nature.* 440:477–483. https://doi.org/10.1038/nature04712
Gao, X., and T.C. Hwang. 2015. Localizing a gate in CFTR. *Proc. Natl. Acad. Sci. USA.* 112:2461–2466. https://doi.org/10.1073/pnas.1420676112
Gao, X., and T.C. Hwang. 2016. Spatial positioning of CFTR's pore-lining residues affirms an asymmetrical contribution of transmembrane segments to the anion permeation pathway. *J. Gen. Physiol.* 147:407–422. https://doi.org/10.1085/jgp.201511557
Gao, X., Y. Bai, and T.C. Hwang. 2013. Cysteine scanning of CFTR's first transmembrane segment reveals its plausible roles in gating and permeation. *Biophys. J.* 104:786–797. https://doi.org/10.1016/j.bpj.2012.12.048
Gené, G.G., A. Llobet, S. Larriba, D. de Semir, I. Martínez, A. Escalada, C. Solsona, T. Casals, and J.M. Aran. 2008. N-terminal CFTR missense variants severely affect the behavior of the CFTR chloride channel. *Hum. Mutat.* 29:738–749. https://doi.org/10.1002/humu.20721
Gong, X., S.M. Burbridge, A.C. Lewis, P.Y. Wong, and P. Linsdell. 2002. Mechanism of lonidamine inhibition of the CFTR chloride channel. *Br. J. Pharmacol.* 137:928–936. https://doi.org/10.1038/sj.bjp.0704932
Guinamard, R., and M.H. Akabas. 1999. Arg352 is a major determinant of charge selectivity in the cystic fibrosis transmembrane conductance regulator chloride channel. *Biochemistry.* 38:5528–5537. https://doi.org/10.1021/bi990155n
Gunderson, K.L., and R.R. Kopito. 1995. Conformational states of CFTR associated with channel gating: the role ATP binding and hydrolysis. *Cell.* 82:231–239. https://doi.org/10.1016/0092-8674(95)90310-0
Hämmerle, M.M., A.A. Aleksandrov, and J.R. Riordan. 2001. Disease-associated mutations in the extracytoplasmic loops of cystic fibrosis transmembrane conductance regulator do not impede biosynthetic processing but impair chloride channel stability. *J. Biol. Chem.* 276:14848–14854. https://doi.org/10.1074/jbc.M011017200
Hanrahan, J.W., H.M. Sampson, and D.Y. Thomas. 2013. Novel pharmacological strategies to treat cystic fibrosis. *Trends Pharmacol. Sci.* 34:119–125. https://doi.org/10.1016/j.tips.2012.11.006
He, L., A.A. Aleksandrov, A.W. Serohijos, T. Hegedus, L.A. Aleksandrov, L. Cui, N.V. Dokholyan, and J.R. Riordan. 2008. Multiple membrane-cytoplasmic domain contacts in the cystic fibrosis transmembrane conductance regulator (CFTR) mediate regulation of channel gating. *J. Biol. Chem.* 283:26383–26390. https://doi.org/10.1074/jbc.M803894200
He, L., P. Kota, A.A. Aleksandrov, L. Cui, T. Jensen, N.V. Dokholyan, and J.R. Riordan. 2013. Correctors of ΔF508 CFTR restore global conformational maturation without thermally stabilizing the mutant protein. *FASEB J.* 27:536–545. https://doi.org/10.1096/fj.12-216119
Higgins, C.F., and K.J. Linton. 2004. The ATP switch model for ABC transporters. *Nat. Struct. Mol. Biol.* 11:918–926. https://doi.org/10.1038/nsmb836
Hoelen, H., B. Kleizen, A. Schmidt, J. Richardson, P. Charitou, P.J. Thomas, and I. Braakman. 2010. The primary folding defect and rescue of ΔF508 CFTR emerge during translation of the mutant domain. *PLoS One.* 5:e15458. https://doi.org/10.1371/journal.pone.0015458
Hopfner, K.-P., A. Karcher, D.S. Shin, L. Craig, L.M. Arthur, J.P. Carney, and J.A. Tainer. 2000. Structural biology of Rad50 ATPase: ATP-driven conformational control in DNA double-strand break repair and the ABC-ATPase superfamily. *Cell.* 101:789–800. https://doi.org/10.1016/S0092-8674(00)80890-9
Huang, S.-Y., D. Bolser, H.-Y. Liu, T.-C. Hwang, and X. Zou. 2009. Molecular modeling of the heterodimer of human CFTR's nucleotide-binding domains using a protein-protein docking approach. *J. Mol. Graph. Model.* 27:822–828. https://doi.org/10.1016/j.jmgm.2008.12.005
Hung, L.W., I.X. Wang, K. Nikaido, P.Q. Liu, G.F. Ames, and S.H. Kim. 1998. Crystal structure of the ATP-binding subunit of an ABC transporter. *Nature.* 396:703–707. https://doi.org/10.1038/25393
Hwang, T.C., and K.L. Kirk. 2013. The CFTR ion channel: gating, regulation, and anion permeation. *Cold Spring Harb. Perspect. Med.* 3:a009498. https://doi.org/10.1101/cshperspect.a009498
Hwang, T.C., and D.N. Sheppard. 1999. Molecular pharmacology of the CFTR Cl- channel. *Trends Pharmacol. Sci.* 20:448–453. https://doi.org/10.1016/S0165-6147(99)01386-3
Hwang, T.C., and D.N. Sheppard. 2009. Gating of the CFTR Cl- channel by ATP-driven nucleotide-binding domain dimerisation. *J. Physiol.* 587:2151–2161. https://doi.org/10.1113/jphysiol.2009.171595
Hwang, T.C., G. Nagel, A.C. Nairn, and D.C. Gadsby. 1994. Regulation of the gating of cystic fibrosis transmembrane conductance regulator C1 channels by phosphorylation and ATP hydrolysis. *Proc. Natl. Acad. Sci. USA.* 91:4698–4702. https://doi.org/10.1073/pnas.91.11.4698
Hwang, T.C., F. Wang, I.C. Yang, and W.W. Reenstra. 1997. Genistein potentiates wild-type and delta F508-CFTR channel activity. *Am. J. Physiol.* 273:C988–C998. https://doi.org/10.1152/ajpcell.1997.273.3.C988
Iakoucheva, L.M., P. Radivojac, C.J. Brown, T.R. O'Connor, J.G. Sikes, Z. Obradovic, and A.K. Dunker. 2004. The importance of intrinsic disorder for protein phosphorylation. *Nucleic Acids Res.* 32:1037–1049. https://doi.org/10.1093/nar/gkh253
Jih, K.Y., and T.C. Hwang. 2012. Nonequilibrium gating of CFTR on an equilibrium theme. *Physiology (Bethesda).* 27:351–361.
Jih, K.Y., and T.C. Hwang. 2013. Vx-770 potentiates CFTR function by promoting decoupling between the gating cycle and ATP hydrolysis cycle. *Proc. Natl. Acad. Sci. USA.* 110:4404–4409. https://doi.org/10.1073/pnas.1215982110
Jih, K.Y., M. Li, T.C. Hwang, and S.G. Bompadre. 2011. The most common cystic fibrosis-associated mutation destabilizes the dimeric state of the nucleotide-binding domains of CFTR. *J. Physiol.* 589:2719–2731. https://doi.org/10.1113/jphysiol.2010.202861
Jih, K.Y., Y. Sohma, and T.C. Hwang. 2012. Nonintegral stoichiometry in CFTR gating revealed by a pore-lining mutation. *J. Gen. Physiol.* 140:347–359. https://doi.org/10.1085/jgp.201210834
Jih, K.Y., W.Y. Lin, Y. Sohma, and T.C. Hwang. 2017. CFTR potentiators: from bench to bedside. *Curr. Opin. Pharmacol.* 34:98–104. https://doi.org/10.1016/j.coph.2017.09.015
Jin, M.S., M.L. Oldham, Q. Zhang, and J. Chen. 2012. Crystal structure of the multidrug transporter P-glycoprotein from Caenorhabditis elegans. *Nature.* 490:566–569. https://doi.org/10.1038/nature11448
Kanelis, V., R.P. Hudson, P.H. Thibodeau, P.J. Thomas, and J.D. Forman-Kay. 2010. NMR evidence for differential phosphorylation-dependent interactions in WT and DeltaF508 CFTR. *EMBO J.* 29:263–277. https://doi.org/10.1038/emboj.2009.329
Karpowich, N., O. Martsinkevich, L. Millen, Y.-R. Yuan, P.L. Dai, K. MacVey, P.J. Thomas, and J.F. Hunt. 2001. Crystal structures of the MJ1267 ATP binding cassette reveal an induced-fit effect at the ATPase active site of an ABC transporter. *Structure.* 9:571–586. https://doi.org/10.1016/S0969-2126(01)00617-7
Khare, D., M.L. Oldham, C. Orelle, A.L. Davidson, and J. Chen. 2009. Alternating access in maltose transporter mediated by rigid-body rotations. *Mol. Cell.* 33:528–536. https://doi.org/10.1016/j.molcel.2009.01.035
Kidd, J.F., M. Ramjeesingh, F. Stratford, L.J. Huan, and C.E. Bear. 2004. A heteromeric complex of the two nucleotide binding domains of cystic fibrosis transmembrane conductance regulator (CFTR) mediates ATPase activity. *J. Biol. Chem.* 279:41664–41669. https://doi.org/10.1074/jbc.M407666200
Kim, Y., M.O. Anderson, J. Park, M.GLee, W. Namkung, and A.S. Verkman. 2015. Benzopyrimido-pyrrolo-oxazine-dione (R)-BPO-27 Inhibits CFTR

Chloride Channel Gating by Competition with ATP. *Mol. Pharmacol.* 88:689–696. https://doi.org/10.1124/mol.115.098368

Kopeikin, Z., Y. Sohma, M. Li, and T.C. Hwang. 2010. On the mechanism of CFTR inhibition by a thiazolidinone derivative. *J. Gen. Physiol.* 136:659–671. https://doi.org/10.1085/jgp.201010518

Kopeikin, Z., Z. Yuksek, H.Y. Yang, and S.G. Bompadre. 2014. Combined effects of VX-770 and VX-809 on several functional abnormalities of F508del-CFTR channels. *J. Cyst. Fibros.* 13:508–514.

Lansdell, K.A., Z. Cai, J.F. Kidd, and D.N. Sheppard. 2000. Two mechanisms of genistein inhibition of cystic fibrosis transmembrane conductance regulator Cl- channels expressed in murine cell line. *J. Physiol.* 524:317–330. https://doi.org/10.1111/j.1469-7793.2000.t01-1-00317.x

Lee, B., and F.M. Richards. 1971. The interpretation of protein structures: estimation of static accessibility. *J. Mol. Biol.* 55:379–400. https://doi.org/10.1016/0022-2836(71)90324-X

Lewis, H.A., S.G. Buchanan, S.K. Burley, K. Conners, M. Dickey, M. Dorwart, R. Fowler, X. Gao, W.B. Guggino, W.A. Hendrickson, et al. 2004. Structure of nucleotide-binding domain 1 of the cystic fibrosis transmembrane conductance regulator. *EMBO J.* 23:282–293. https://doi.org/10.1038/sj.emboj.7600040

Lewis, H.A., X. Zhao, C. Wang, J.M. Sauder, I. Rooney, B.W. Noland, D. Lorimer, M.C. Kearins, K. Conners, B. Condon, et al. 2005. Impact of the deltaF508 mutation in first nucleotide-binding domain of human cystic fibrosis transmembrane conductance regulator on domain folding and structure. *J. Biol. Chem.* 280:1346–1353. https://doi.org/10.1074/jbc.M410968200

Li, C., M. Ramjeesingh, W. Wang, E. Garami, M. Hewryk, D. Lee, J.M. Rommens, K. Galley, and C.E. Bear. 1996. ATPase activity of the cystic fibrosis transmembrane conductance regulator. *J. Biol. Chem.* 271:28463–28468. https://doi.org/10.1074/jbc.271.45.28463

Li, M.S., E.A. Cowley, Y. El Hiani, and P. Linsdell. 2018. Functional organization of cytoplasmic portals controlling access to the cystic fibrosis transmembrane conductance regulator (CFTR) chloride channel pore. *J. Biol. Chem.* https://doi.org/10.1074/jbc.RA117.001373

Lin, S., J. Sui, S. Cotard, B. Fung, J. Andersen, P. Zhu, N. El Messadi, J. Lehar, M. Lee, and J. Staunton. 2010. Identification of synergistic combinations of F508del cystic fibrosis transmembrane conductance regulator (CFTR) modulators. *Assay Drug Dev. Technol.* 8:669–684. https://doi.org/10.1089/adt.2010.0313

Lin, W.Y., K.Y. Jih, and T.C. Hwang. 2014. A single amino acid substitution in CFTR converts ATP to an inhibitory ligand. *J. Gen. Physiol.* 144:311–320. https://doi.org/10.1085/jgp.201411247

Lin, W.Y., Y. Sohma, and T.C. Hwang. 2016. Synergistic Potentiation of Cystic Fibrosis Transmembrane Conductance Regulator Gating by Two Chemically Distinct Potentiators, Ivacaftor (VX-770) and 5-Nitro-2-(3-Phenylpropylamino) Benzoate. *Mol. Pharmacol.* 90:275–285. https://doi.org/10.1124/mol.116.104570

Linsdell, P. 2001. Relationship between anion binding and anion permeability revealed by mutagenesis within the cystic fibrosis transmembrane conductance regulator chloride channel pore. *J. Physiol.* 531:51–66. https://doi.org/10.1111/j.1469-7793.2001.0051j.x

Linsdell, P. 2005. Location of a common inhibitor binding site in the cytoplasmic vestibule of the cystic fibrosis transmembrane conductance regulator chloride channel pore. *J. Biol. Chem.* 280:8945–8950. https://doi.org/10.1074/jbc.M414354200

Linsdell, P. 2006. Mechanism of chloride permeation in the cystic fibrosis transmembrane conductance regulator chloride channel. *Exp. Physiol.* 91:123–129. https://doi.org/10.1113/expphysiol.2005.031757

Linsdell, P. 2014a. Cystic fibrosis transmembrane conductance regulator chloride channel blockers: Pharmacological, biophysical and physiological relevance. *World J. Biol. Chem.* 5:26–39. https://doi.org/10.4331/wjbc.v5.i1.26

Linsdell, P. 2014b. State-dependent blocker interactions with the CFTR chloride channel: implications for gating the pore. *Pflugers Arch.* 466:2243–2255. https://doi.org/10.1007/s00424-014-1501-7

Linsdell, P. 2016. Anion conductance selectivity mechanism of the CFTR chloride channel. *Biochim. Biophys. Acta.* 1858:740–747. https://doi.org/10.1016/j.bbamem.2016.01.009

Linsdell, P. 2017. Architecture and functional properties of the CFTR channel pore. *Cell. Mol. Life Sci.* 74:67–83. https://doi.org/10.1007/s00018-016-2389-5

Linsdell, P., and J.W. Hanrahan. 1998. Adenosine triphosphate-dependent asymmetry of anion permeation in the cystic fibrosis transmembrane conductance regulator chloride channel. *J. Gen. Physiol.* 111:601–614. https://doi.org/10.1085/jgp.111.4.601

Linsdell, P., S.X. Zheng, and J.W. Hanrahan. 1998. Non-pore lining amino acid side chains influence anion selectivity of the human CFTR Cl- channel expressed in mammalian cell lines. *J. Physiol.* 512:1–16. https://doi.org/10.1111/j.1469-7793.1998.001bf.x

Linsdell, P., A. Evagelidis, and J.W. Hanrahan. 2000. Molecular determinants of anion selectivity in the cystic fibrosis transmembrane conductance regulator chloride channel pore. *Biophys. J.* 78:2973–2982. https://doi.org/10.1016/S0006-3495(00)76836-6

Linton, K.J. 2015. Lipid flopping in the liver. *Biochem. Soc. Trans.* 43:1003–1010. https://doi.org/10.1042/BST20150132

Liu, F., Z. Zhang, L. Csanady, D.C. Gadsby, and J. Chen. 2017. Molecular Structure of the Human CFTR Ion Channel. *Cell.* 169:85–95.

Liu, Y., M. Holmgren, M.E. Jurman, and G. Yellen. 1997. Gated access to the pore of a voltage-dependent K+ channel. *Neuron.* 19:175–184. https://doi.org/10.1016/S0896-6273(00)80357-8

Lomize, M.A., I.D. Pogozheva, H. Joo, H.I. Mosberg, and A.L. Lomize. 2012. OPM database and PPM web server: resources for positioning of proteins in membranes. *Nucleic Acids Res.* 40(D1):D370–D376. https://doi.org/10.1093/nar/gkr703

Long, S.B., E.B. Campbell, and R. Mackinnon. 2005. Crystal structure of a mammalian voltage-dependent Shaker family K+ channel. *Science.* 309:897–903. https://doi.org/10.1126/science.1116269

Loo, T.W., M.C. Bartlett, and D.M. Clarke. 2013. Corrector VX-809 stabilizes the first transmembrane domain of CFTR. *Biochem. Pharmacol.* 86:612–619. https://doi.org/10.1016/j.bcp.2013.06.028

Lukacs, G.L., and A.S. Verkman. 2012. CFTR: folding, misfolding and correcting the ΔF508 conformational defect. *Trends Mol. Med.* 18:81–91. https://doi.org/10.1016/j.molmed.2011.10.003

Lukacs, G.L., X.B. Chang, C. Bear, N. Kartner, A. Mohamed, J.R. Riordan, and S. Grinstein. 1993. The delta F508 mutation decreases the stability of cystic fibrosis transmembrane conductance regulator in the plasma membrane. Determination of functional half-lives on transfected cells. *J. Biol. Chem.* 268:21592–21598.

Ma, T., J.R. Thiagarajah, H. Yang, N.D. Sonawane, C. Folli, L.J. Galietta, and A.S. Verkman. 2002. Thiazolidinone CFTR inhibitor identified by high-throughput screening blocks cholera toxin-induced intestinal fluid secretion. *J. Clin. Invest.* 110:1651–1658. https://doi.org/10.1172/JCI0216112

McCarty, N.A., and Z.R. Zhang. 2001. Identification of a region of strong discrimination in the pore of CFTR. *Am. J. Physiol. Lung Cell. Mol. Physiol.* 281:L852–L867. https://doi.org/10.1152/ajplung.2001.281.4.L852

Mendoza, J.L., A. Schmidt, Q. Li, E. Nuvaga, T. Barrett, R.J. Bridges, A.P. Feranchak, C.A. Brautigam, and P.J. Thomas. 2012. Requirements for efficient correction of ΔF508 CFTR revealed by analyses of evolved sequences. *Cell.* 148:164–174. https://doi.org/10.1016/j.cell.2011.11.023

Mense, M., P. Vergani, D.M. White, G. Altberg, A.C. Nairn, and D.C. Gadsby. 2006. In vivo phosphorylation of CFTR promotes formation of a nucleotide-binding domain heterodimer. *EMBO J.* 25:4728–4739. https://doi.org/10.1038/sj.emboj.7601373

Miki, H., Z. Zhou, M. Li, T.C. Hwang, and S.G. Bompadre. 2010. Potentiation of disease-associated cystic fibrosis transmembrane conductance regulator mutants by hydrolyzable ATP analogs. *J. Biol. Chem.* 285:19967–19975. https://doi.org/10.1074/jbc.M109.092684

Mio, K., T. Ogura, M. Mio, H. Shimizu, T.C. Hwang, C. Sato, and Y. Sohma. 2008. Three-dimensional reconstruction of human cystic fibrosis transmembrane conductance regulator chloride channel revealed an ellipsoidal structure with orifices beneath the putative transmembrane domain. *J. Biol. Chem.* 283:30300–30310. https://doi.org/10.1074/jbc.M803185200

Moran, O., L.J.V. Galietta, and O. Zegarra-Moran. 2005. Binding site of activators of the cystic fibrosis transmembrane conductance regulator in the nucleotide binding domains. *Cell. Mol. Life Sci.* 62:446–460. https://doi.org/10.1007/s00018-004-4422-3

Mornon, J.P., P. Lehn, and I. Callebaut. 2008. Atomic model of human cystic fibrosis transmembrane conductance regulator: membrane-spanning domains and coupling interfaces. *Cell. Mol. Life Sci.* 65:2594–2612. https://doi.org/10.1007/s00018-008-8249-1

Mornon, J.P., B. Hoffmann, S. Jonic, P. Lehn, and I. Callebaut. 2015. Full-open and closed CFTR channels, with lateral tunnels from the cytoplasm and an alternative position of the F508 region, as revealed by molecular dynamics. *Cell. Mol. Life Sci.* 72:1377–1403. https://doi.org/10.1007/s00018-014-1749-2

Muanprasat, C., N.D. Sonawane, D. Salinas, A. Taddei, L.J. Galietta, and A.S. Verkman. 2004. Discovery of glycine hydrazide pore-occluding CFTR inhibitors: Mechanism, structure-activity analysis, and in vivo efficacy. *J. Gen. Physiol.* 124:125–137. https://doi.org/10.1085/jgp.200409059

Nagel, G., T.C. Hwang, K.L. Nastiuk, A.C. Nairn, and D.C. Gadsby. 1992. The protein kinase A-regulated cardiac Cl- channel resembles the cystic fibrosis transmembrane conductance regulator. *Nature.* 360:81–84. https://doi.org/10.1038/360081a0

Naren, A.P., E. Cormet-Boyaka, J. Fu, M. Villain, J.E. Blalock, M.W. Quick, and K.L. Kirk. 1999. CFTR chloride channel regulation by an interdomain interaction. *Science.* 286:544–548. https://doi.org/10.1126/science.286.5439.544

Negoda, A., Y. El Hiani, E.A. Cowley, and P. Linsdell. 2017. Contribution of a leucine residue in the first transmembrane segment to the selectivity filter region in the CFTR chloride channel. *Biochim. Biophys. Acta.* 1859:1049–1058. https://doi.org/10.1016/j.bbamem.2017.02.014

Negoda, A., E.A. Cowley, Y. El Hiani, and P. Linsdell. 2018. Conformational change of the extracellular parts of the CFTR protein during channel gating. *Cell. Mol. Life Sci.* https://doi.org/10.1007/s00018-018-2777-0

Norimatsu, Y., A. Ivetac, C. Alexander, J. Kirkham, N. O'Donnell, D.C. Dawson, and M.S.P. Sansom. 2012a. Cystic fibrosis transmembrane conductance regulator: a molecular model defines the architecture of the anion conduction path and locates a "bottleneck" in the pore. *Biochemistry.* 51:2199–2212. https://doi.org/10.1021/bi201888a

Norimatsu, Y., A. Ivetac, C. Alexander, N. O'Donnell, L. Frye, M.S. Sansom, and D.C. Dawson. 2012b. Locating a plausible binding site for an open-channel blocker, GlyH-101, in the pore of the cystic fibrosis transmembrane conductance regulator. *Mol. Pharmacol.* 82:1042–1055. https://doi.org/10.1124/mol.112.080267

Obayashi, K., M. Horie, T. Washizuka, T. Nishimoto, and S. Sasayama. 1999. On the mechanism of genistein-induced activation of protein kinase A-dependent Cl- conductance in cardiac myocytes. *Pflugers Arch.* 438:269–277. https://doi.org/10.1007/s004240050909

Okiyoneda, T., G. Veit, J.F. Dekkers, M. Bagdany, N. Soya, H. Xu, A. Roldan, A.S. Verkman, M. Kurth, A. Simon, et al. 2013. Mechanism-based corrector combination restores ΔF508-CFTR folding and function. *Nat. Chem. Biol.* 9:444–454. https://doi.org/10.1038/nchembio.1253

Oldfield, C.J., and A.K. Dunker. 2014. Intrinsically disordered proteins and intrinsically disordered protein regions. *Annu. Rev. Biochem.* 83:553–584. https://doi.org/10.1146/annurev-biochem-072711-164947

Oldham, M.L., A.L. Davidson, and J. Chen. 2008. Structural insights into ABC transporter mechanism. *Curr. Opin. Struct. Biol.* 18:726–733. https://doi.org/10.1016/j.sbi.2008.09.007

Ostedgaard, L.S., O. Baldursson, D.W. Vermeer, M.J. Welsh, and A.D. Robertson. 2000. A functional R domain from cystic fibrosis transmembrane conductance regulator is predominantly unstructured in solution. *Proc. Natl. Acad. Sci. USA.* 97:5657–5662. https://doi.org/10.1073/pnas.100588797

Ostedgaard, L.S., O. Baldursson, and M.J. Welsh. 2001. Regulation of the cystic fibrosis transmembrane conductance regulator Cl- channel by its R domain. *J. Biol. Chem.* 276:7689–7692. https://doi.org/10.1074/jbc.R100001200

Pedemonte, N., N.D. Sonawane, A. Taddei, J. Hu, O. Zegarra-Moran, Y.F. Suen, L.I. Robins, C.W. Dicus, D. Willenbring, M.H. Nantz, et al. 2005. Phenylglycine and sulfonamide correctors of defective delta F508 and G551D cystic fibrosis transmembrane conductance regulator chloride-channel gating. *Mol. Pharmacol.* 67:1797–1807. https://doi.org/10.1124/mol.105.010959

Price, M.P., H. Ishihara, D.N. Sheppard, and M.J. Welsh. 1996. Function of Xenopus cystic fibrosis transmembrane conductance regulator (CFTR) Cl channels and use of human-Xenopus chimeras to investigate the pore properties of CFTR. *J. Biol. Chem.* 271:25184–25191. https://doi.org/10.1074/jbc.271.41.25184

Qian, F., Y. El Hiani, and P. Linsdell. 2011. Functional arrangement of the 12th transmembrane region in the CFTR chloride channel pore based on functional investigation of a cysteine-less CFTR variant. *Pflugers Arch.* 462:559–571. https://doi.org/10.1007/s00424-011-0998-2

Rabeh, W.M., F. Bossard, H. Xu, T. Okiyoneda, M. Bagdany, C.M. Mulvihill, K. Du, S. di Bernardo, Y. Liu, L. Konermann, et al. 2012. Correction of both NBD1 energetics and domain interface is required to restore ΔF508 CFTR folding and function. *Cell.* 148:150–163. https://doi.org/10.1016/j.cell.2011.11.024

Ramsey, B.W., J. Davies, N.G. McElvaney, E. Tullis, S.C. Bell, P. Dřevínek, M. Griese, E.F. McKone, C.E. Wainwright, M.W. Konstan, et al. VX08-770-102 Study Group. 2011. A CFTR potentiator in patients with cystic fibrosis and the G551D mutation. *N. Engl. J. Med.* 365:1663–1672. https://doi.org/10.1056/NEJMoa1105185

Randak, C., and M.J. Welsh. 2003. An intrinsic adenylate kinase activity regulates gating of the ABC transporter CFTR. *Cell.* 115:837–850. https://doi.org/10.1016/S0092-8674(03)00983-8

Randak, C.O., and M.J. Welsh. 2005. ADP inhibits function of the ABC transporter cystic fibrosis transmembrane conductance regulator via its adenylate kinase activity. *Proc. Natl. Acad. Sci. USA.* 102:2216–2220. https://doi.org/10.1073/pnas.0409787102

Rees, D.C., E. Johnson, and O. Lewinson. 2009. ABC transporters: the power to change. *Nat. Rev. Mol. Cell Biol.* 10:218–227. https://doi.org/10.1038/nrm2646

Ren, H.Y., D.E. Grove, O. De La Rosa, S.A. Houck, P. Sopha, F. Van Goor, B.J. Hoffman, and D.M. Cyr. 2013. VX-809 corrects folding defects in cystic fibrosis transmembrane conductance regulator protein through action on membrane-spanning domain 1. *Mol. Biol. Cell.* 24:3016–3024. https://doi.org/10.1091/mbc.E13-05-0240

Riordan, J.R., J.M. Rommens, B. Kerem, N. Alon, R. Rozmahel, Z. Grzelczak, J. Zielenski, S. Lok, N. Plavsic, J.L. Chou, et al. 1989. Identification of the cystic fibrosis gene: cloning and characterization of complementary DNA. *Science.* 245:1066–1073. https://doi.org/10.1126/science.2475911

Rosser, M.F.N., D.E. Grove, L. Chen, and D.M. Cyr. 2008. Assembly and misassembly of cystic fibrosis transmembrane conductance regulator: folding defects caused by deletion of F508 occur before and after the calnexin-dependent association of membrane spanning domain (MSD) 1 and MSD2. *Mol. Biol. Cell.* 19:4570–4579. https://doi.org/10.1091/mbc.E08-04-0357

Rowe, S.M., and A.S. Verkman. 2013. Cystic fibrosis transmembrane regulator correctors and potentiators. *Cold Spring Harb. Perspect. Med.* 3:a009761. https://doi.org/10.1101/cshperspect.a009761

Rubaiy, H.N., and P. Linsdell. 2015. Location of a permeant anion binding site in the cystic fibrosis transmembrane conductance regulator chloride channel pore. *J. Physiol. Sci.* 65:233–241. https://doi.org/10.1007/s12576-015-0359-6

Rusnati, M., D. Sala, A. Orro, A. Bugatti, G. Trombetti, E. Cichero, C. Urbinati, M. Di Somma, E. Millo, L.J.V. Galietta, et al. 2018. Speeding Up the Identification of Cystic Fibrosis Transmembrane Conductance Regulator-Targeted Drugs: An Approach Based on Bioinformatics Strategies and Surface Plasmon Resonance. *Molecules.* 23:120. https://doi.org/10.3390/molecules23010120

Sauna, Z.E., and S.V. Ambudkar. 2007. About a switch: how P-glycoprotein (ABCB1) harnesses the energy of ATP binding and hydrolysis to do mechanical work. *Mol. Cancer Ther.* 6:13–23. https://doi.org/10.1158/1535-7163.MCT-06-0155

Schmitt, L. 2002. The first view of an ABC transporter: the X-ray crystal structure of MsbA from E. coli. *ChemBioChem.* 3:161–165. https://doi.org/10.1002/1439-7633(20020301)3:2/3%3C161::AID-CBIC161%3E3.0.CO;2-F

Schultz, B.D., A.D. DeRoos, C.J. Venglarik, A.K. Singh, R.A. Frizzell, and R.J. Bridges. 1996. Glibenclamide blockade of CFTR chloride channels. *Am. J. Physiol.* 271:L192–L200.

Scott-Ward, T.S., Z. Cai, E.S. Dawson, A. Doherty, A.C. Da Paula, H. Davidson, D.J. Porteous, B.J. Wainwright, M.D. Amaral, D.N. Sheppard, and A.C. Boyd. 2007. Chimeric constructs endow the human CFTR Cl- channel with the gating behavior of murine CFTR. *Proc. Natl. Acad. Sci. USA.* 104:16365–16370. https://doi.org/10.1073/pnas.0701562104

Sebastian, A., L. Rishishwar, J. Wang, K.F. Bernard, A.B. Conley, N.A. McCarty, and I.K. Jordan. 2013. Origin and evolution of the cystic fibrosis transmembrane regulator protein R domain. *Gene.* 523:137–146. https://doi.org/10.1016/j.gene.2013.02.050

Seibert, F.S., X.B. Chang, A.A. Aleksandrov, D.M. Clarke, J.W. Hanrahan, and J.R. Riordan. 1999. Influence of phosphorylation by protein kinase A on CFTR at the cell surface and endoplasmic reticulum. *Biochim. Biophys. Acta.* 1461:275–283. https://doi.org/10.1016/S0005-2736(99)00163-7

Serohijos, A.W., T. Hegedus, A.A. Aleksandrov, L. He, L. Cui, N.V. Dokholyan, and J.R. Riordan. 2008. Phenylalanine-508 mediates a cytoplasmic-membrane domain contact in the CFTR 3D structure crucial to assembly and channel function. *Proc. Natl. Acad. Sci. USA.* 105:3256–3261. https://doi.org/10.1073/pnas.0800254105

Sheppard, D.N., and K.A. Robinson. 1997. Mechanism of glibenclamide inhibition of cystic fibrosis transmembrane conductance regulator Cl- channels expressed in a murine cell line. *J. Physiol.* 503:333–346. https://doi.org/10.1111/j.1469-7793.1997.333bh.x

Sheppard, D.N., D.P. Rich, L.S. Ostedgaard, R.J. Gregory, A.E. Smith, and M.J. Welsh. 1993. Mutations in CFTR associated with mild-disease-form Cl- channels with altered pore properties. *Nature.* 362:160–164. https://doi.org/10.1038/362160a0

Smith, P.C., N. Karpowich, L. Millen, J.E. Moody, J. Rosen, P.J. Thomas, and J.F. Hunt. 2002. ATP binding to the motor domain from an ABC transporter drives formation of a nucleotide sandwich dimer. *Mol. Cell.* 10:139–149. https://doi.org/10.1016/S1097-2765(02)00576-2

Smith, S.S., E.D. Steinle, M.E. Meyerhoff, and D.C. Dawson. 1999. Cystic fibrosis transmembrane conductance regulator. Physical basis for lyotropic anion selectivity patterns. *J. Gen. Physiol.* 114:799–818. https://doi.org/10.1085/jgp.114.6.799

Smith, S.S., X. Liu, Z.R. Zhang, F. Sun, T.E. Kriewall, N.A. McCarty, and D.C. Dawson. 2001. CFTR: Covalent and noncovalent modification suggests a role for fixed charges in anion conduction. *J. Gen. Physiol.* 118:407–431. https://doi.org/10.1085/jgp.118.4.407

Snyder, D.S., L. Tradtrantip, S. Battula, C. Yao, P.W. Phuan, J.C. Fettinger, M.J. Kurth, and A.S. Verkman. 2013. Absolute Configuration and Biological Properties of Enantiomers of CFTR Inhibitor BPO-27. *ACS Med. Chem. Lett.* 4:456–459. https://doi.org/10.1021/ml400069k

Sohma, Y., and T.C. Hwang. 2015. Cystic fibrosis and the CFTR anion channel. *In* Handbook of Ion Channels. J. Zheng and M.C. Trudeau, editors. Taylor & Francis Group, LLC, Boca Raton, FL. 627–648. https://doi.org/10.1201/b18027-48

Sorum, B., D. Czégé, and L. Csanády. 2015. Timing of CFTR pore opening and structure of its transition state. *Cell.* 163:724–733. https://doi.org/10.1016/j.cell.2015.09.052

Sorum, B., B. Töröcsik, and L. Csanády. 2017. Asymmetry of movements in CFTR's two ATP sites during pore opening serves their distinct functions. *eLife.* 6. https://doi.org/10.7554/eLife.29013

Stahl, M., K. Stahl, M.B. Brubacher, and J.N. Forrest Jr. 2012. Divergent CFTR orthologs respond differently to the channel inhibitors CFTRinh-172, glibenclamide, and GlyH-101. *Am. J. Physiol. Cell Physiol.* 302:C67–C76. https://doi.org/10.1152/ajpcell.00225.2011

St. Aubin, C.N., J.J. Zhou, and P. Linsdell. 2007. Identification of a second blocker binding site at the cytoplasmic mouth of the cystic fibrosis transmembrane conductance regulator chloride channel pore. *Mol. Pharmacol.* 71:1360–1368. https://doi.org/10.1124/mol.106.031732

Szellas, T., and G. Nagel. 2003. Apparent affinity of CFTR for ATP is increased by continuous kinase activity. *FEBS Lett.* 535:141–146. https://doi.org/10.1016/S0014-5793(02)03892-9

Szollosi, A., D.R. Muallem, L. Csanády, and P. Vergani. 2011. Mutant cycles at CFTR's non-canonical ATP-binding site support little interface separation during gating. *J. Gen. Physiol.* 137:549–562. https://doi.org/10.1085/jgp.201110608

Tabcharani, J.A., J.M. Rommens, Y.X. Hou, X.B. Chang, L.C. Tsui, J.R. Riordan, and J.W. Hanrahan. 1993. Multi-ion pore behaviour in the CFTR chloride channel. *Nature.* 366:79–82. https://doi.org/10.1038/366079a0

Taddei, A., C. Folli, O. Zegarra-Moran, P. Fanen, A.S. Verkman, and L.J.V. Galietta. 2004. Altered channel gating mechanism for CFTR inhibition by a high-affinity thiazolidinone blocker. *FEBS Lett.* 558:52–56. https://doi.org/10.1016/S0014-5793(04)00011-0

Thibodeau, P.H., C.A. Brautigam, M. Machius, and P.J. Thomas. 2005. Side chain and backbone contributions of Phe508 to CFTR folding. *Nat. Struct. Mol. Biol.* 12:10–16. https://doi.org/10.1038/nsmb881

Thibodeau, P.H., J.M. Richardson III, W. Wang, L. Millen, J. Watson, J.L. Mendoza, K. Du, S. Fischman, H. Senderowitz, G.L. Lukacs, et al. 2010. The cystic fibrosis-causing mutation deltaF508 affects multiple steps in cystic fibrosis transmembrane conductance regulator biogenesis. *J. Biol. Chem.* 285:35825–35835. https://doi.org/10.1074/jbc.M110.131623

Tsai, M.F., H. Shimizu, Y. Sohma, M. Li, and T.C. Hwang. 2009. State-dependent modulation of CFTR gating by pyrophosphate. *J. Gen. Physiol.* 133:405–419. https://doi.org/10.1085/jgp.200810186

Tsai, M.F., M. Li, and T.C. Hwang. 2010. Stable ATP binding mediated by a partial NBD dimer of the CFTR chloride channel. *J. Gen. Physiol.* 135:399–414. https://doi.org/10.1085/jgp.201010399

Uversky, V.N. 2011. Intrinsically disordered proteins from A to Z. *Int. J. Biochem. Cell Biol.* 43:1090–1103. https://doi.org/10.1016/j.biocel.2011.04.001

Van Goor, F., S. Hadida, P.D. Grootenhuis, B. Burton, D. Cao, T. Neuberger, A. Turnbull, A. Singh, J. Joubran, A. Hazlewood, et al. 2009. Rescue of CF airway epithelial cell function in vitro by a CFTR potentiator, VX-770. *Proc. Natl. Acad. Sci. USA.* 106:18825–18830. https://doi.org/10.1073/pnas.0904709106

Van Goor, F., S. Hadida, P.D. Grootenhuis, B. Burton, J.H. Stack, K.S. Straley, C.J. Decker, M. Miller, J. McCartney, E.R. Olson, et al. 2011. Correction of the F508del-CFTR protein processing defect in vitro by the investigational drug VX-809. *Proc. Natl. Acad. Sci. USA.* 108:18843–18848. https://doi.org/10.1073/pnas.1105787108

Van Goor, F., H. Yu, B. Burton, and B.J. Hoffman. 2014. Effect of ivacaftor on CFTR forms with missense mutations associated with defects in protein processing or function. *J. Cyst. Fibros.* 13:29–36.

Vankeerberghen, A., L. Wei, M. Jaspers, J.J. Cassiman, B. Nilius, and H. Cuppens. 1998. Characterization of 19 disease-associated missense mutations in the regulatory domain of the cystic fibrosis transmembrane conductance regulator. *Hum. Mol. Genet.* 7:1761–1769. https://doi.org/10.1093/hmg/7.11.1761

Vergani, P., S.W. Lockless, A.C. Nairn, and D.C. Gadsby. 2005. CFTR channel opening by ATP-driven tight dimerization of its nucleotide-binding domains. *Nature.* 433:876–880. https://doi.org/10.1038/nature03313

Wang, W., and P. Linsdell. 2012a. Alternating access to the transmembrane domain of the ATP-binding cassette protein cystic fibrosis transmembrane conductance regulator (ABCC7). *J. Biol. Chem.* 287:10156–10165. https://doi.org/10.1074/jbc.M112.342972

Wang, W., and P. Linsdell. 2012b. Conformational change opening the CFTR chloride channel pore coupled to ATP-dependent gating. *Biochim. Biophys. Acta.* 1818:851–860. https://doi.org/10.1016/j.bbamem.2011.12.025

Wang, F., S. Zeltwanger, I.C. Yang, A.C. Nairn, and T.C. Hwang. 1998. Actions of genistein on cystic fibrosis transmembrane conductance regulator channel gating. Evidence for two binding sites with opposite effects. *J. Gen. Physiol.* 111:477–490. https://doi.org/10.1085/jgp.111.3.477

Wang, F., S. Zeltwanger, S. Hu, and T.C. Hwang. 2000. Deletion of phenylalanine 508 causes attenuated phosphorylation-dependent activation of CFTR chloride channels. *J. Physiol.* 524:637–648. https://doi.org/10.1111/j.1469-7793.2000.00637.x

Wang, W., G. Li, J.P. Clancy, and K.L. Kirk. 2005. Activating cystic fibrosis transmembrane conductance regulator channels with pore blocker analogs. *J. Biol. Chem.* 280:23622–23630. https://doi.org/10.1074/jbc.M503118200

Wang, W., K. Bernard, G. Li, and K.L. Kirk. 2007. Curcumin opens cystic fibrosis transmembrane conductance regulator channels by a novel mechanism that requires neither ATP binding nor dimerization of the nucleotide-binding domains. *J. Biol. Chem.* 282:4533–4544. https://doi.org/10.1074/jbc.M609942200

Wang, W., Y. El Hiani, and P. Linsdell. 2011. Alignment of transmembrane regions in the cystic fibrosis transmembrane conductance regulator chloride channel pore. *J. Gen. Physiol.* 138:165–178. https://doi.org/10.1085/jgp.201110605

Wang, W., Y. El Hiani, H.N. Rubaiy, and P. Linsdell. 2014a. Relative contribution of different transmembrane segments to the CFTR chloride channel pore. *Pflugers Arch.* 466:477–490. https://doi.org/10.1007/s00424-013-1317-x

Wang, Y., J.A. Wrennall, Z. Cai, H. Li, and D.N. Sheppard. 2014b. Understanding how cystic fibrosis mutations disrupt CFTR function: from single molecules to animal models. *Int. J. Biochem. Cell Biol.* 52:47–57. https://doi.org/10.1016/j.biocel.2014.04.001

Ward, A., C.L. Reyes, J. Yu, C.B. Roth, and G. Chang. 2007. Flexibility in the ABC transporter MsbA: Alternating access with a twist. *Proc. Natl. Acad. Sci. USA.* 104:19005–19010. https://doi.org/10.1073/pnas.0709388104

Weinreich, F., P.G. Wood, J.R. Riordan, and G. Nagel. 1997. Direct action of genistein on CFTR. *Pflugers Arch.* 434:484–491. https://doi.org/10.1007/s004240050424

Wilkinson, D.J., T.V. Strong, M.K. Mansoura, D.L. Wood, S.S. Smith, F.S. Collins, and D.C. Dawson. 1997. CFTR activation: additive effects of stimulatory and inhibitory phosphorylation sites in the R domain. *Am. J. Physiol.* 273:L127–L133.

Wright, P.E., and H.J. Dyson. 1999. Intrinsically unstructured proteins: re-assessing the protein structure-function paradigm. *J. Mol. Biol.* 293:321–331. https://doi.org/10.1006/jmbi.1999.3110

Xie, J., L.M. Adams, J. Zhao, T.A. Gerken, P.B. Davis, and J. Ma. 2002. A short segment of the R domain of cystic fibrosis transmembrane conductance regulator contains channel stimulatory and inhibitory activities that are separable by sequence modification. *J. Biol. Chem.* 277:23019–23027. https://doi.org/10.1074/jbc.M201661200

Yang, H., A.A. Shelat, R.K. Guy, V.S. Gopinath, T. Ma, K. Du, G.L. Lukacs, A. Taddei, C. Folli, N. Pedemonte, et al. 2003. Nanomolar affinity small molecule correctors of defective Delta F508-CFTR chloride channel gating. *J. Biol. Chem.* 278:35079–35085. https://doi.org/10.1074/jbc.M303098200

Yeh, H.I., J.T. Yeh, and T.C. Hwang. 2015. Modulation of CFTR gating by permeant ions. *J. Gen. Physiol.* 145:47–60. https://doi.org/10.1085/jgp.201411272

Yeh, H.I., Y. Sohma, K. Conrath, and T.C. Hwang. 2017. A common mechanism for CFTR potentiators. *J. Gen. Physiol.* 149:1105–1118. https://doi.org/10.1085/jgp.201711886

Yu, H., B. Burton, C.J. Huang, J. Worley, D. Cao, J.P. Johnson Jr., A. Urrutia, J. Joubran, S. Seepersaud, K. Sussky, et al. 2012. Ivacaftor potentiation of multiple CFTR channels with gating mutations. *J. Cyst. Fibros.* 11:237–245.

Yu, Y.C., Y. Sohma, and T.C. Hwang. 2016. On the mechanism of gating defects caused by the R117H mutation in cystic fibrosis transmembrane conductance regulator. *J. Physiol.* 594:3227–3244. https://doi.org/10.1113/JP271723

Yuan, Y.R., S. Blecker, O. Martsinkevich, L. Millen, P.J. Thomas, and J.F. Hunt. 2001. The crystal structure of the MJ0796 ATP-binding cassette. Implications for the structural consequences of ATP hydrolysis in the active site of an ABC transporter. *J. Biol. Chem.* 276:32313–32321. https://doi.org/10.1074/jbc.M100758200

Zeltwanger, S., F. Wang, G.T. Wang, K.D. Gillis, and T.C. Hwang. 1999. Gating of cystic fibrosis transmembrane conductance regulator chloride channels by adenosine triphosphate hydrolysis. Quantitative analysis of a cyclic gating scheme. *J. Gen. Physiol.* 113:541–554. https://doi.org/10.1085/jgp.113.4.541

Zhang, J., and T.C. Hwang. 2015. The Fifth Transmembrane Segment of Cystic Fibrosis Transmembrane Conductance Regulator Contributes to Its Anion Permeation Pathway. *Biochemistry.* 54:3839–3850. https://doi.org/10.1021/acs.biochem.5b00427

Zhang, J., and T.C. Hwang. 2017. Electrostatic tuning of the pre- and post-hydrolytic open states in CFTR. *J. Gen. Physiol.* 149:355–372. https://doi.org/10.1085/jgp.201611664

Zhang, Z., and J. Chen. 2016. Atomic Structure of the Cystic Fibrosis Transmembrane Conductance Regulator. *Cell.* 167:1586–1597.

Zhang, Z., F. Liu, and J. Chen. 2017. Conformational Changes of CFTR upon Phosphorylation and ATP Binding. *Cell.* 170:483–491.e8. https://doi.org/10.1016/j.cell.2017.06.041

Zhao, Y., M. Ishigami, K. Nagao, K. Hanada, N. Kono, H. Arai, M. Matsuo, N. Kioka, and K. Ueda. 2015. ABCB4 exports phosphatidylcholine in a sphingomyelin-dependent manner. *J. Lipid Res.* 56:644–652. https://doi.org/10.1194/jlr.M056622

Zhou, J.J., M. Fatehi, and P. Linsdell. 2008. Identification of positive charges situated at the outer mouth of the CFTR chloride channel pore. *Pflugers Arch.* 457:351–360. https://doi.org/10.1007/s00424-008-0521-6

Zhou, J.J., M.S. Li, J. Qi, and P. Linsdell. 2010. Regulation of conductance by the number of fixed positive charges in the intracellular vestibule of the CFTR chloride channel pore. *J. Gen. Physiol.* 135:229–245. https://doi.org/10.1085/jgp.200910327

Zhou, S.S., A. Hazama, and Y. Okada. 1998. Tyrosine kinase-independent extracellular action of genistein on the CFTR Cl- channel in guinea pig ventricular myocytes and CFTR-transfected mouse fibroblasts. *Jpn. J. Physiol.* 48:389–396. https://doi.org/10.2170/jjphysiol.48.389

Zhou, Z., S. Hu, and T.C. Hwang. 2002. Probing an open CFTR pore with organic anion blockers. *J. Gen. Physiol.* 120:647–662. https://doi.org/10.1085/jgp.20028685

Zhou, Z., X. Wang, M. Li, Y. Sohma, X. Zou, and T.C. Hwang. 2005. High affinity ATP/ADP analogues as new tools for studying CFTR gating. *J. Physiol.* 569:447–457. https://doi.org/10.1113/jphysiol.2005.095083